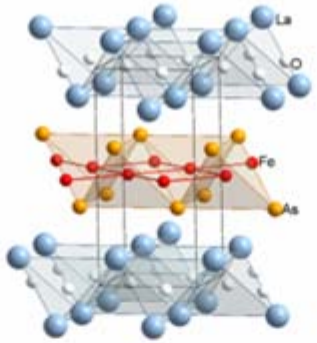

Explaining the band structure and itinerant magnetism of iron-arsenide superconductors

Lilia Boeri, Alexander Yaresko, and O. K. Andersen

Max-Planck-Institute for Solid-State Research, Stuttgart

Superconductivity in F-doped iron pnictides (d^6) was discovered early in 2008. Within a few months, T_c was increased from 26 K in LaOFeAs to 55 K in SmOFeAs. In addition to the LnOFeAs compounds, $A_{½}FeAs$, and $Fe_{1+x}Se$ superconducting compounds have been found.

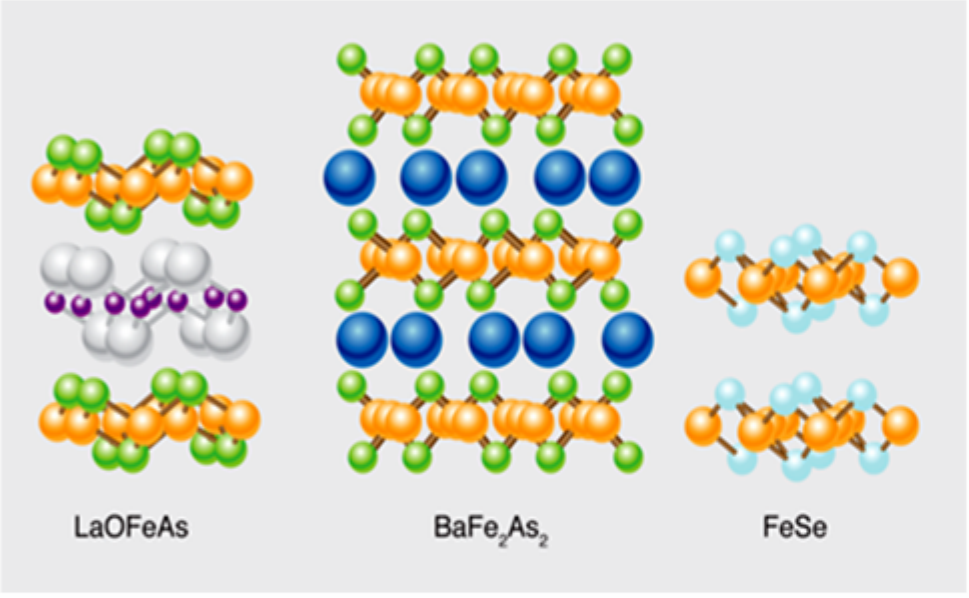

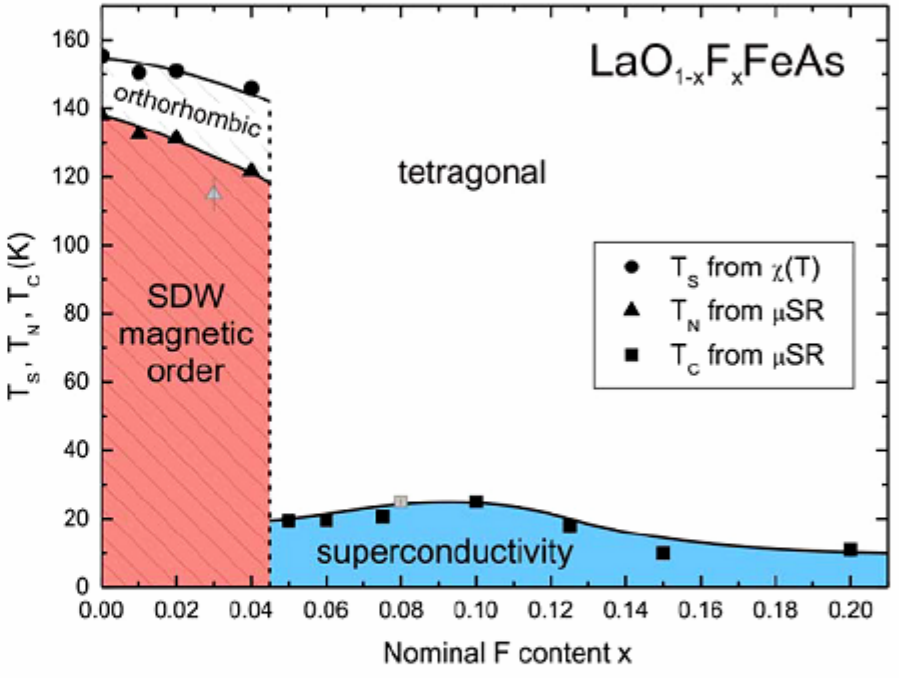

The superconductivity seems to be unconventional ($s_{+/-}$, d, s+id) since the calculated electron-phonon interaction is weak (Boeri: $\lambda \sim 0.2$) and the parent compound displays a transition to a striped AFM state, with a small moment $m \sim 0.3\ \mu_B$ in LnOFeAs and $\sim 0.9\ \mu_B$ in $Ba_{1/2}FeAs$.

The common motive is square **Fe** lattice with **As** atoms placed alternatingly above and below the centers of the squares.

The $FeAs_4$ tetrahedron is squeezed.

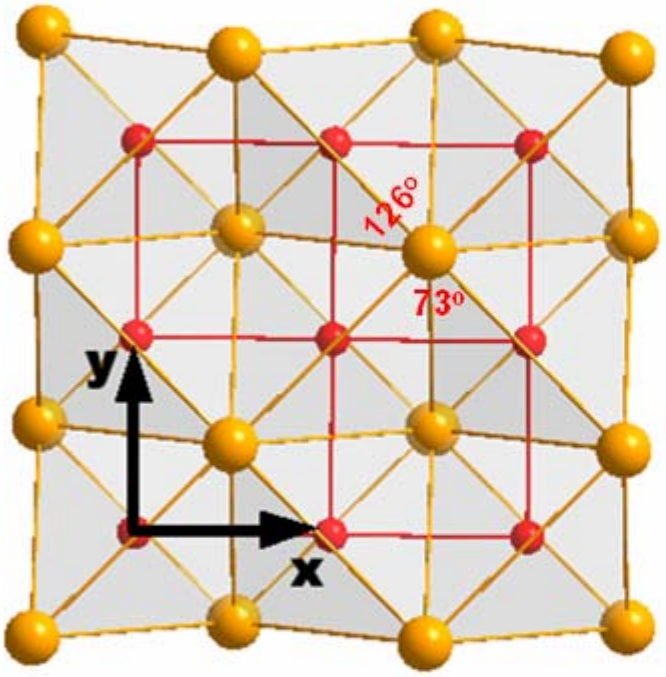

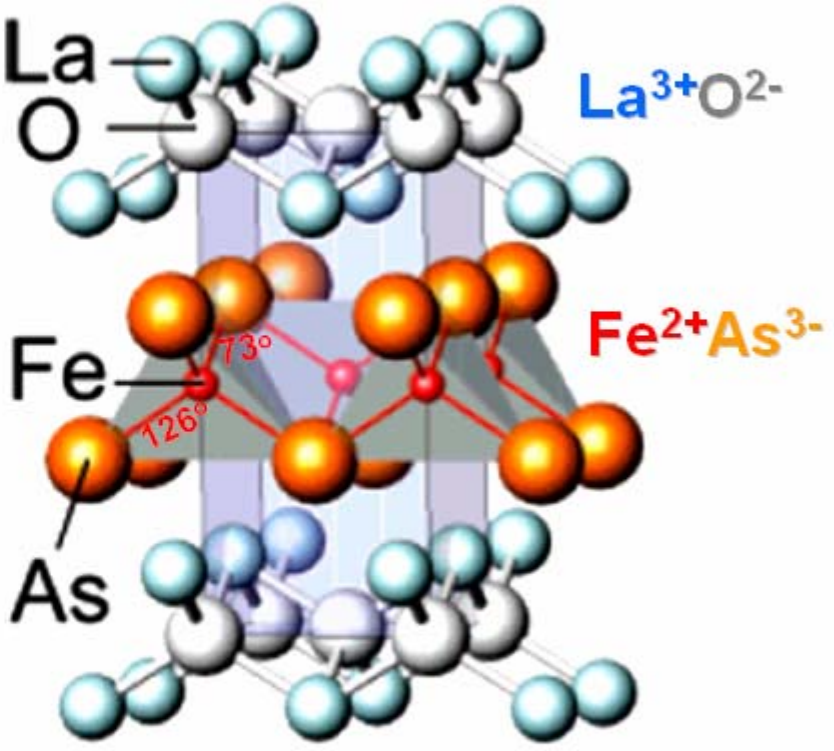

The physical properties and even the basic electronic structure of these materials are not well understood. In contrast to the cuprates, the Fe compunds are always metals, the electronic correlations seem to be weak, the magnetism itinerant, and the LSDA seems to work.

Published band structures are complicated. Even without magnetism they have 2x5 *d* bands and 2x3 *p* bands in the Fe_2As_2 translational cell. We simplify them by using the space group generated by a primitive translation of the square lattice *followed by mirroring* in the Fe plane. This reduces the formula unit to FeAs and makes the 2D Brillouin zone identical to the one used for the cuprate superconductors. Below we show the **unfolding** (red) of the LAPW bands (black) and Fermi surface.

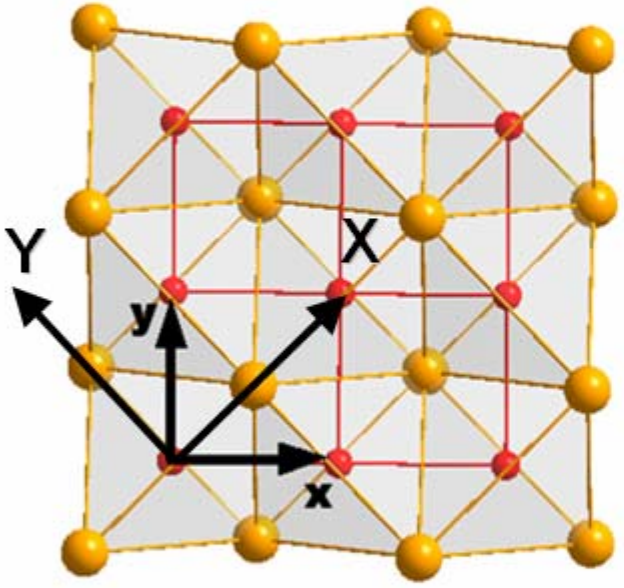

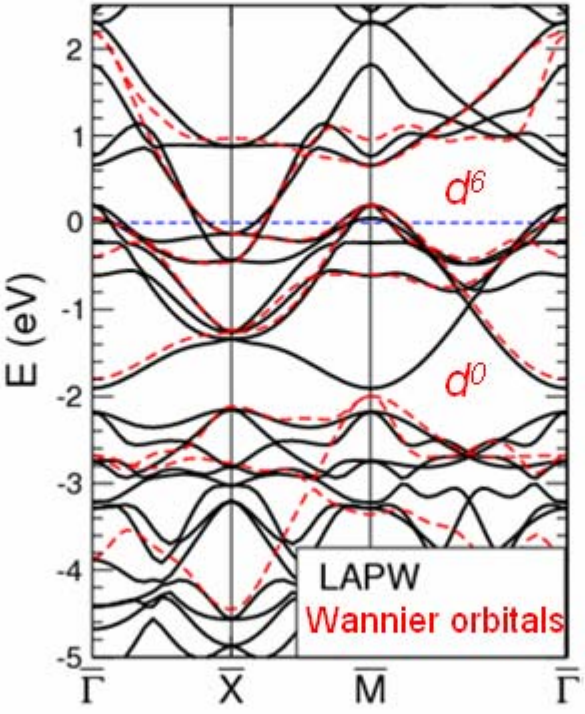

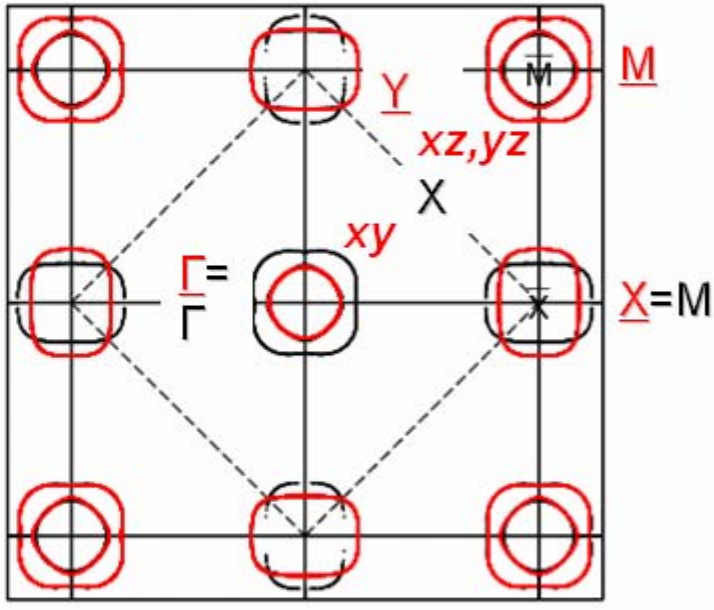

We have derived a generally applicable (e.g. for studies of magnetism and superconductivity) and accurate tight-binding (TB) model describing the LDA single-particle wavefunctions of the bands near the Fermi level in terms of the 3 As *p* and 5 Fe *d* Wannier orbitals by means of downfolding plus N-ization (NMTO).

Positions of the hole pockets in the large BZ:

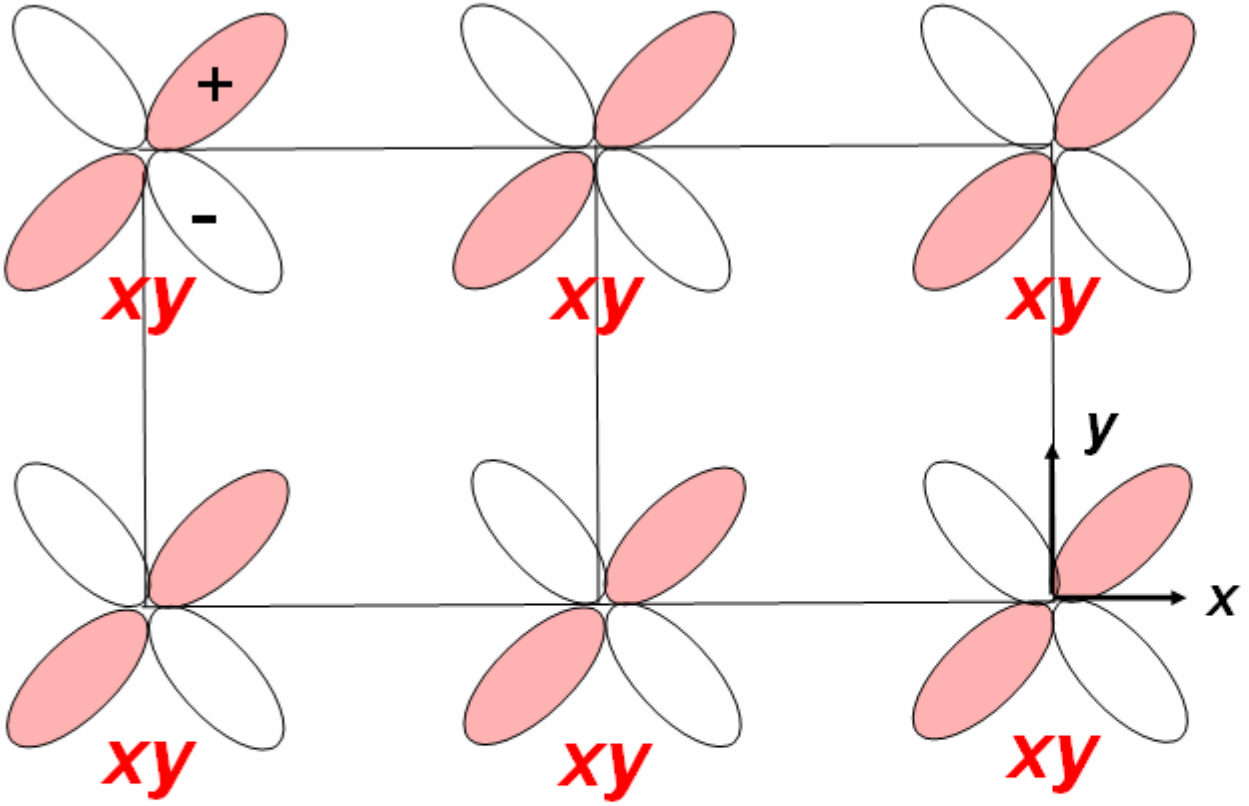

At ***k*** =(0,0) the **Fe *xy*** Blochwave is anti-bonding, i.e. the ***xy*** band has its **top at Γ.**

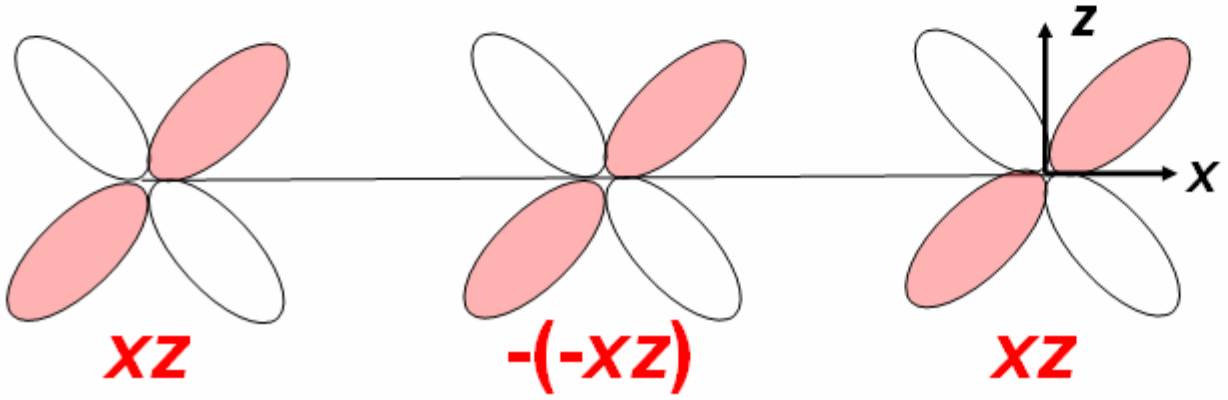

At ***k*** = (π, π) the **Fe *xz*** Blochwave is anti-bonding, i.e. the ***xz*** band has its **top at M.**

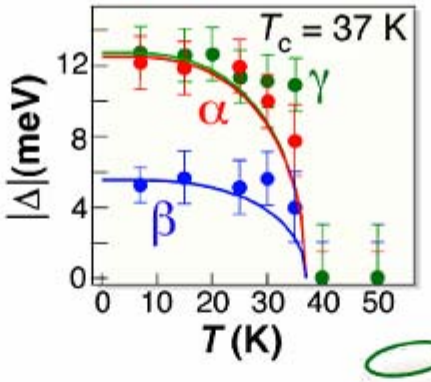

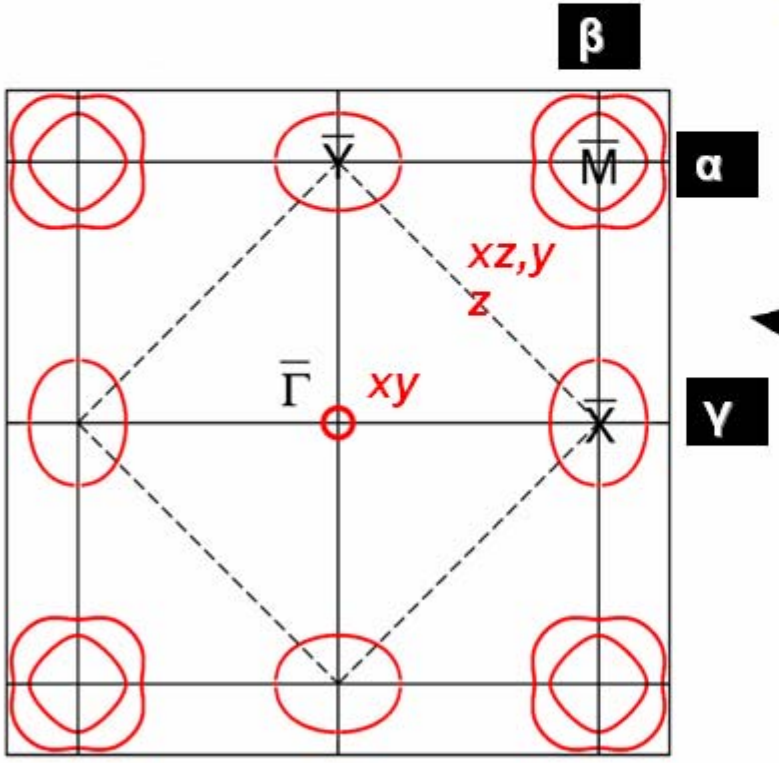

Observation of Fermi-surface-dependent nodeless superconducting gaps in $Ba_{0.6}K_{0.4}Fe_2As_2$

H. Ding[1], P. Richard[2], K. Nakayama[3], T. Sugawara[3], T. Arakane[3], Y. Sekiba[3], A. Takayama[3], S. Souma[2], T. Sato[3], T. Takahashi[2,3], Z. Wang[4], X. Dai[1], Z. Fang[1], G. F. Chen[1], J. L. Luo[1], and N. L. Wang[1]

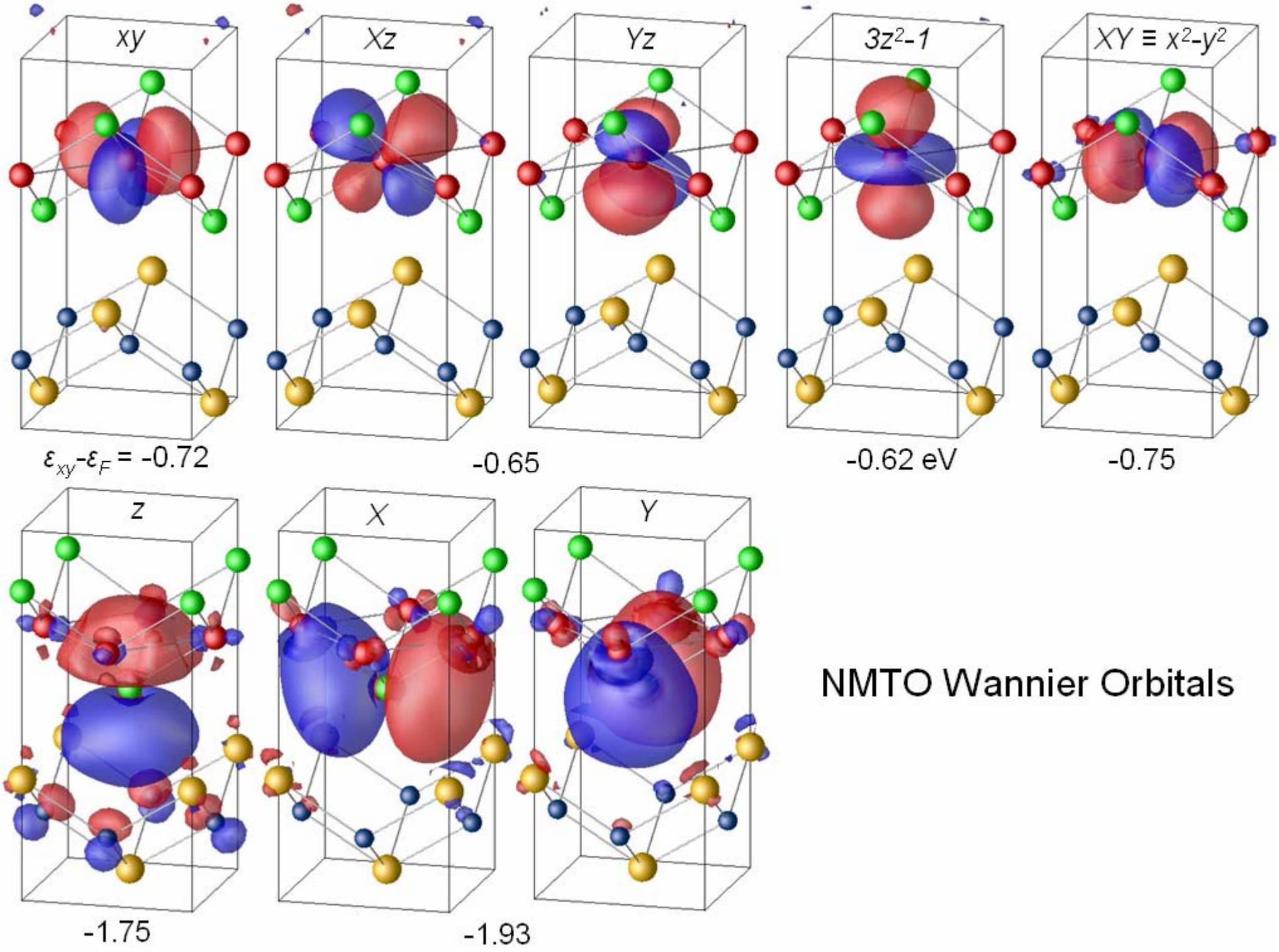
xy
Xz
Yz
3z²-1
XY ≡ x²-y²
z
X
Y
$\varepsilon_{xy}-\varepsilon_F$ = -0.72
-0.65
-0.62 eV
-0.75
-1.75
-1.93
NMTO Wannier Orbitals

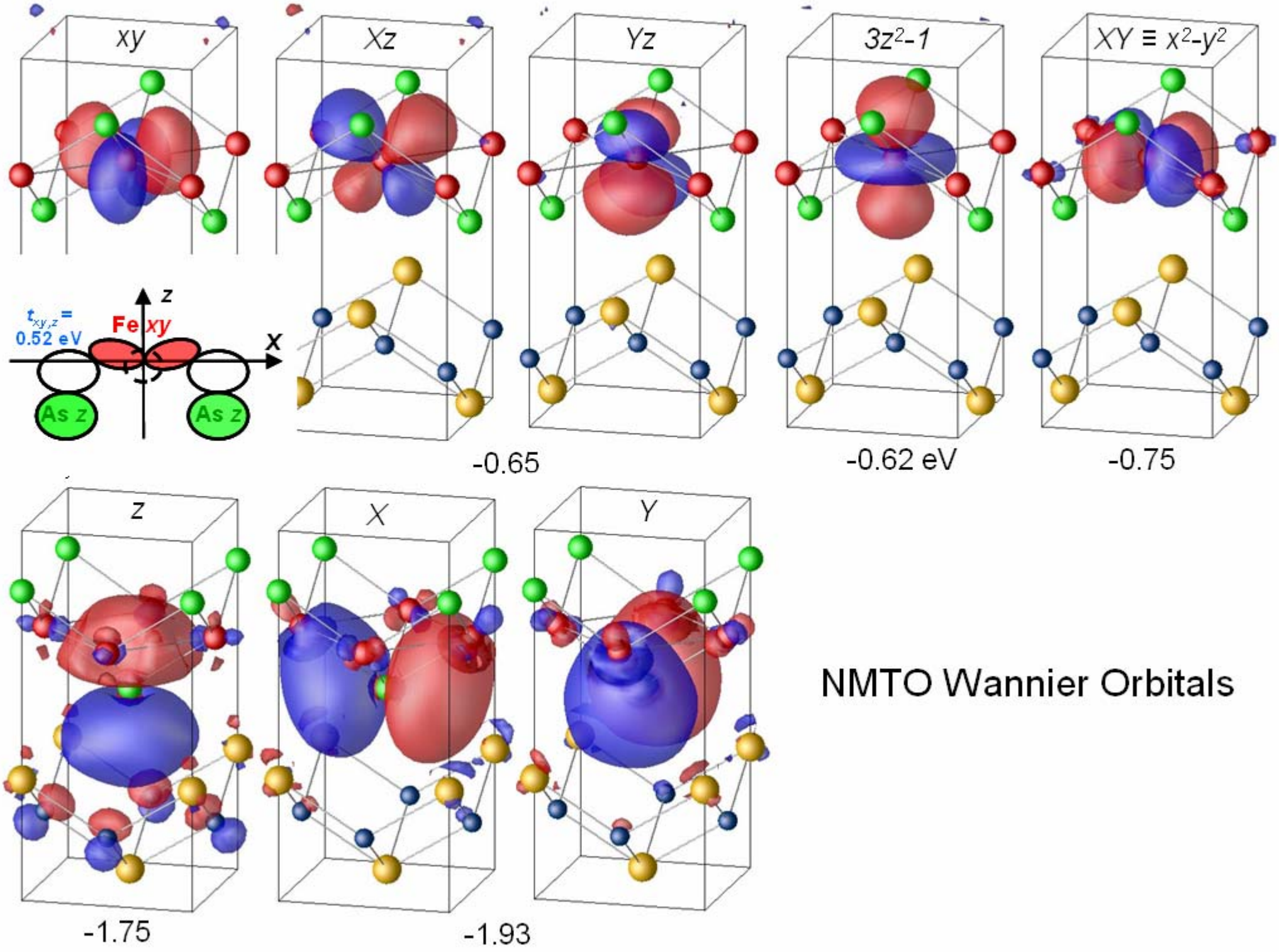

NMTO Wannier Orbitals

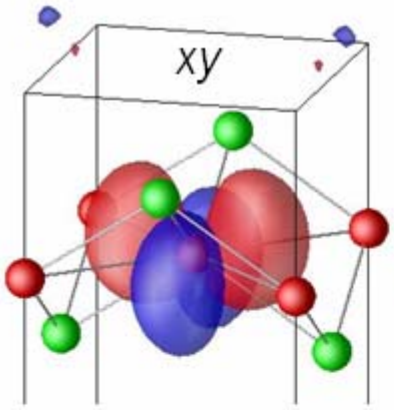

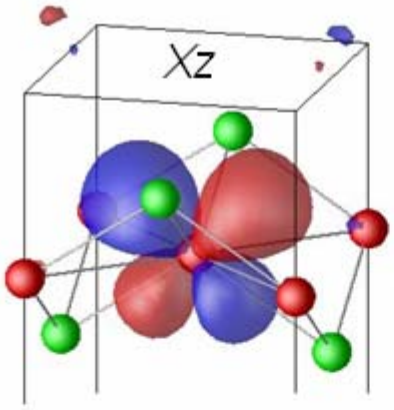

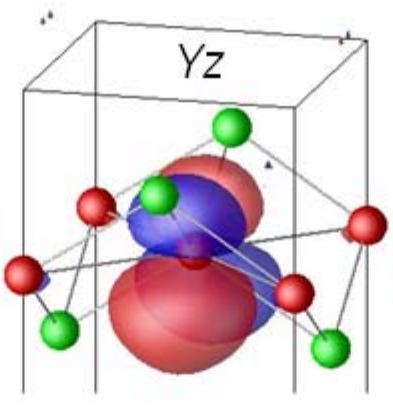

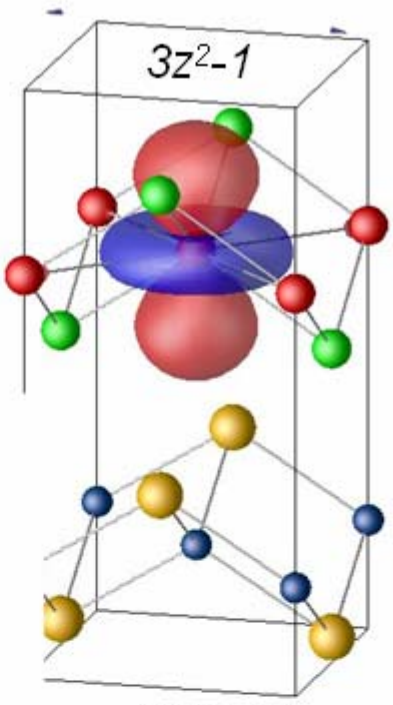

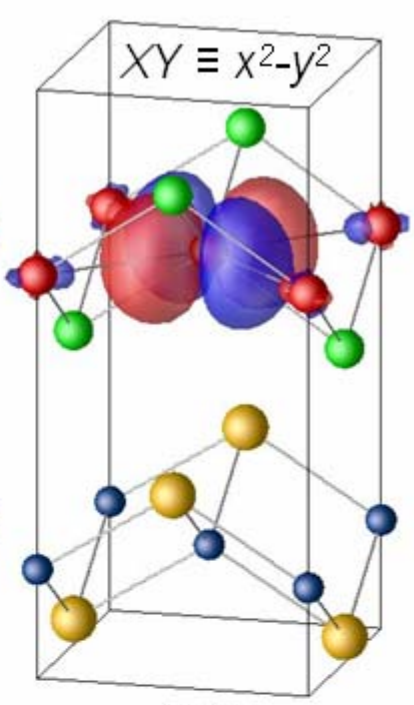

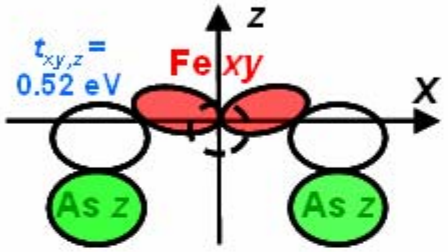

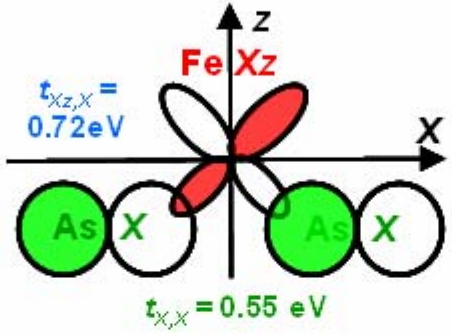

-0.62 eV

-0.75

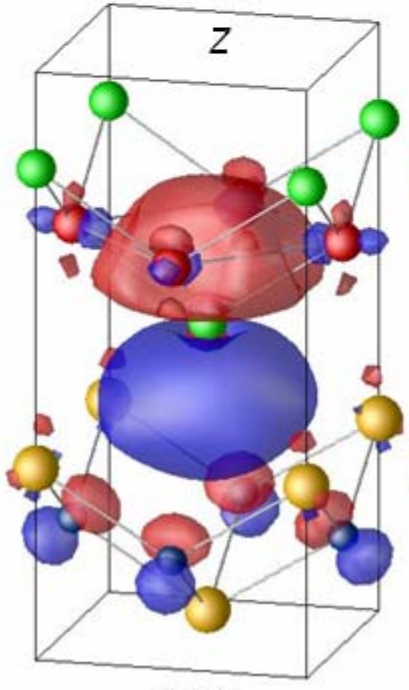

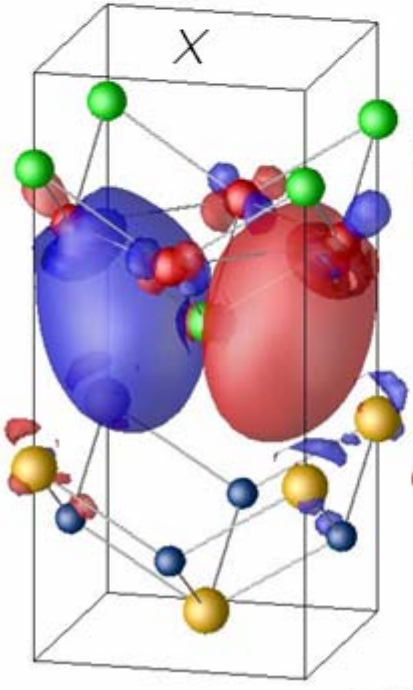

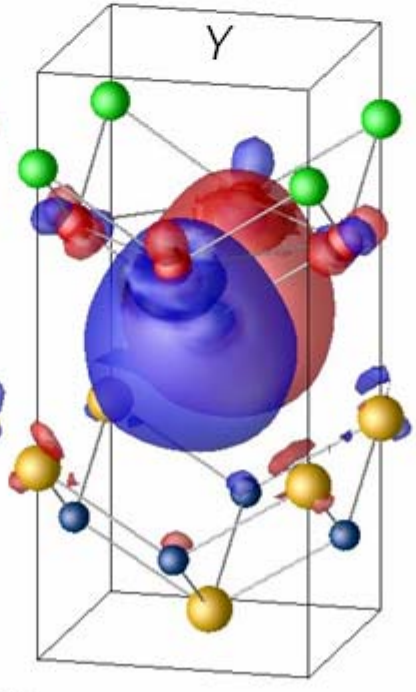

-1.75

-1.93

NMTO Wannier Orbitals

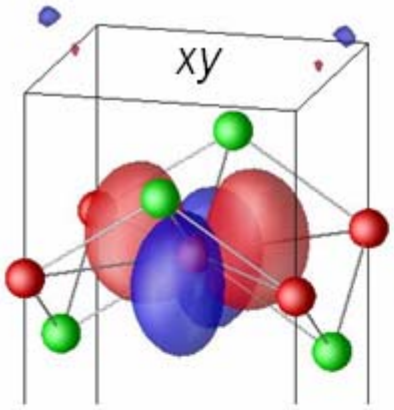

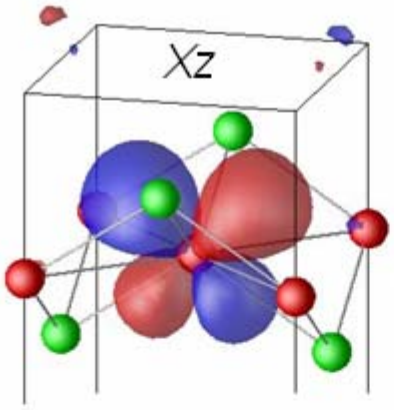

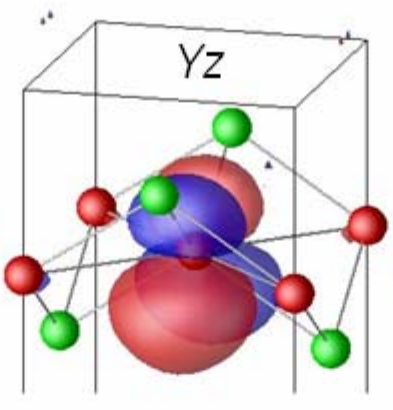

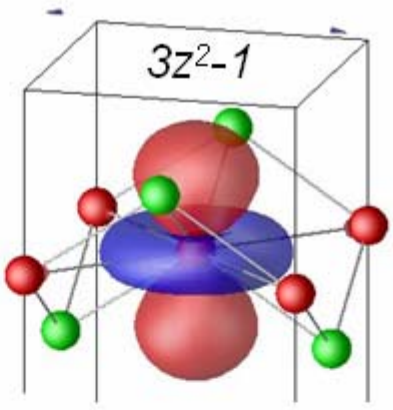

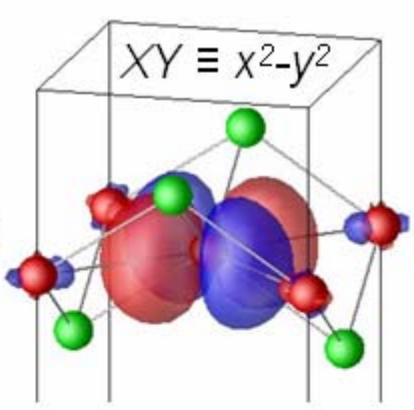

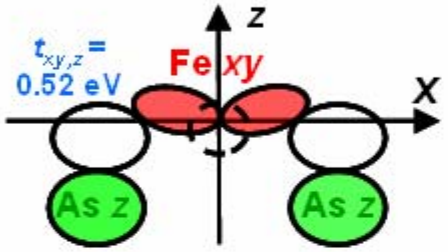

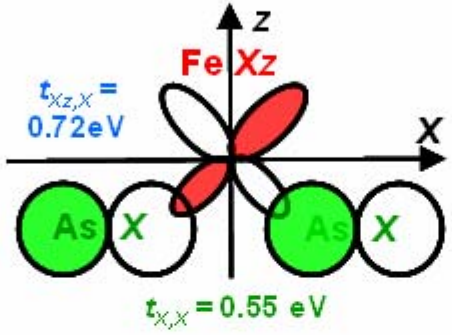

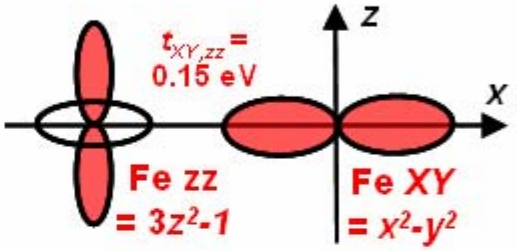

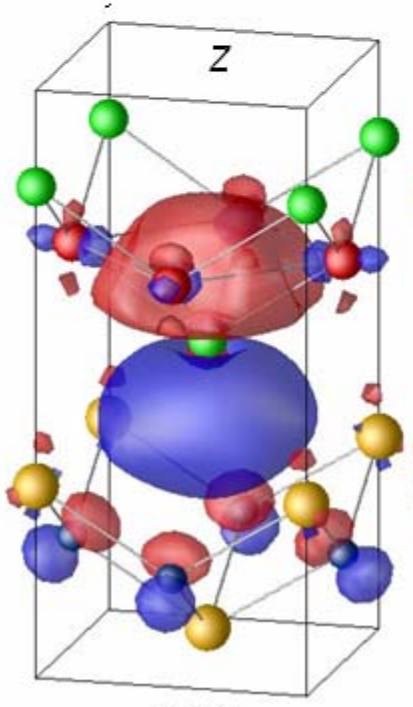

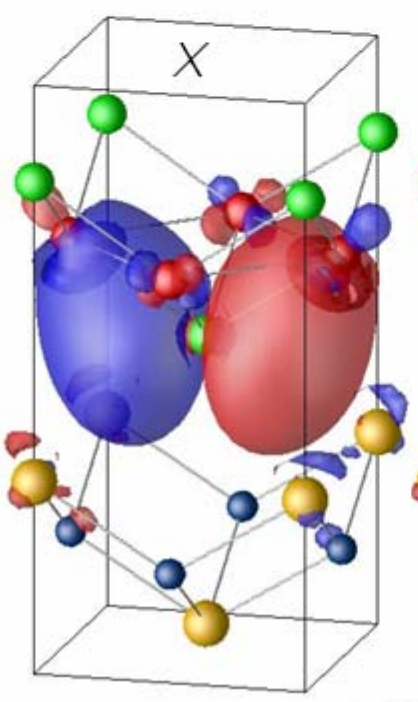

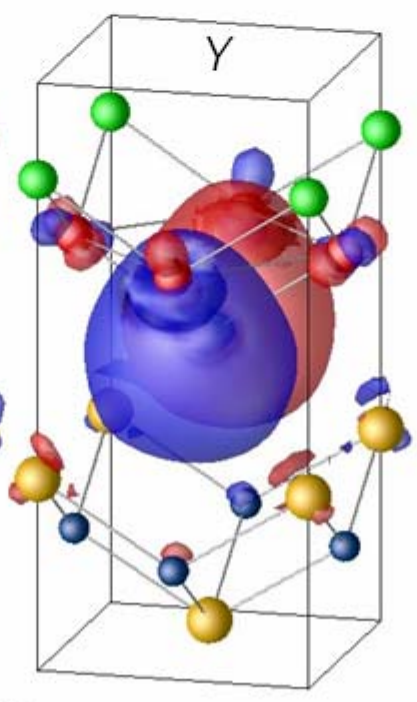

NMTO Wannier Orbitals

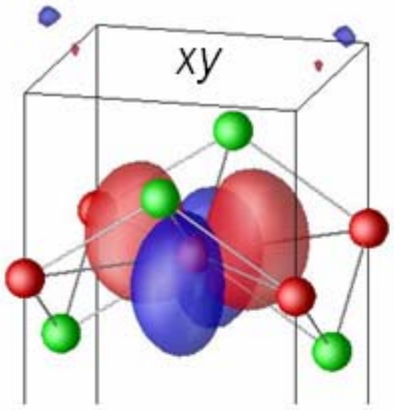

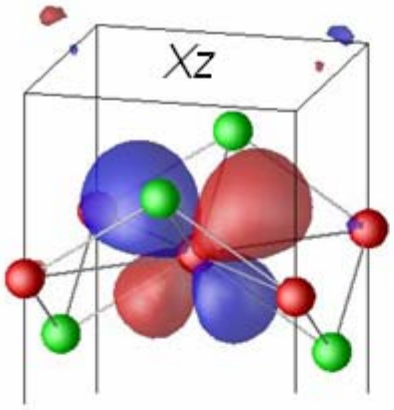

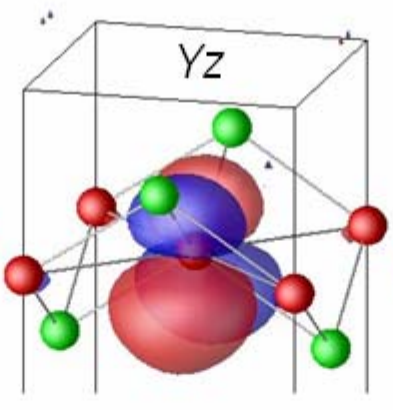

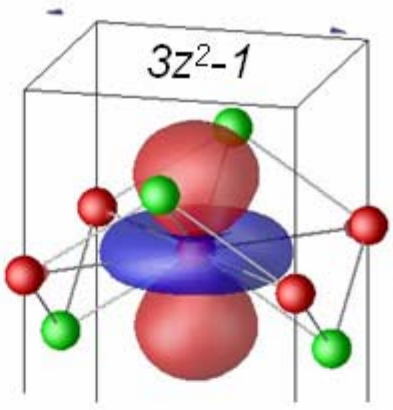

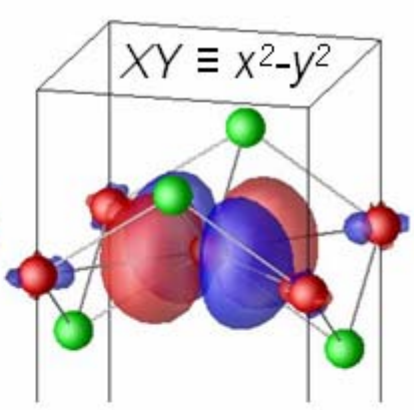

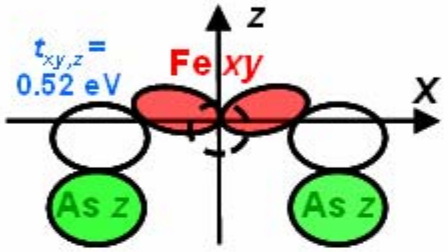

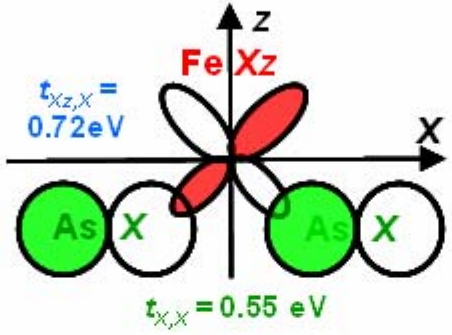

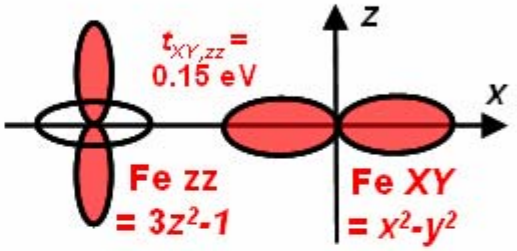

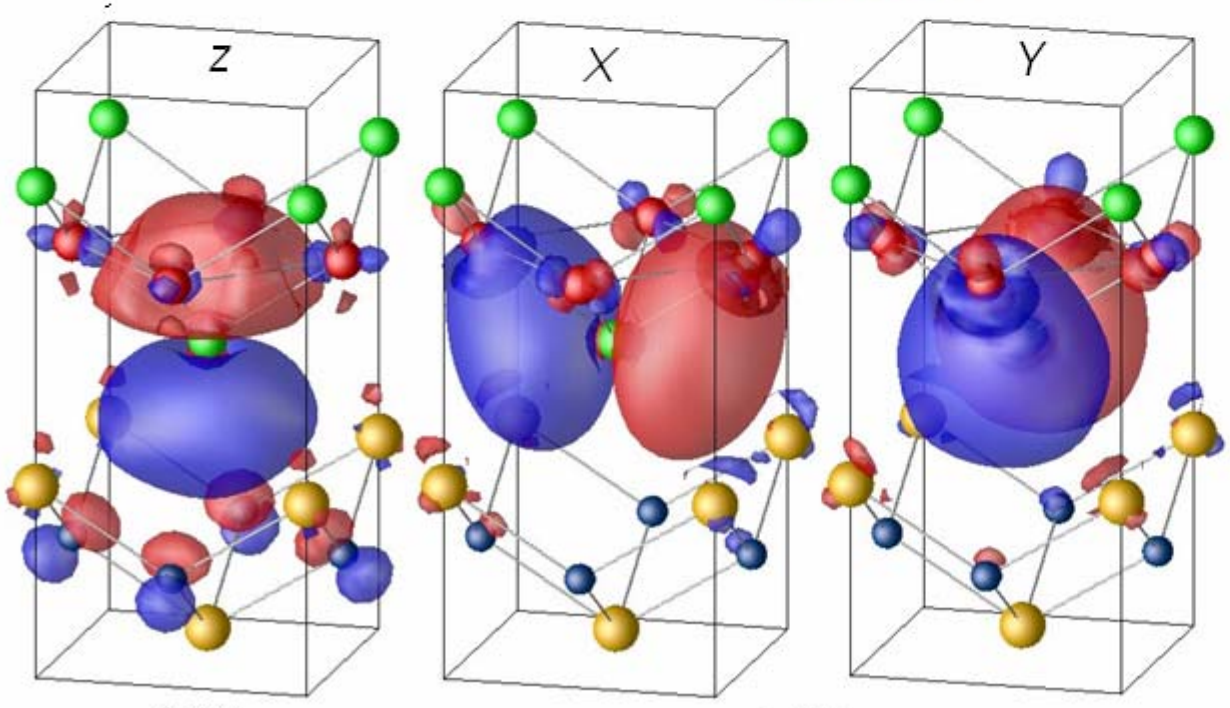

NMTO Wannier Orbitals

Hopping ranges are long due to incomplete covalent pairing of orbitals, i.e. the bonding is partly covalent and partly metallic.

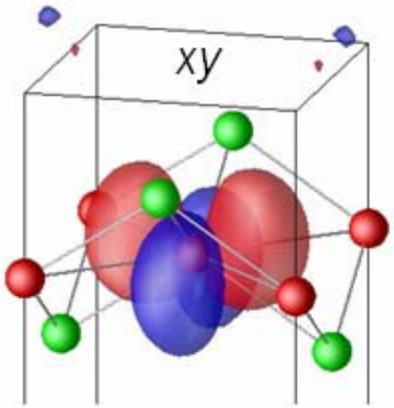

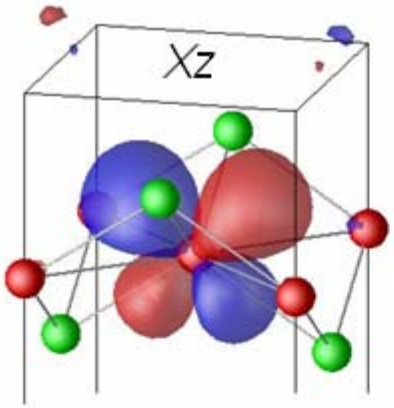

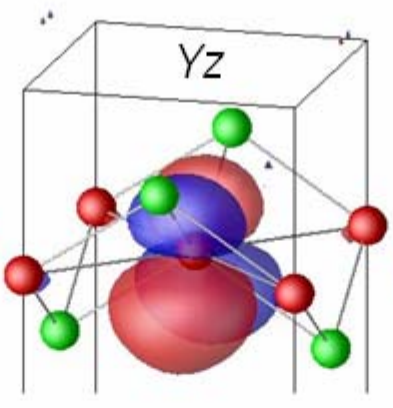

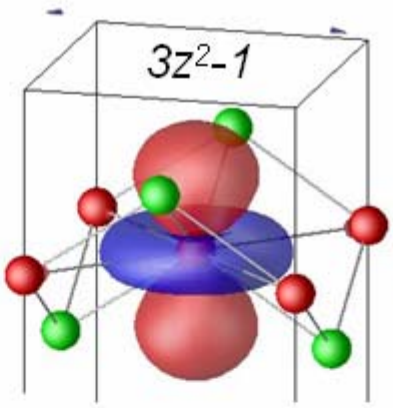

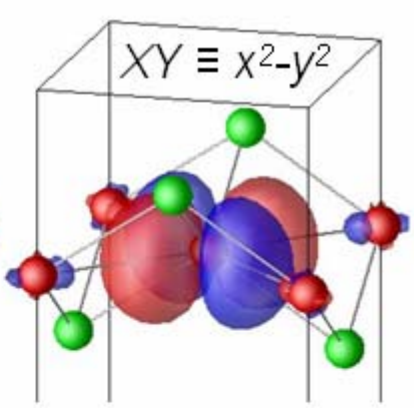

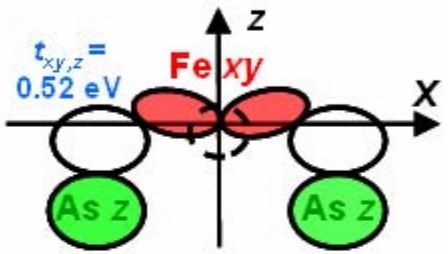

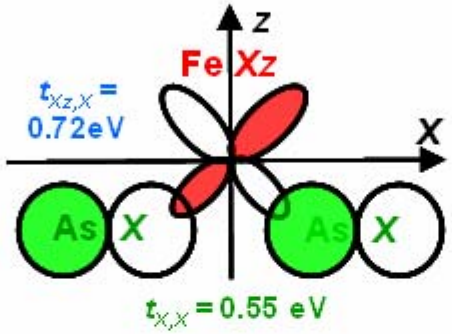

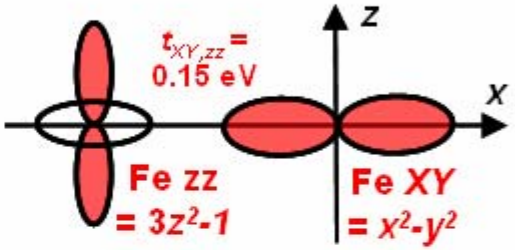

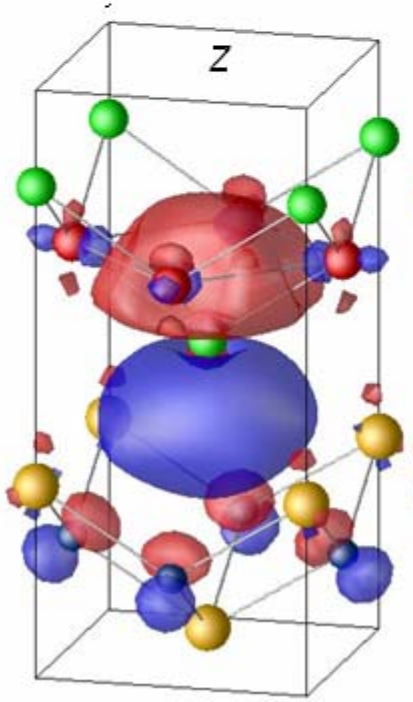

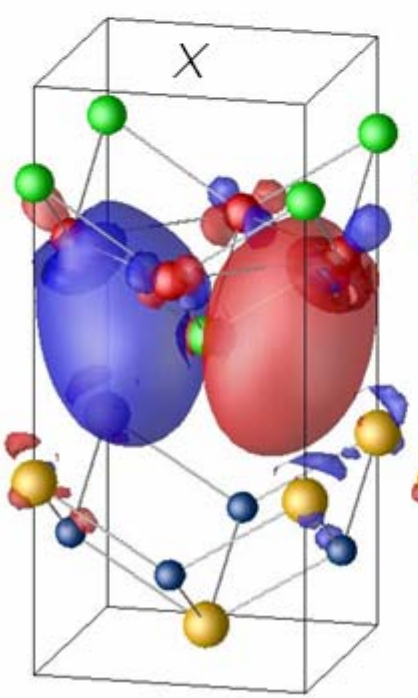

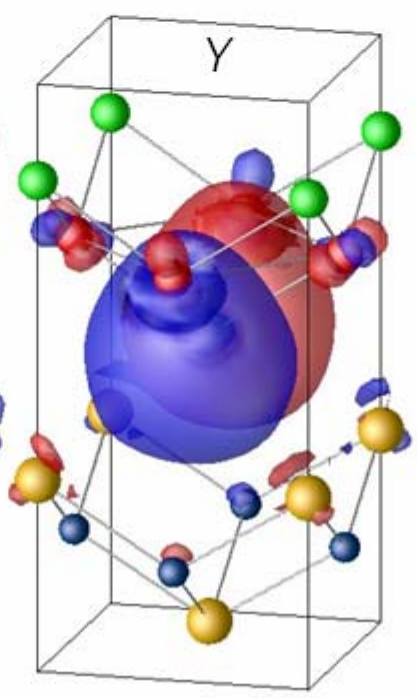

NMTO Wannier Orbitals

Hopping ranges are long due to incomplete covalent pairing of orbitals, i.e. the bonding is partly covalent and partly metallic.

Cuprates have $pd\sigma$ geometry and d^9

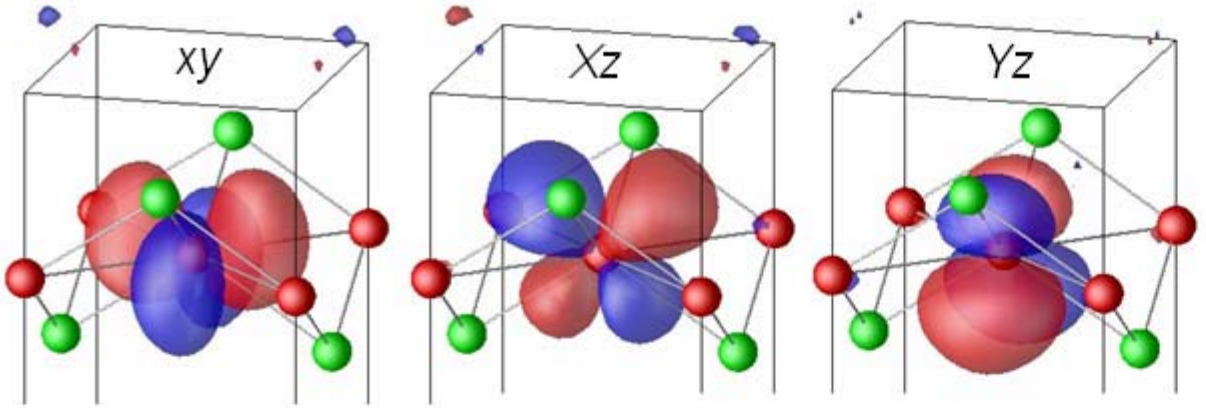

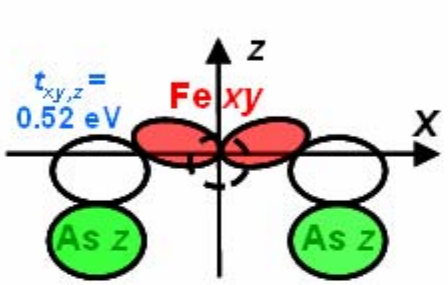

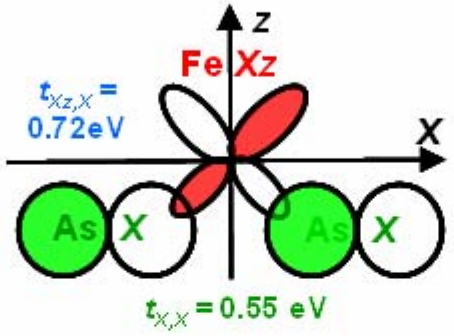

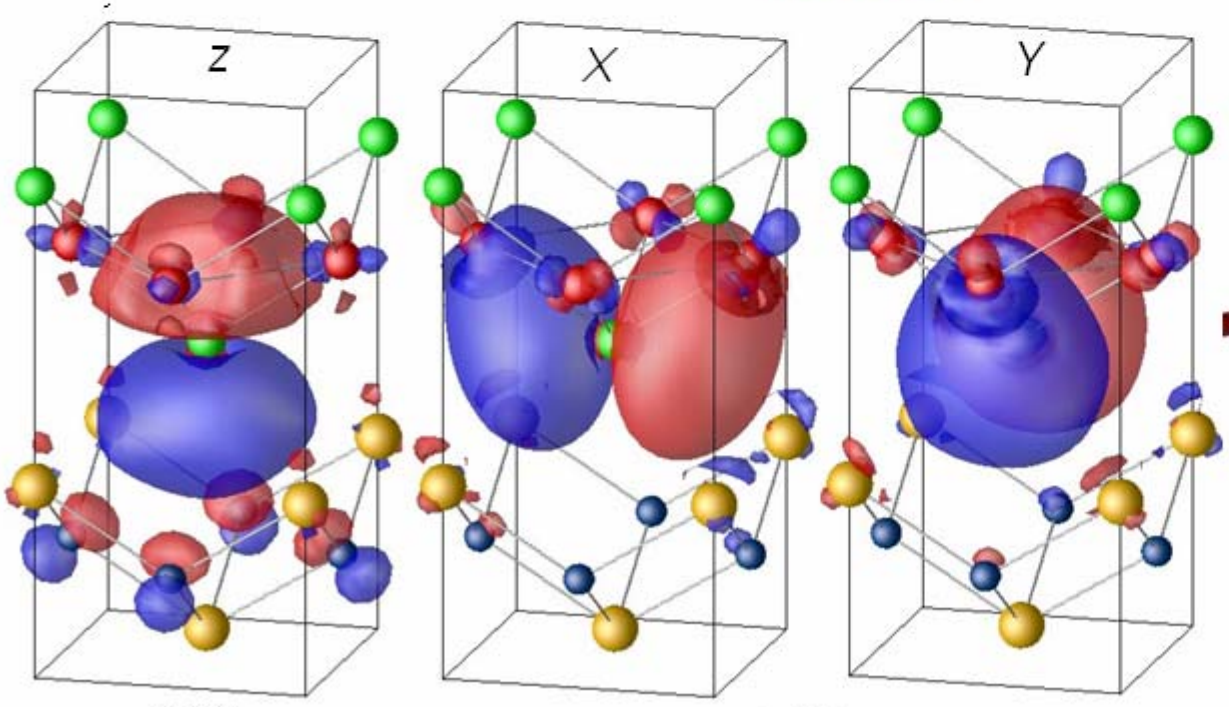

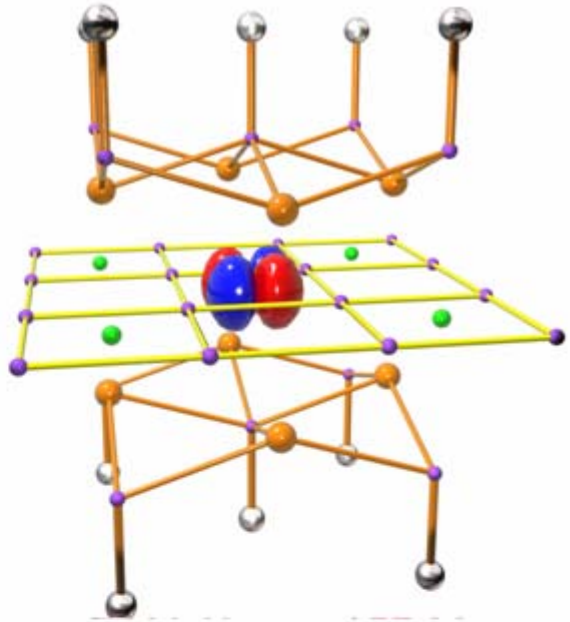

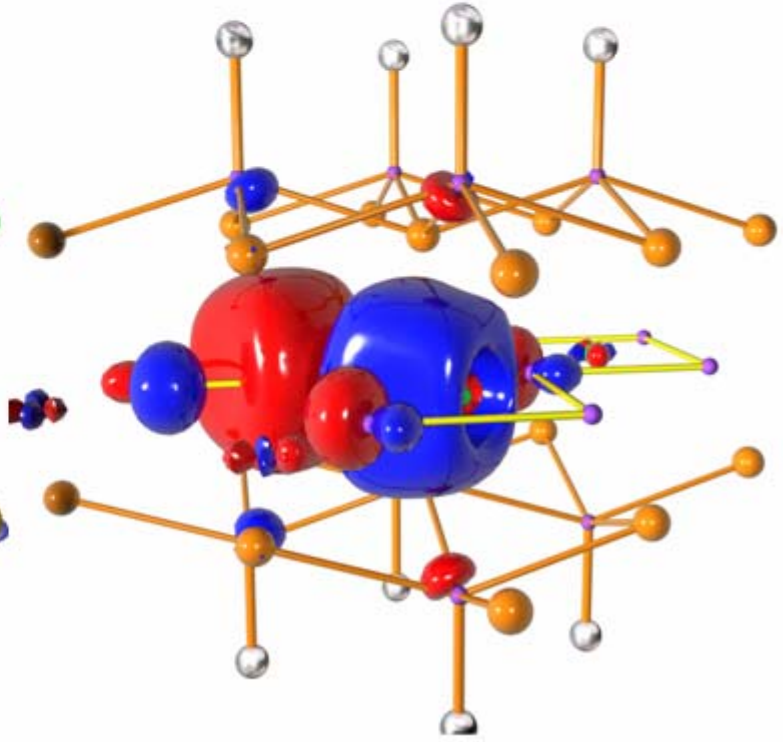

Cuprates have $pd\sigma$ geometry and d^9

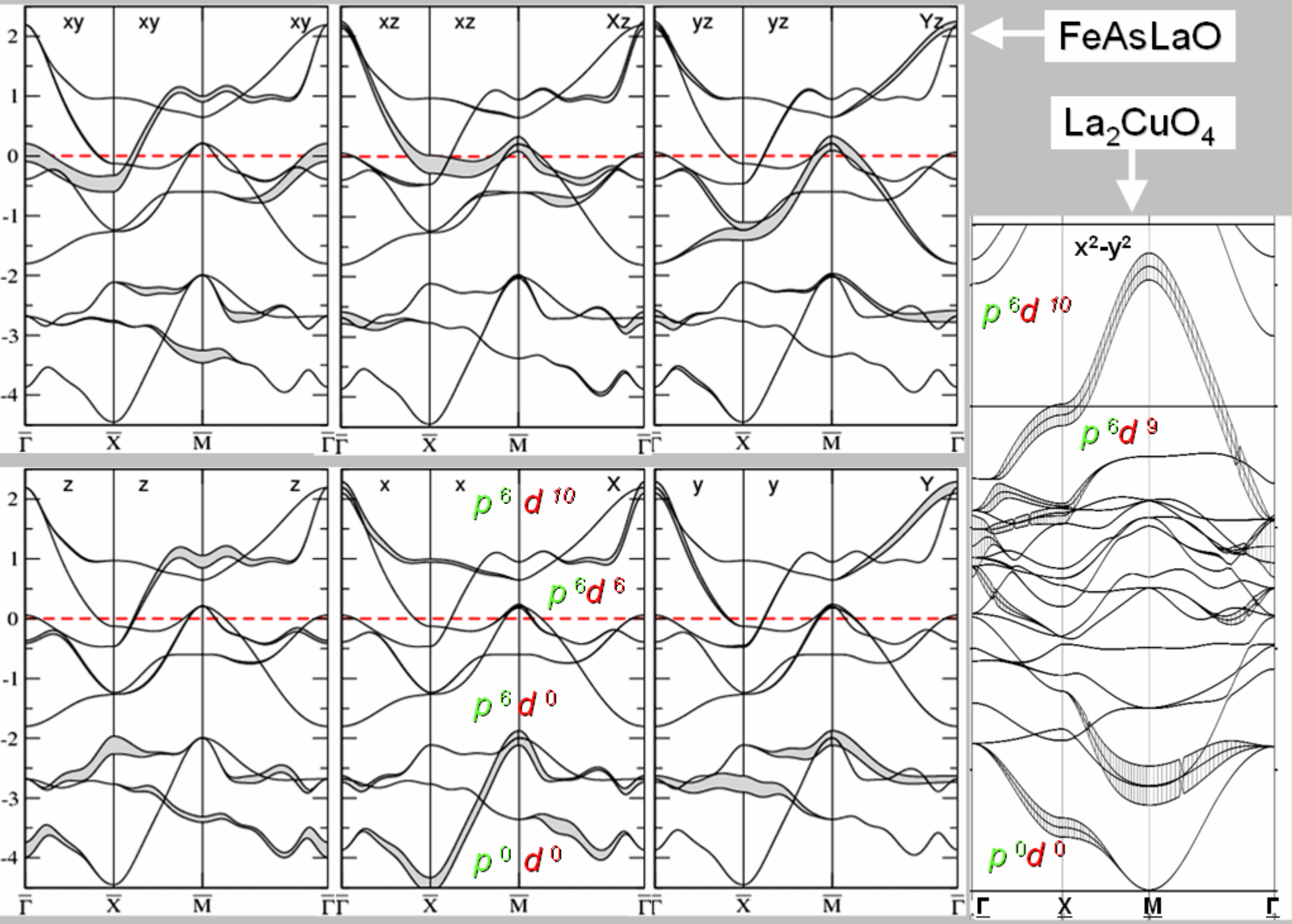
FeAsLaO
La2CuO4
xy
xz
Xz
yz
Yz
z
x
X
y
Y
x²-y²
p 6d 10
p 6d 9
p 6d 6
p 6d 0
p 0d 0
Γ̄
X̄
M̄
Γ
X
M

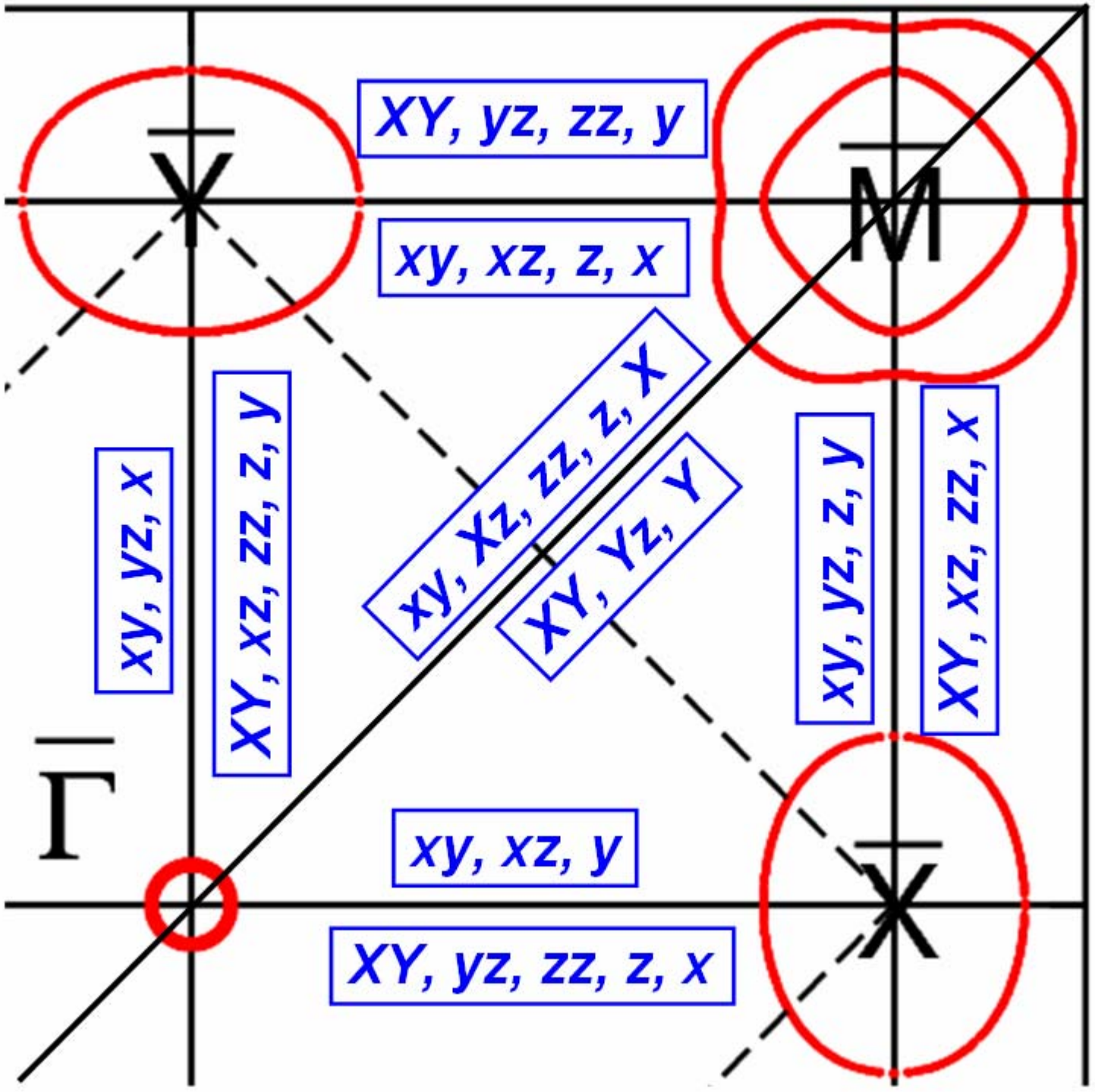
XY, yz, zz, y
xy, xz, z, x
xy, Xz, zz, z, X
XY, Yz, Y
xy, yz, x
XY, xz, zz, z, y
xy, yz, z, y
XY, xz, zz, x
xy, xz, y
XY, yz, zz, z, x
Γ
M
X
X

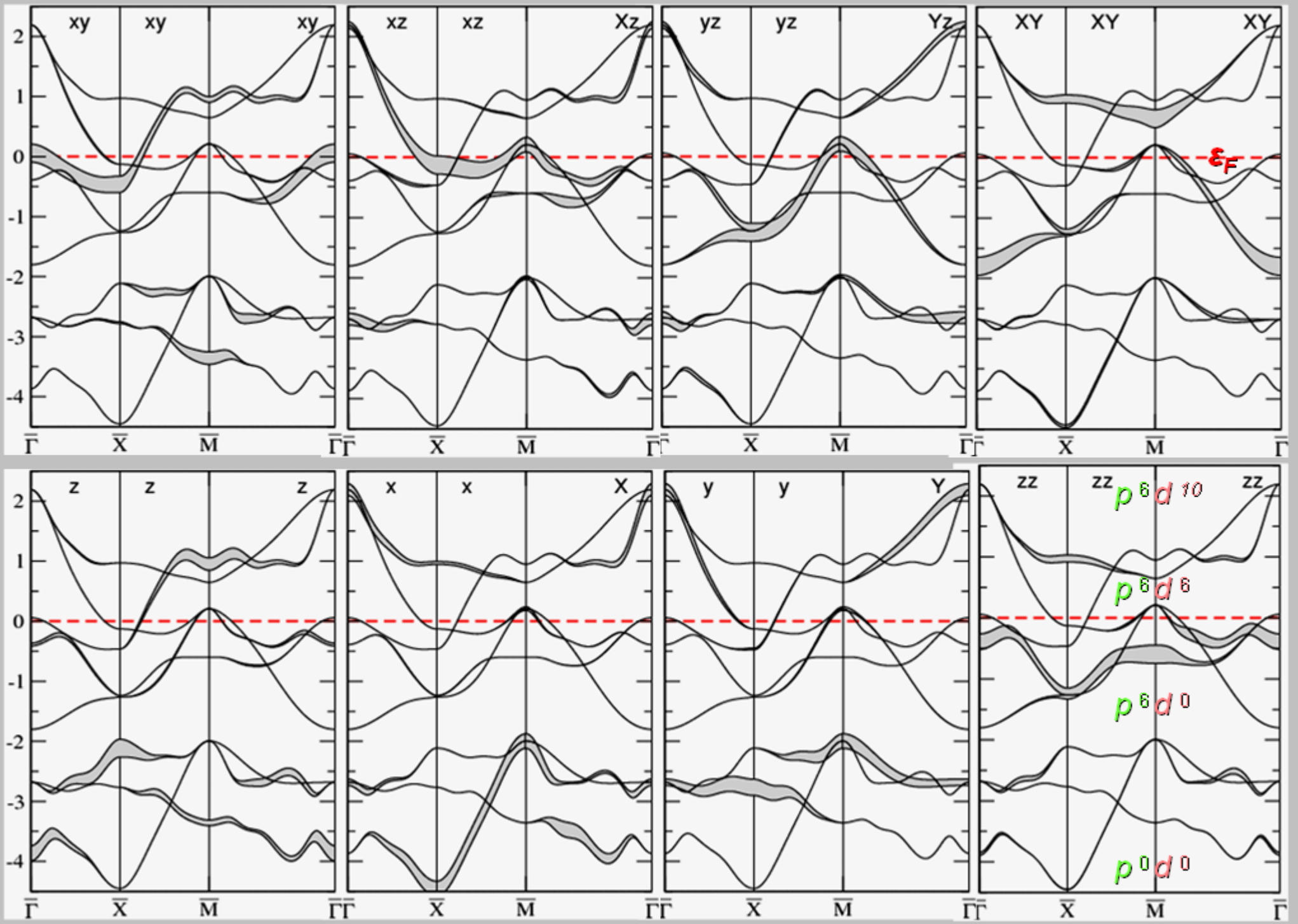
xy
xy
xy
xz
xz
Xz
yz
yz
Yz
XY
XY
XY
ε_F
z
z
z
x
x
X
y
y
Y
zz
zz
zz
$p^6 d^{10}$
$p^6 d^6$
$p^6 d^0$
$p^0 d^0$
2
1
0
-1
-2
-3
-4
$\bar{\Gamma}$
$\bar{X}$
$\bar{M}$
$\bar{\Gamma}\bar{\Gamma}$

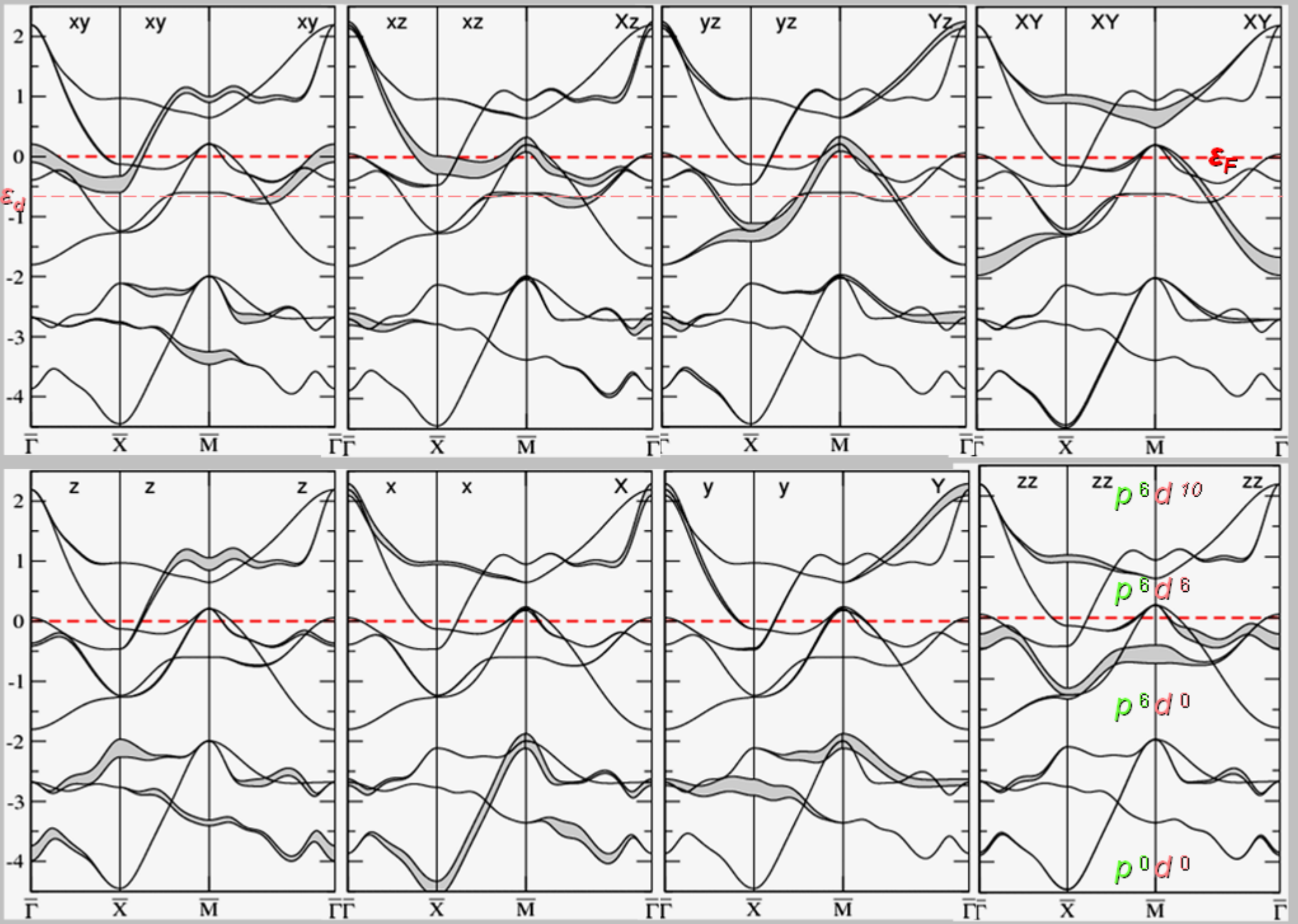
xy
xy
xy
xz
xz
Xz
yz
yz
Yz
XY
XY
XY
z
z
z
x
x
X
y
y
Y
zz
zz
zz
ε_F
ε_d
$p^6 d^{10}$
$p^6 d^6$
$p^6 d^0$
$p^0 d^0$
2
1
0
-1
-2
-3
-4
$\bar{\Gamma}$
$\bar{X}$
$\bar{M}$
$\bar{\Gamma}$

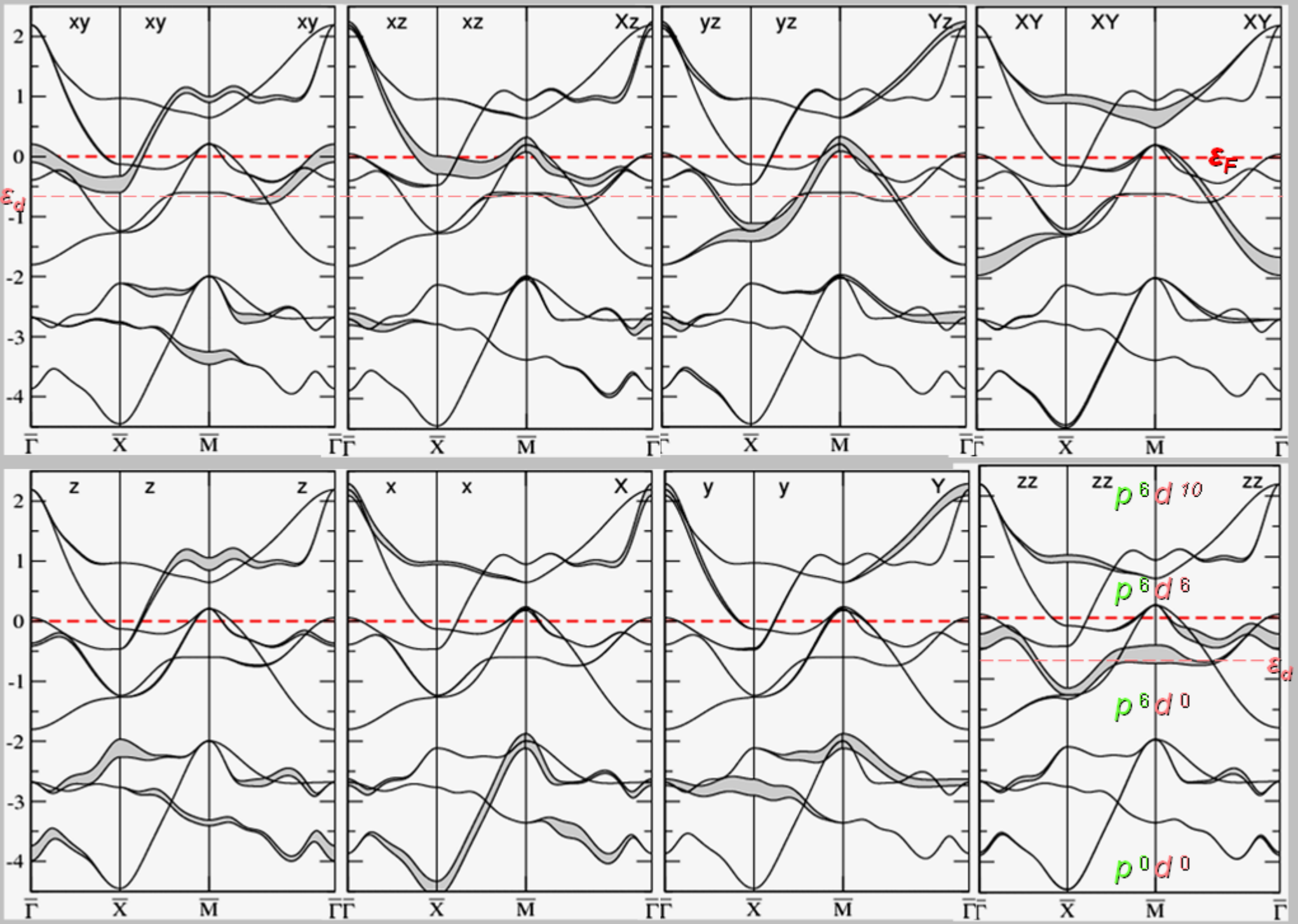
xy
xy
xy
xz
xz
Xz
yz
yz
Yz
XY
XY
XY
z
z
z
x
x
X
y
y
Y
zz
zz
zz
ε_F
ε_d
$p^6 d^{10}$
$p^6 d^6$
$p^6 d^0$
$p^0 d^0$
2
1
0
-1
-2
-3
-4
Γ̄
X̄
M̄
Γ̄

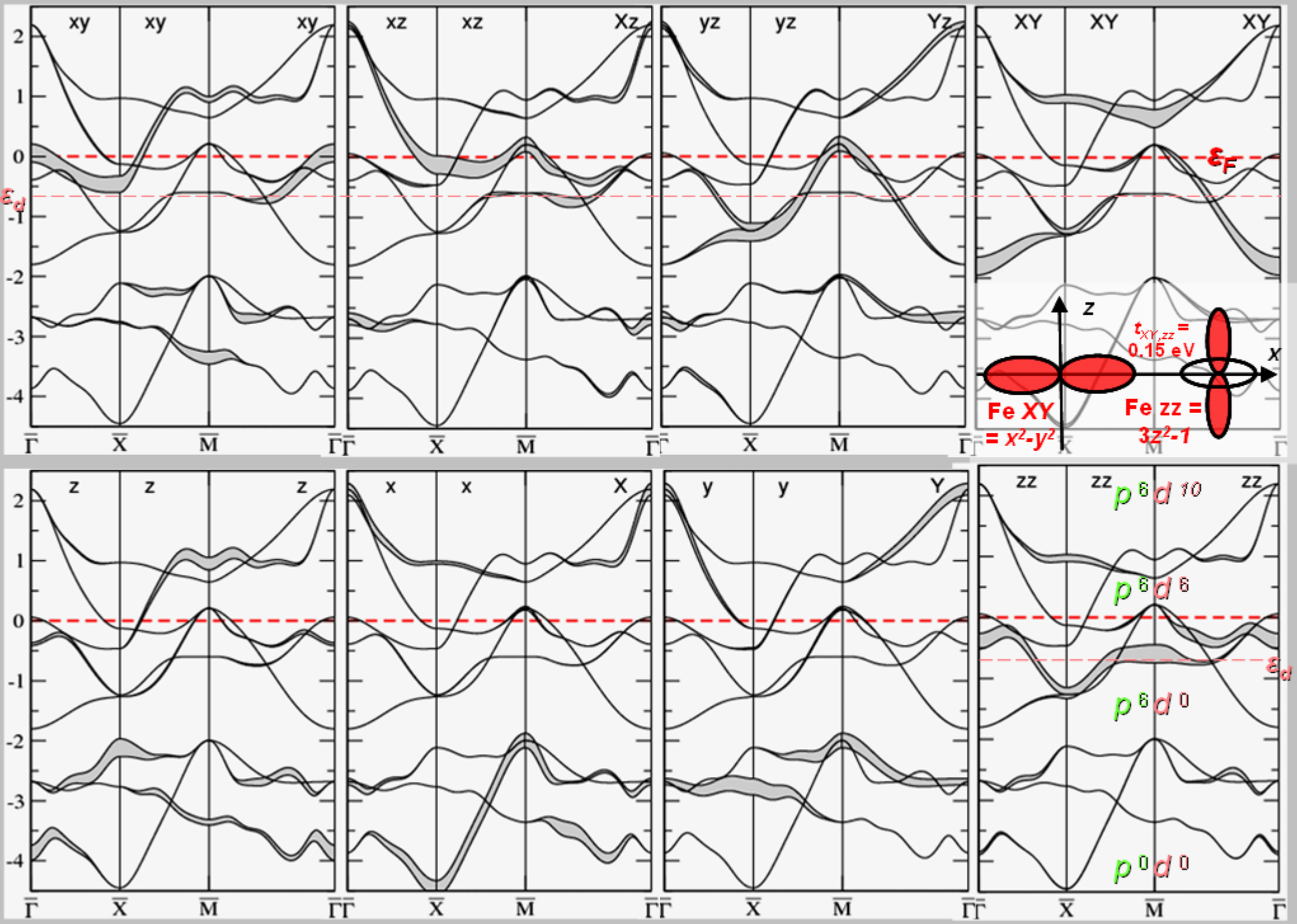
xy
xy
xy
xz
xz
Xz
yz
yz
Yz
XY
XY
XY
ε_F
ε_d
z
x
$t_{XY,zz}$ = 0.15 eV
Fe XY = x^2-y^2
Fe zz = $3z^2$-1
z
z
z
x
x
X
y
y
Y
zz
zz
zz
$p^6 d^{10}$
$p^6 d^6$
$p^6 d^0$
$p^0 d^0$
ε_d
2
1
0
-1
-2
-3
-4
$\bar{\Gamma}$
$\bar{X}$
$\bar{M}$
$\bar{\Gamma}\bar{\Gamma}$

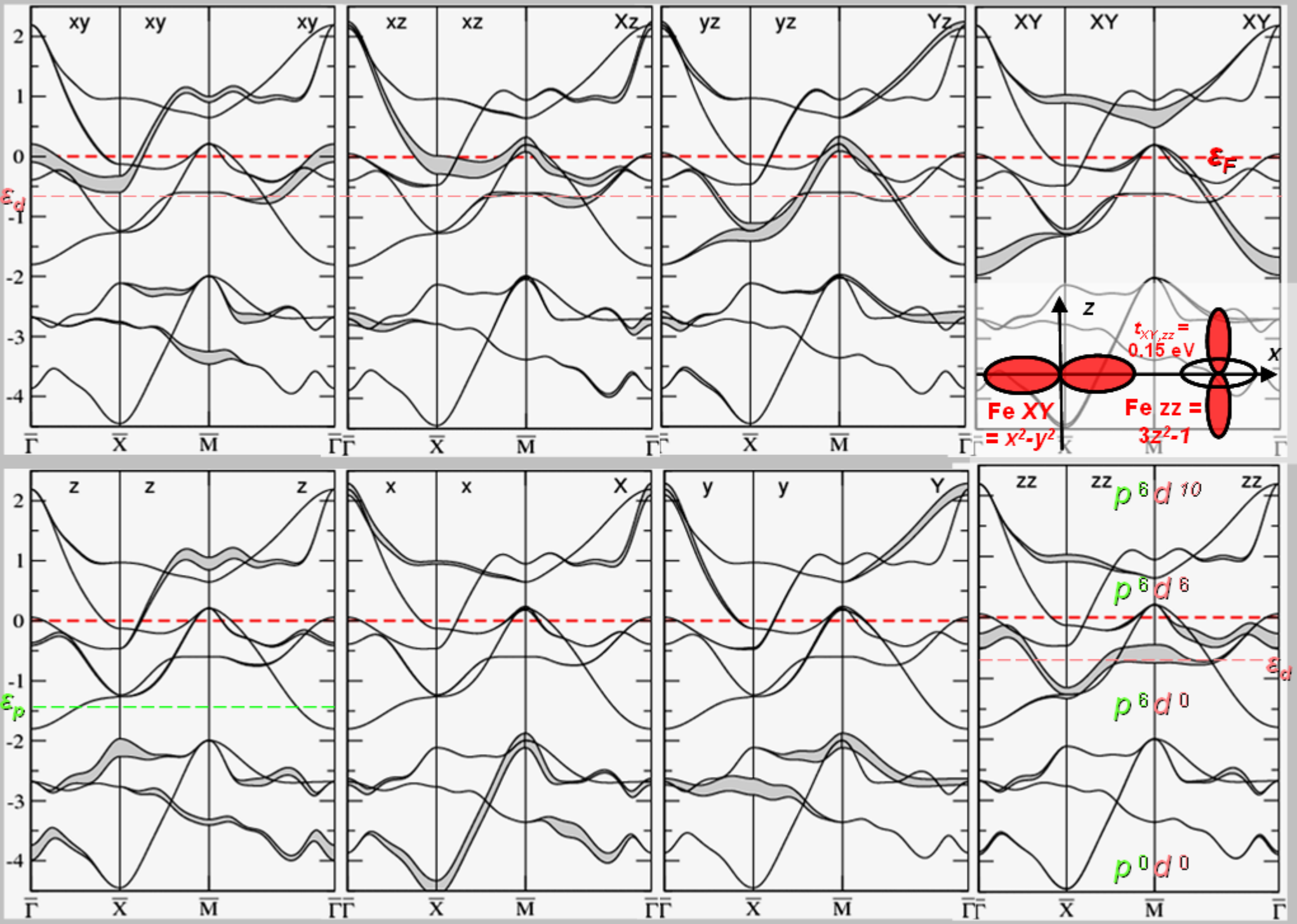
xy
xy
xy
xz
xz
Xz
yz
yz
Yz
XY
XY
XY
ε_F
ε_d
z
x
$t_{XY,zz}$ = 0.15 eV
Fe XY = x^2-y^2
Fe zz = $3z^2$-1
z
z
z
x
x
X
y
y
Y
zz
zz
zz
ε_p
ε_d
$p^6 d^{10}$
$p^6 d^6$
$p^6 d^0$
$p^0 d^0$
2
1
0
-1
-2
-3
-4
$\bar{\Gamma}$
$\bar{X}$
$\bar{M}$
$\bar{\Gamma}$

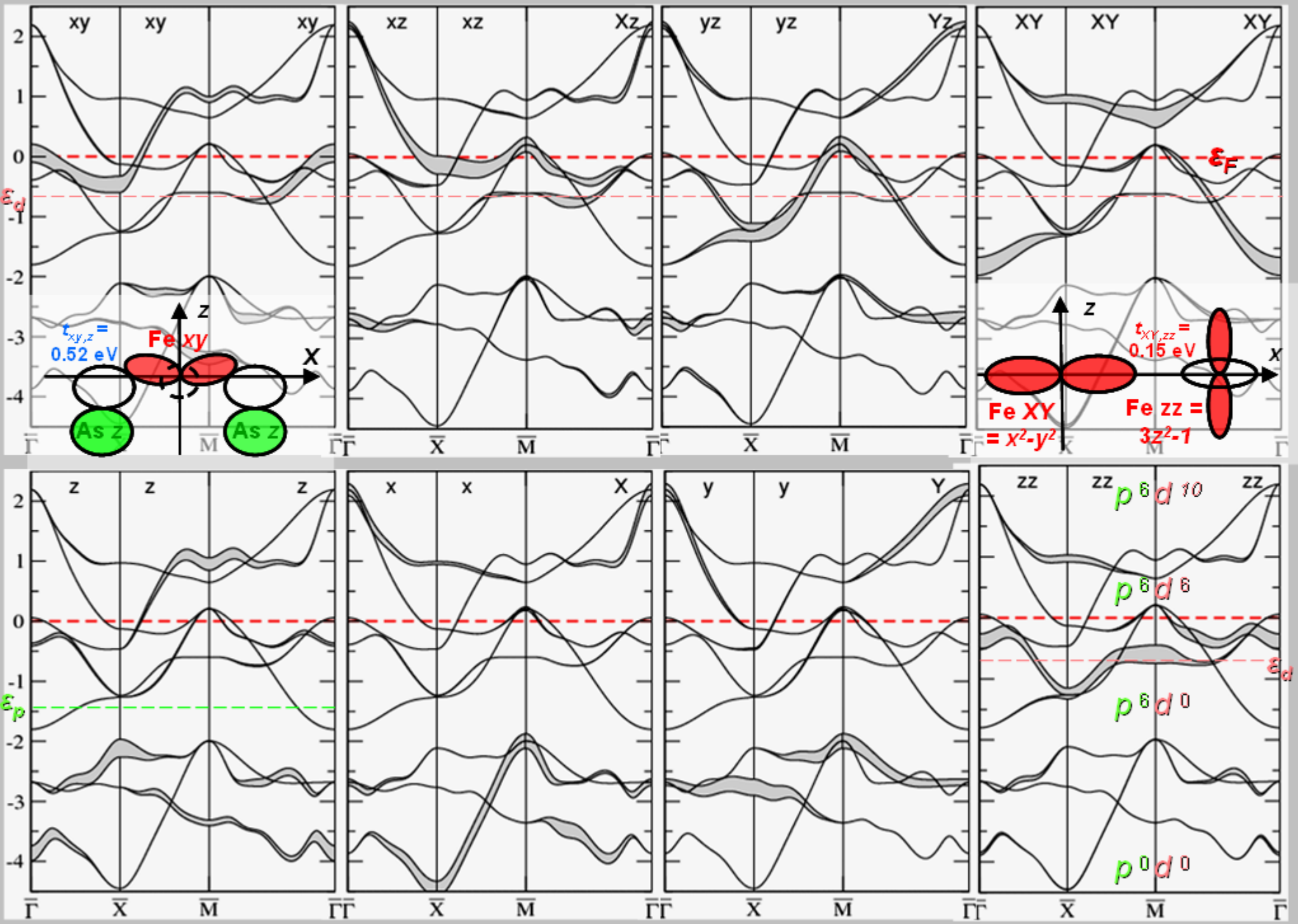
xy
xy
xy
xz
xz
Xz
yz
yz
Yz
XY
XY
XY
2
1
0
-1
-2
-3
-4
ε_d
ε_F
$t_{xy,z}$ = 0.52 eV
Fe xy
z
x
As z
As z
$t_{XY,zz}$ = 0.15 eV
Fe XY = x^2-y^2
Fe zz = $3z^2$-1
z
z
z
x
x
X
y
y
Y
zz
zz
zz
ε_p
$p^6 d^{10}$
$p^6 d^6$
$p^6 d^0$
$p^0 d^0$
Γ̄
X̄
M̄
Γ̄Γ̄

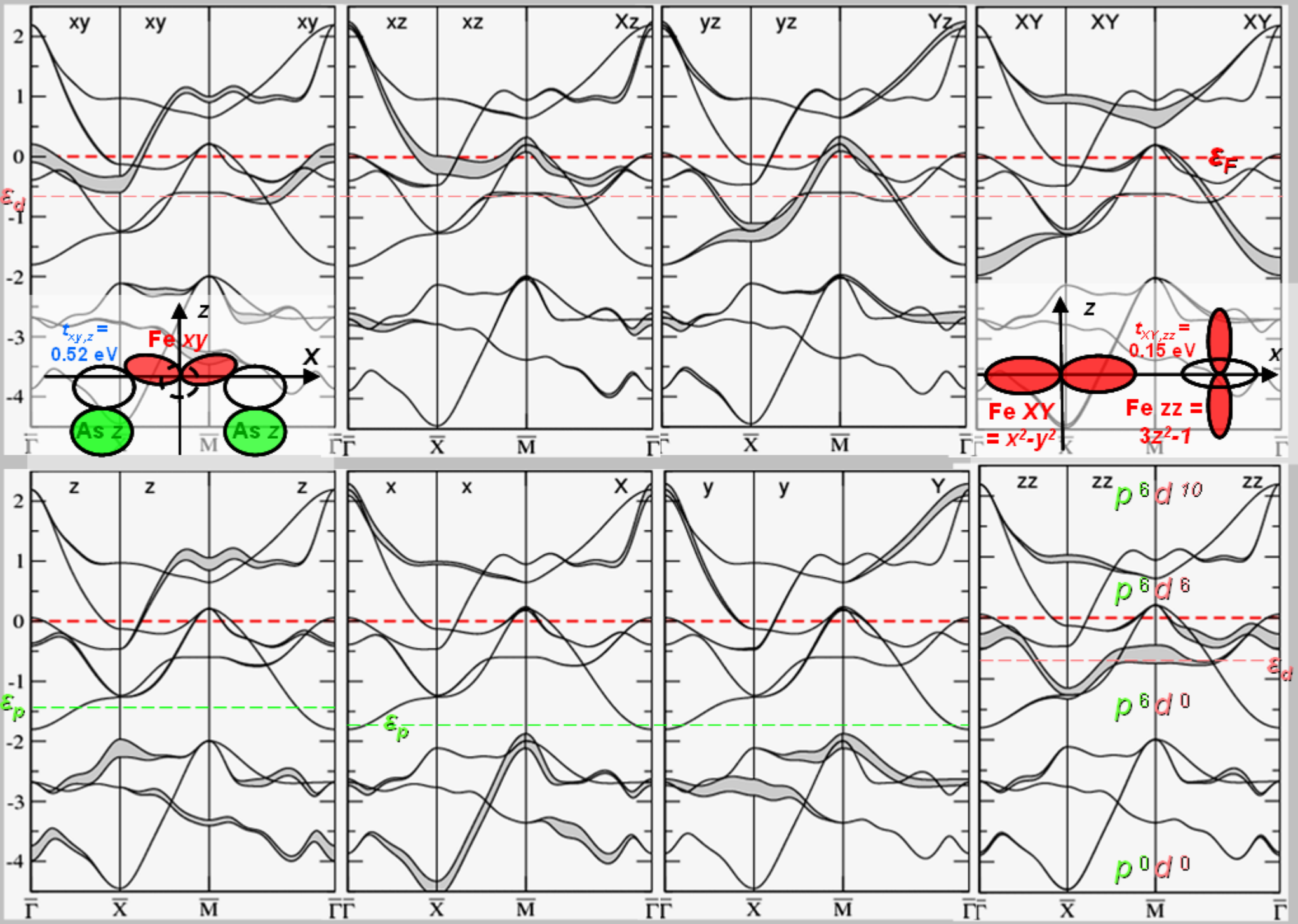
xy
xz
Xz
yz
Yz
XY
ε_F
ε_d
$t_{xy,z}$ = 0.52 eV
Fe xy
As z
As z
z
x
$t_{XY,zz}$ = 0.15 eV
Fe XY = x^2-y^2
Fe zz = $3z^2$-1
z
x
y
Y
zz
ε_p
$p^6 d^{10}$
$p^6 d^6$
$p^6 d^0$
$p^0 d^0$
Γ̄ X̄ M̄ Γ̄Γ̄

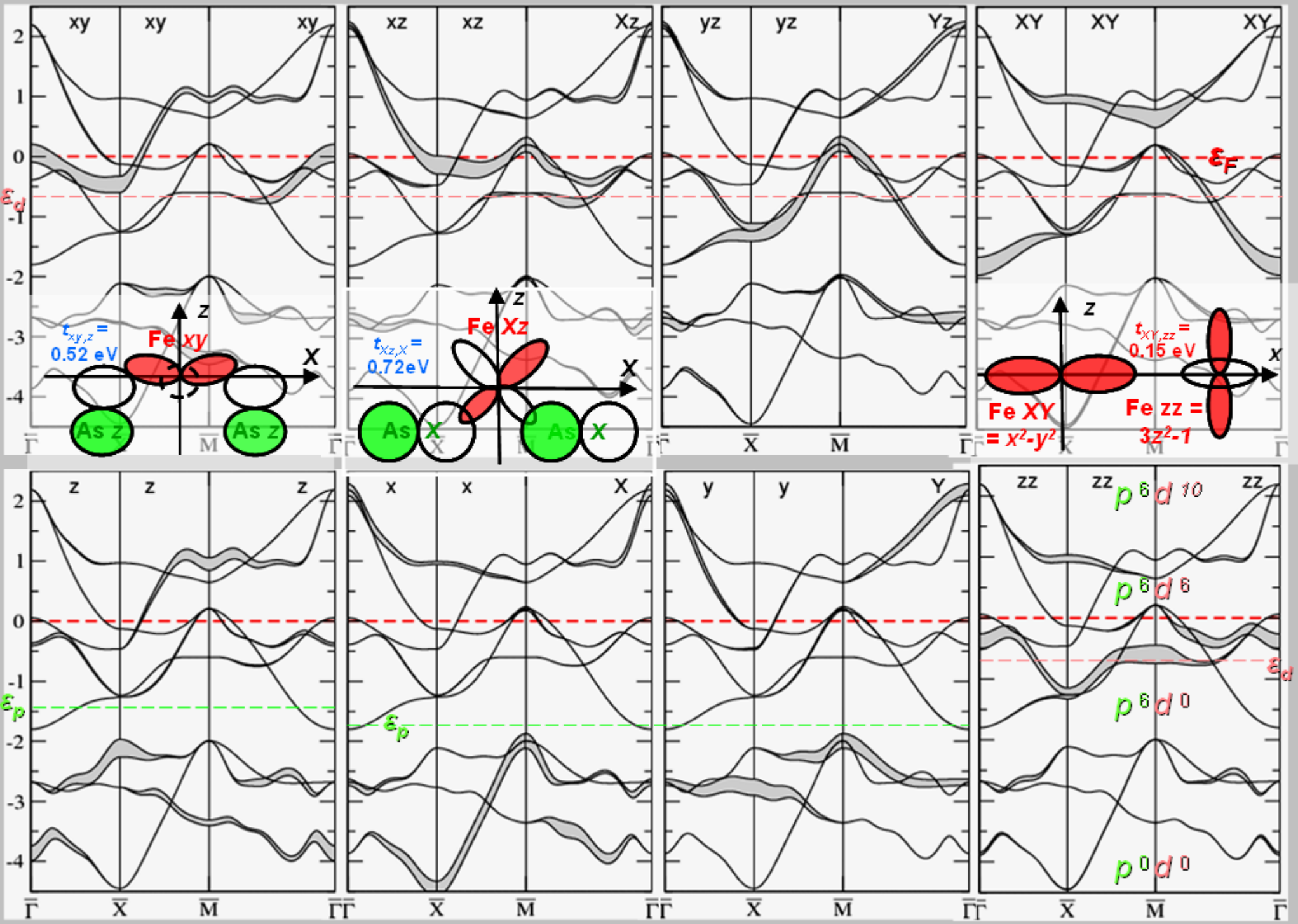
xy
xz
Xz
yz
Yz
XY
z
Fe xy
$t_{xy,z}$ = 0.52 eV
As z
Fe Xz
$t_{Xz,X}$ = 0.72eV
As
X
ε_F
ε_d
Fe XY = x^2-y^2
$t_{XY,zz}$ = 0.15 eV
Fe zz = $3z^2$-1
z
x
y
Y
zz
ε_p
$p^6 d^{10}$
$p^6 d^6$
$p^6 d^0$
$p^0 d^0$
Γ̄
X̄
M̄

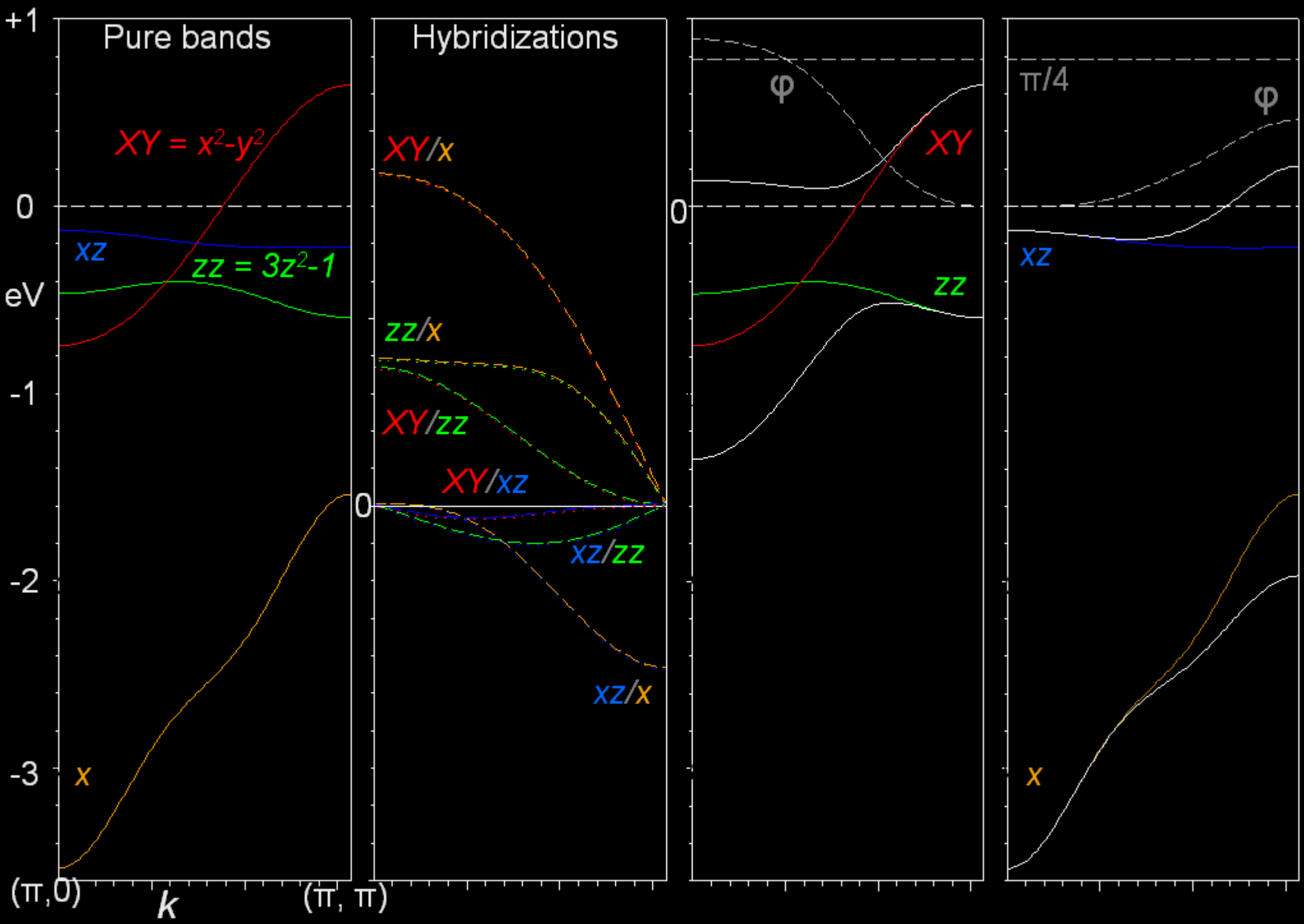
Pure bands
Hybridizations
+1
0
-1
-2
-3
eV
XY = x²-y²
xz
zz = 3z²-1
x
XY/x
zz/x
XY/zz
XY/xz
xz/zz
xz/x
φ
XY
zz
π/4
(π,0)
k
(π, π)

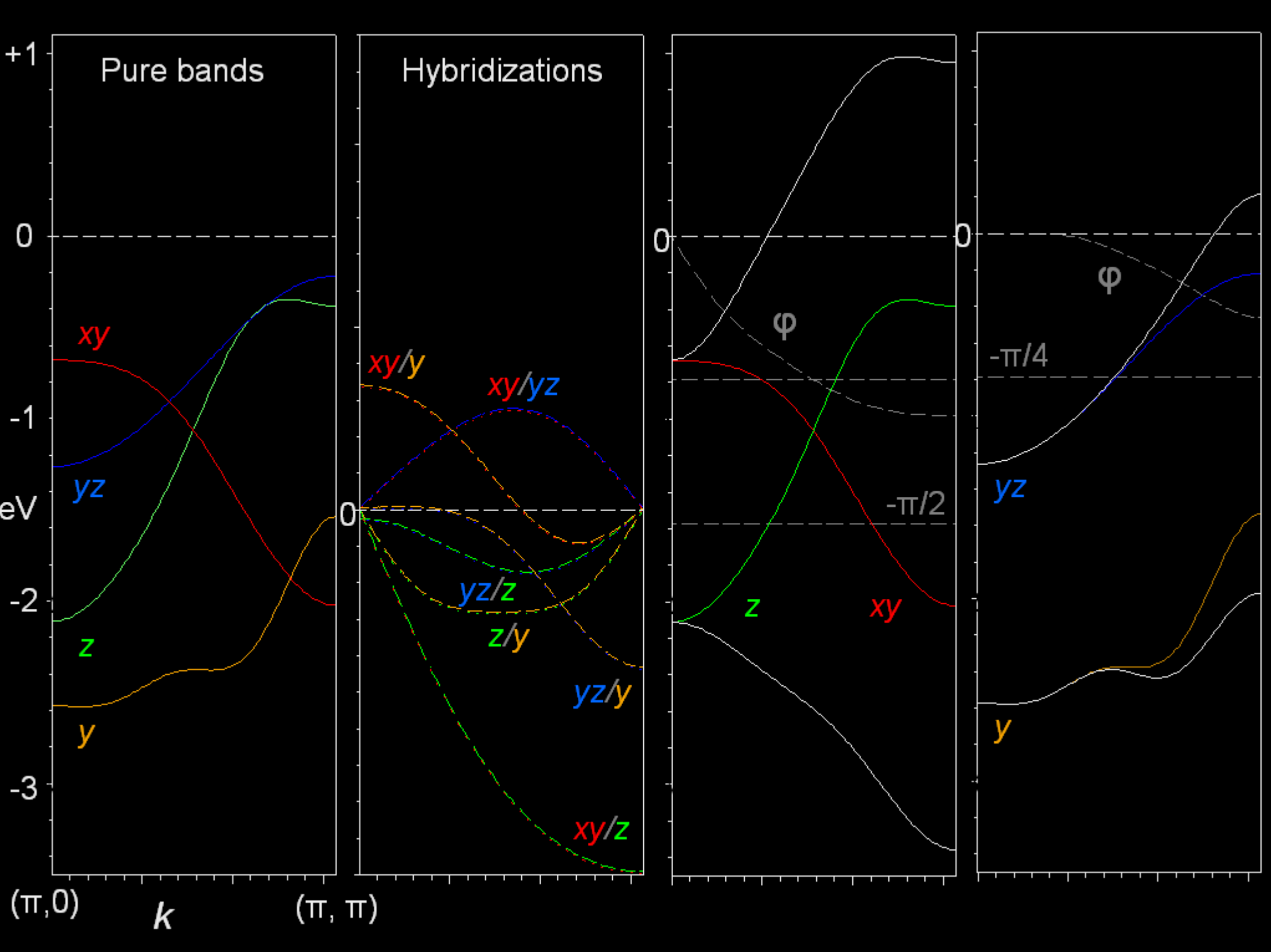
Pure bands
Hybridizations
+1
0
-1
-2
-3
eV
xy
yz
z
y
xy/y
xy/yz
yz/z
z/y
yz/y
xy/z
φ
-π/4
-π/2
(π,0)
k
(π, π)

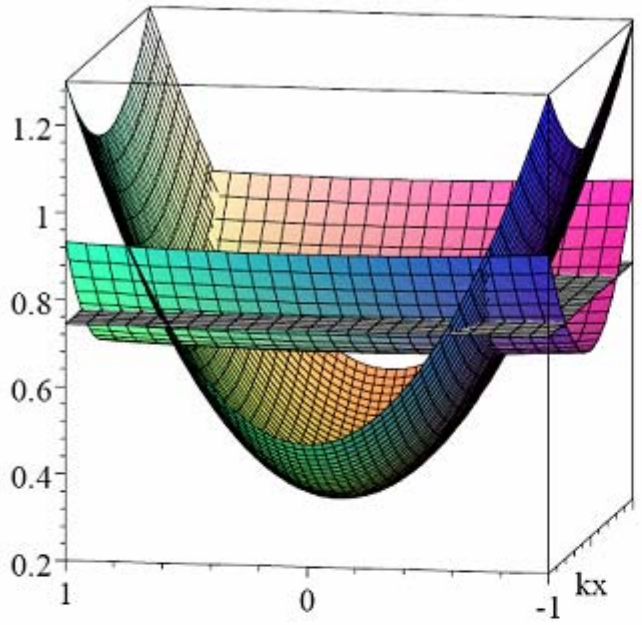

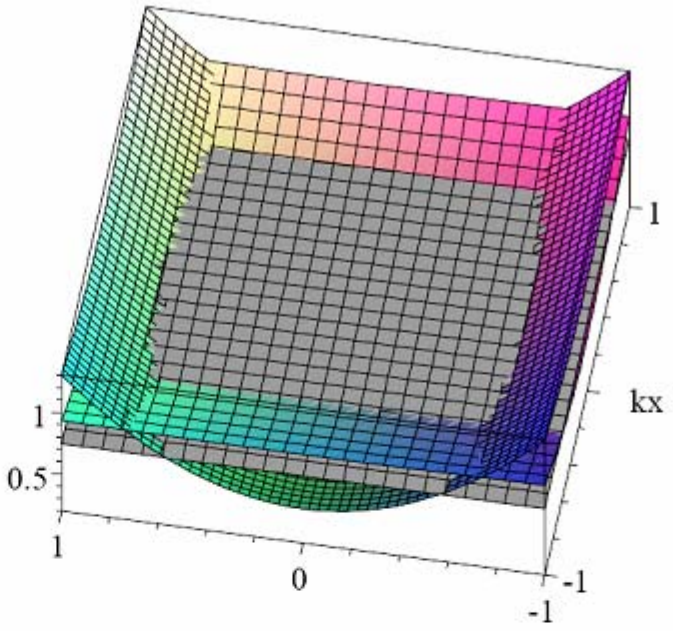

Non-hybridized *xy*-*z* and *xz*-*y* like bands near X

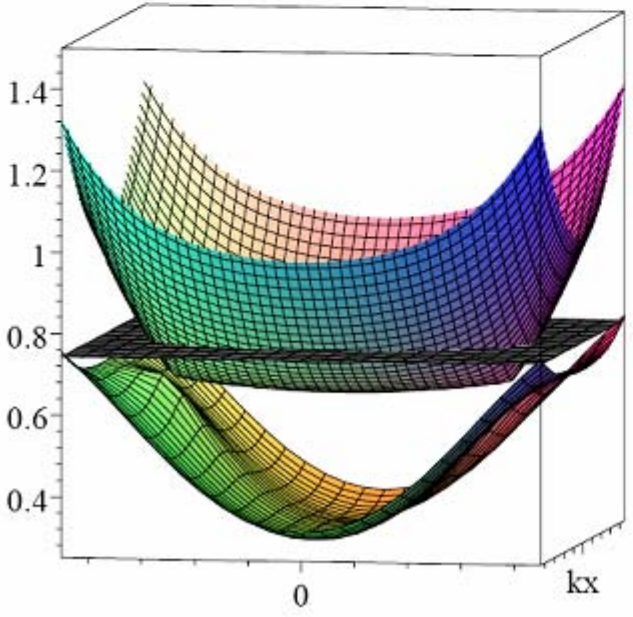

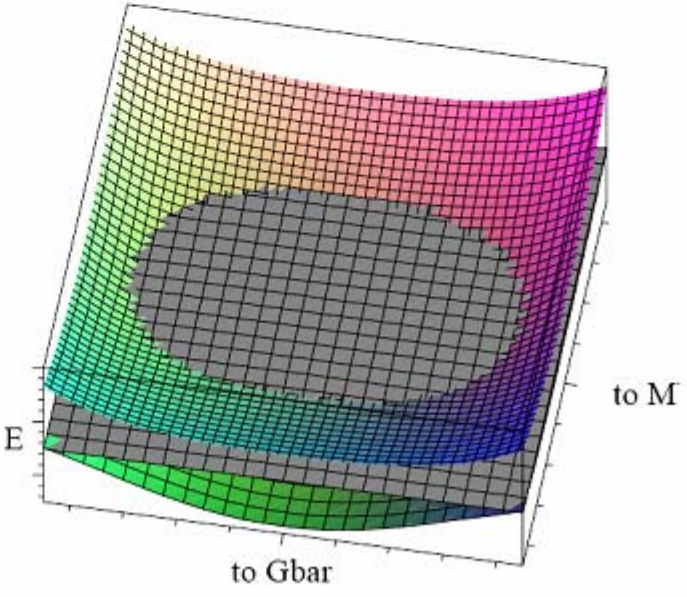

Hybridized *xy*-*z* and *xz*-*y* like bands near X

This super-ellipsoidal electron pocket points towards the doubly degenerate hole pockets at M

1/5 ×

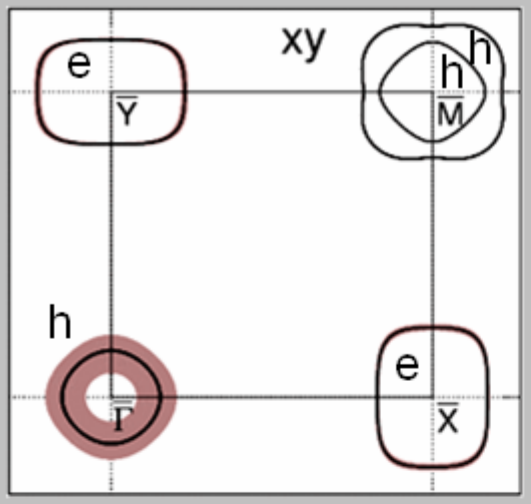
xy
e
h
h
h
e
Y
M
Γ
X

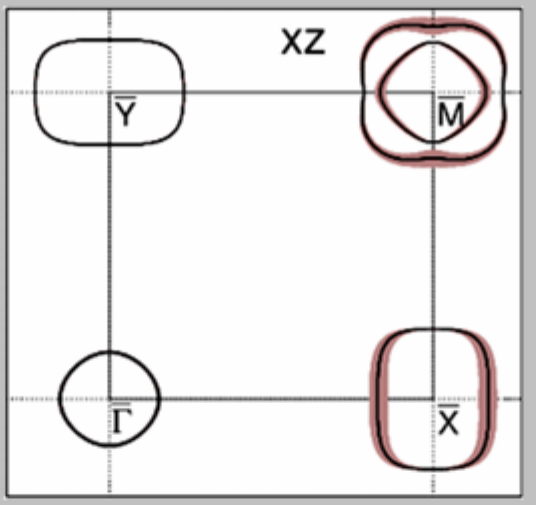
xz
Y
M
Γ
X

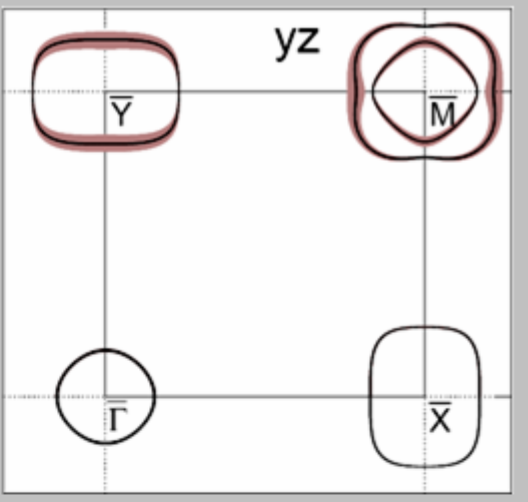
yz
Y
M
Γ
X

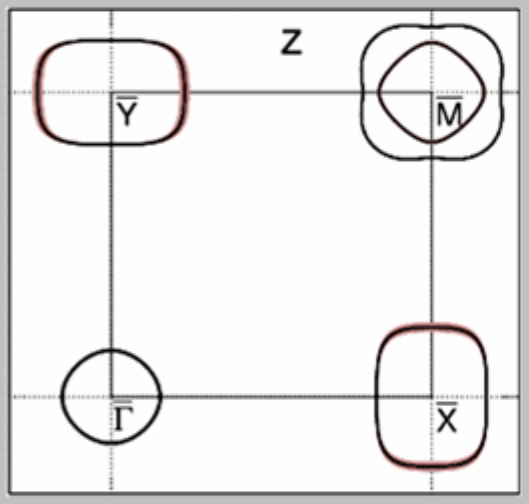
z
Y
M
Γ
X

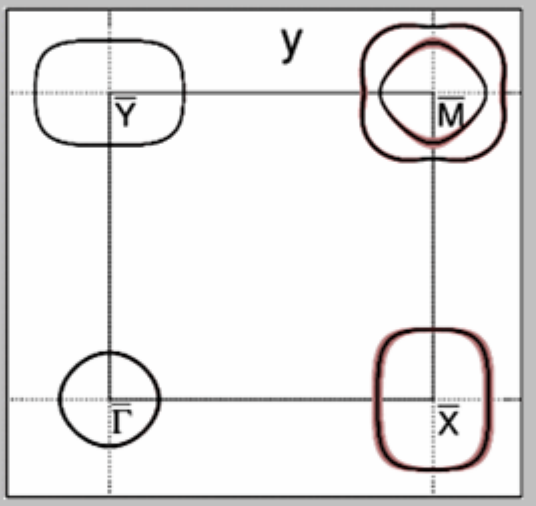
y
Y
M
Γ
X

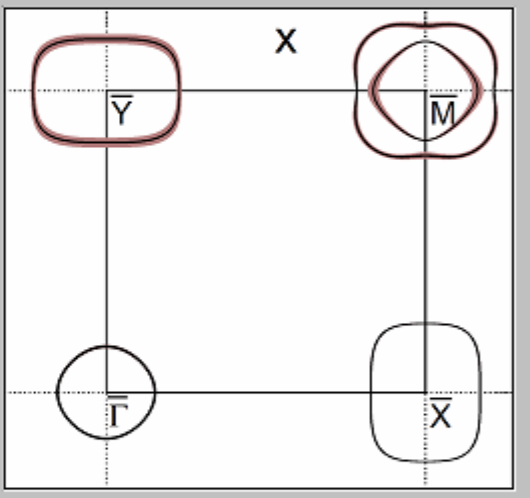
x
Y
M
Γ
X

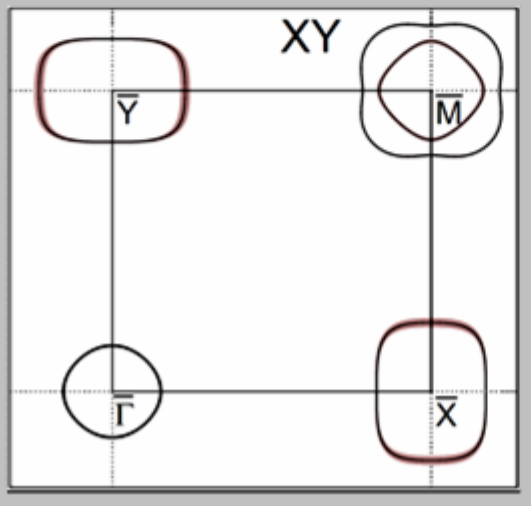
XY
Y
M
Γ
X

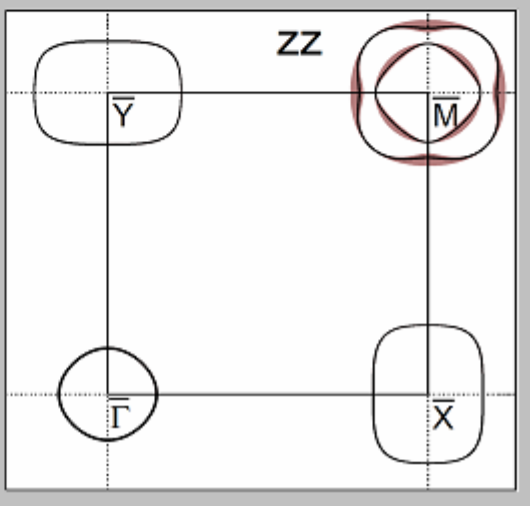
zz
Y
M
Γ
X

One reason for the small mass (~1m_0) of the inner, M-centered hole pocket

Hybridized *Xz*-*X* band

Pure *Xz* band
thin line: (1,0) hops only

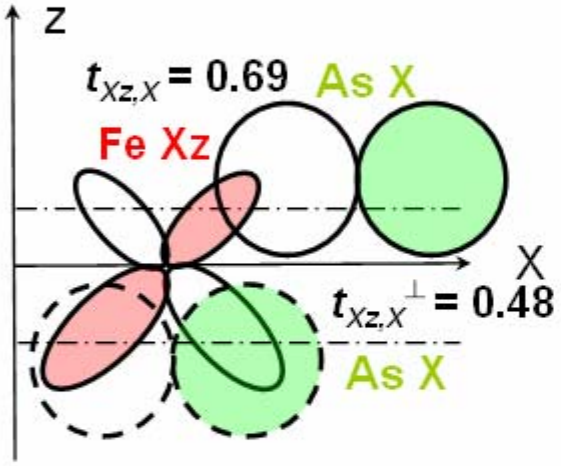

Xz-*X* hybridization (- abs. value)
dashed line: (½,½) hops only

Pure *X* band
dotted line: (1,0) and (1,1) hops only

For the small band mass (~1m_0) of the Fe *d*-like hole pockets, the long range of the As *p* - Fe *d* hybridization is crucial.

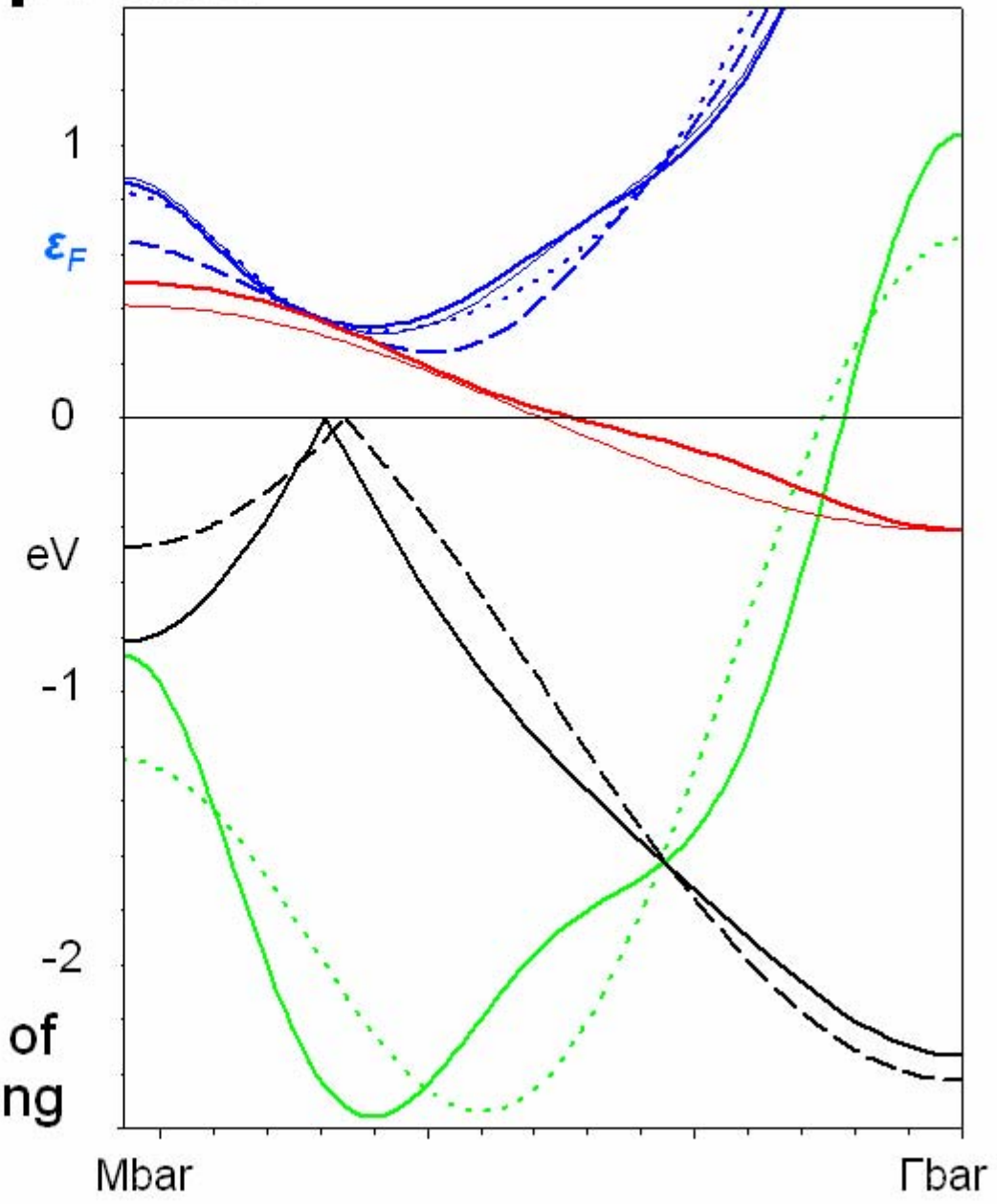

Another -more interesting- reason, causing the materials' trend

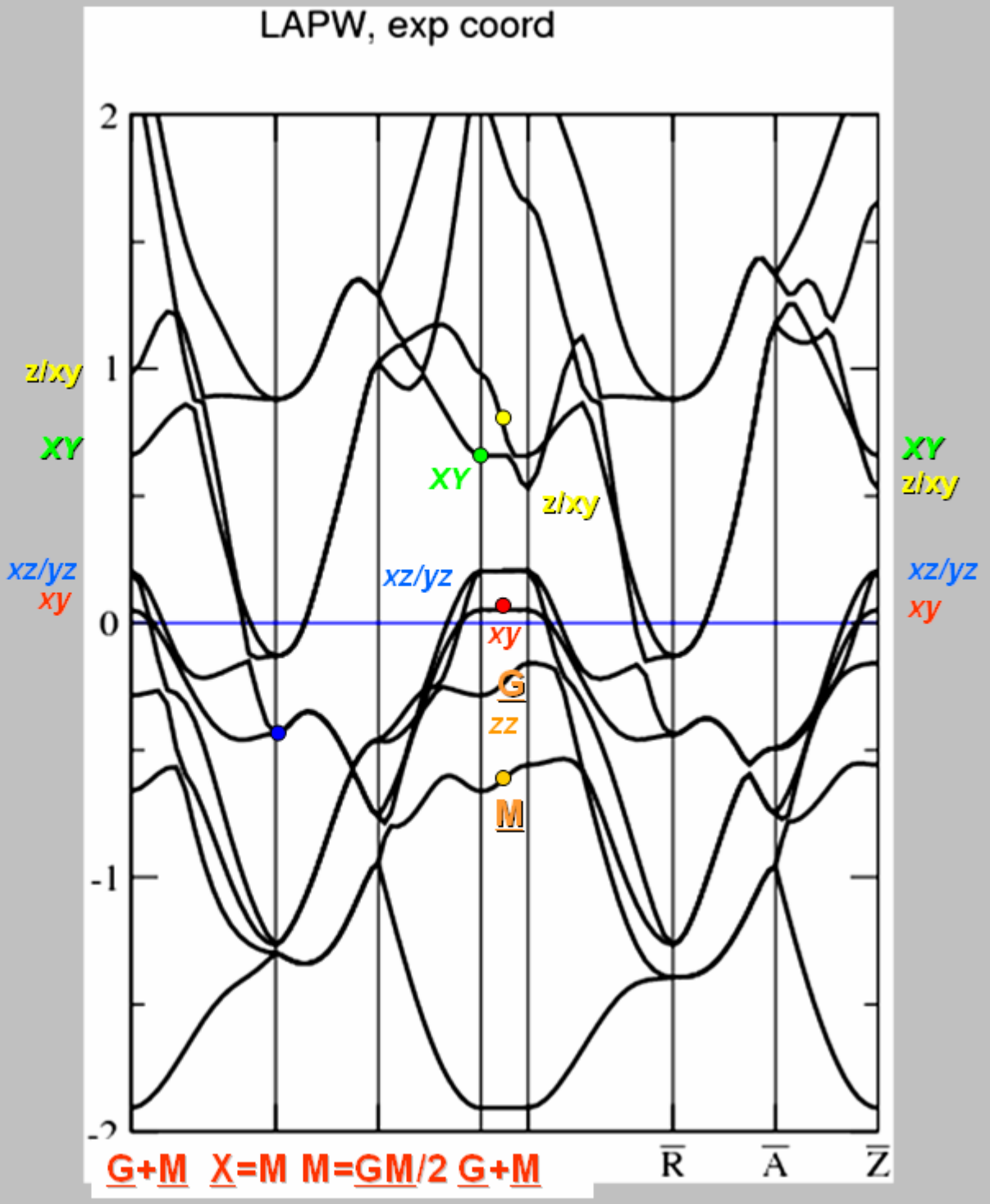

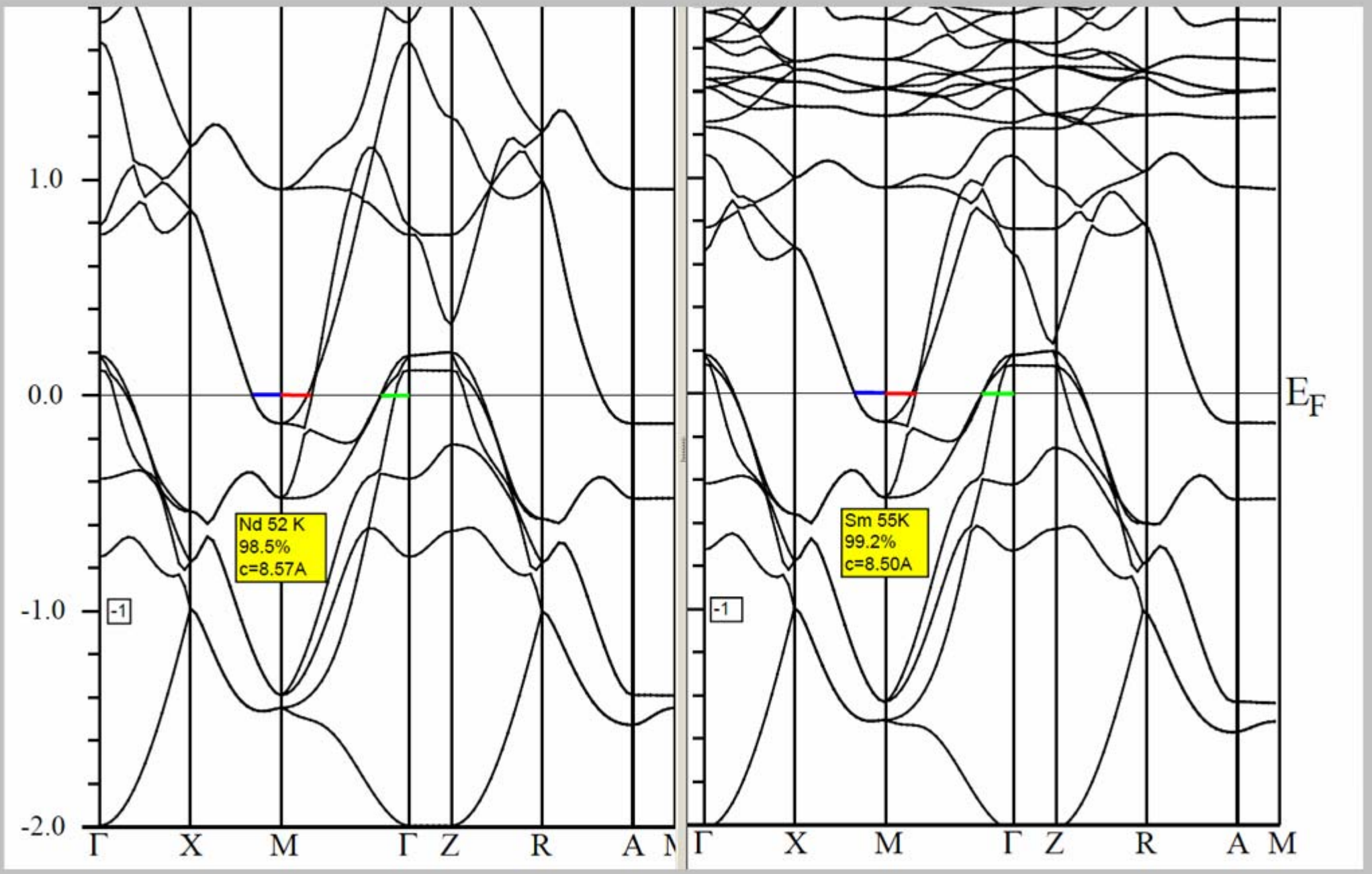
NdOFeAs
SmOFeAs
1.0
0.0
-1.0
-2.0
Nd 52 K
98.5%
c=8.57A
Sm 55K
99.2%
c=8.50A
-1
-1
Γ X M Γ Z R A M
Γ X M Γ Z R A M
E_F

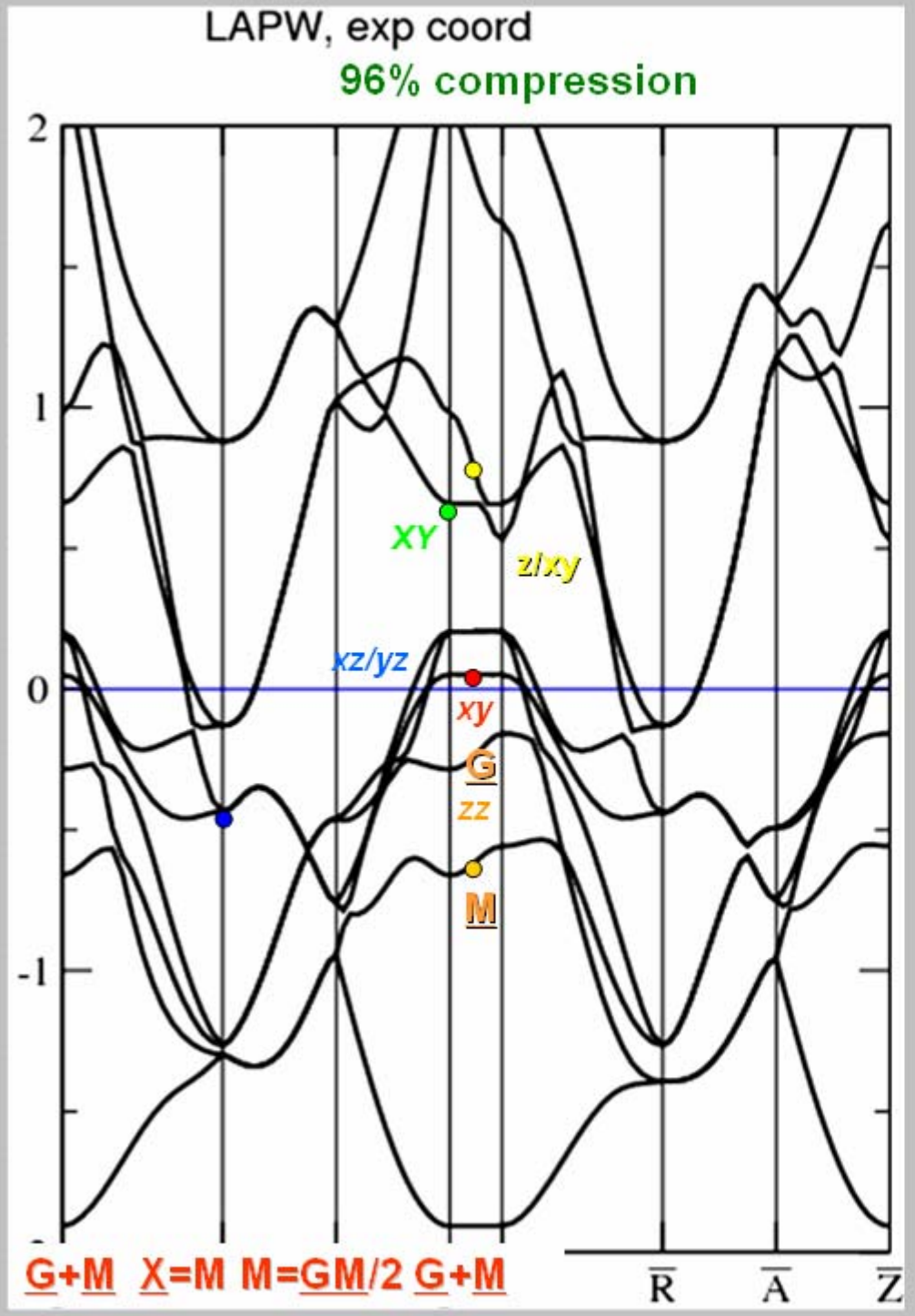
LAPW, exp coord
96% compression
2
1
0
-1
XY
z/xy
xz/yz
xy
G
zz
M
G+M X=M M=GM/2 G+M
R
A
Z

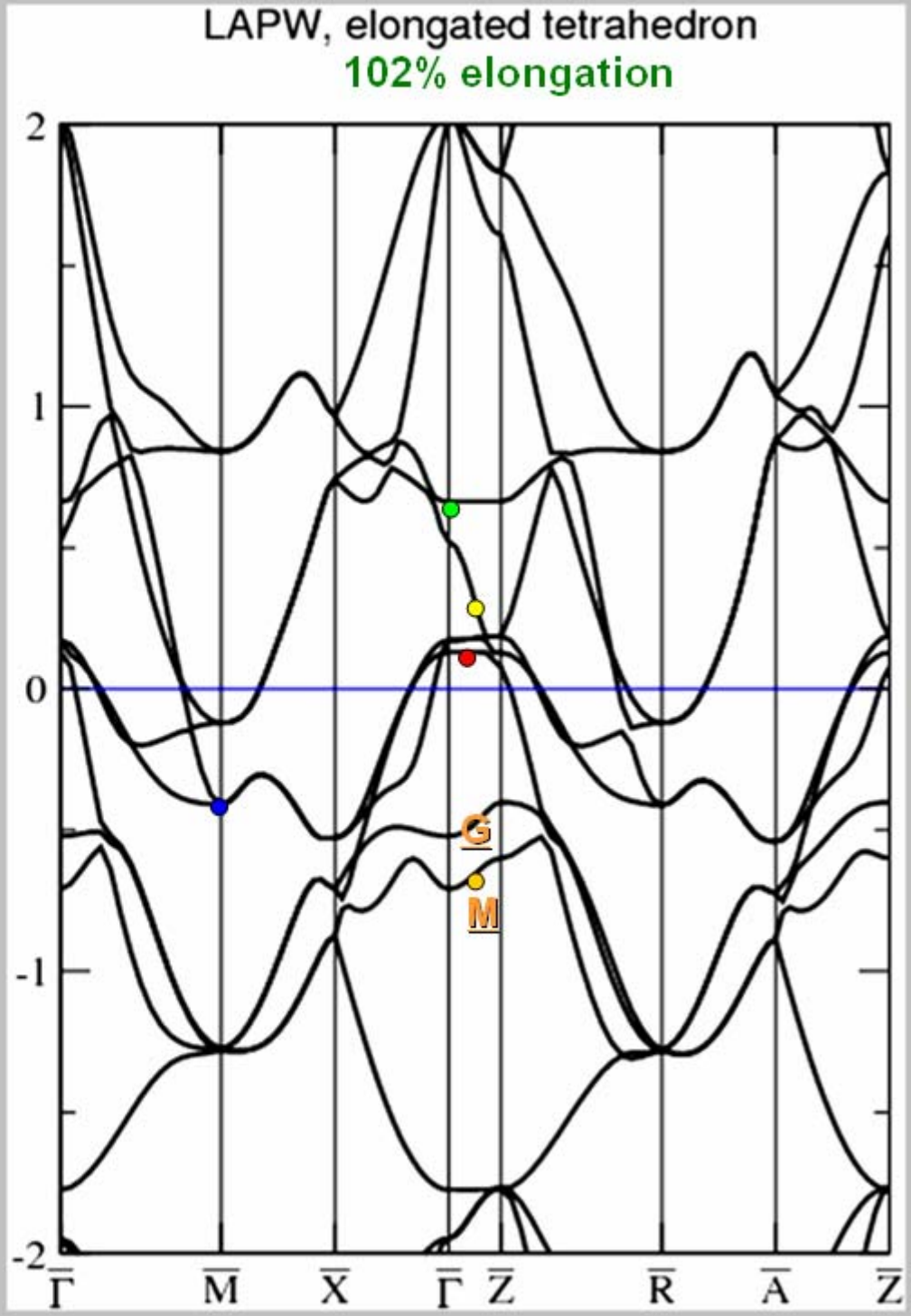
LAPW, elongated tetrahedron
102% elongation
2
1
0
-1
-2
G
M
Γ
M
X
Γ
Z
R
A
Z

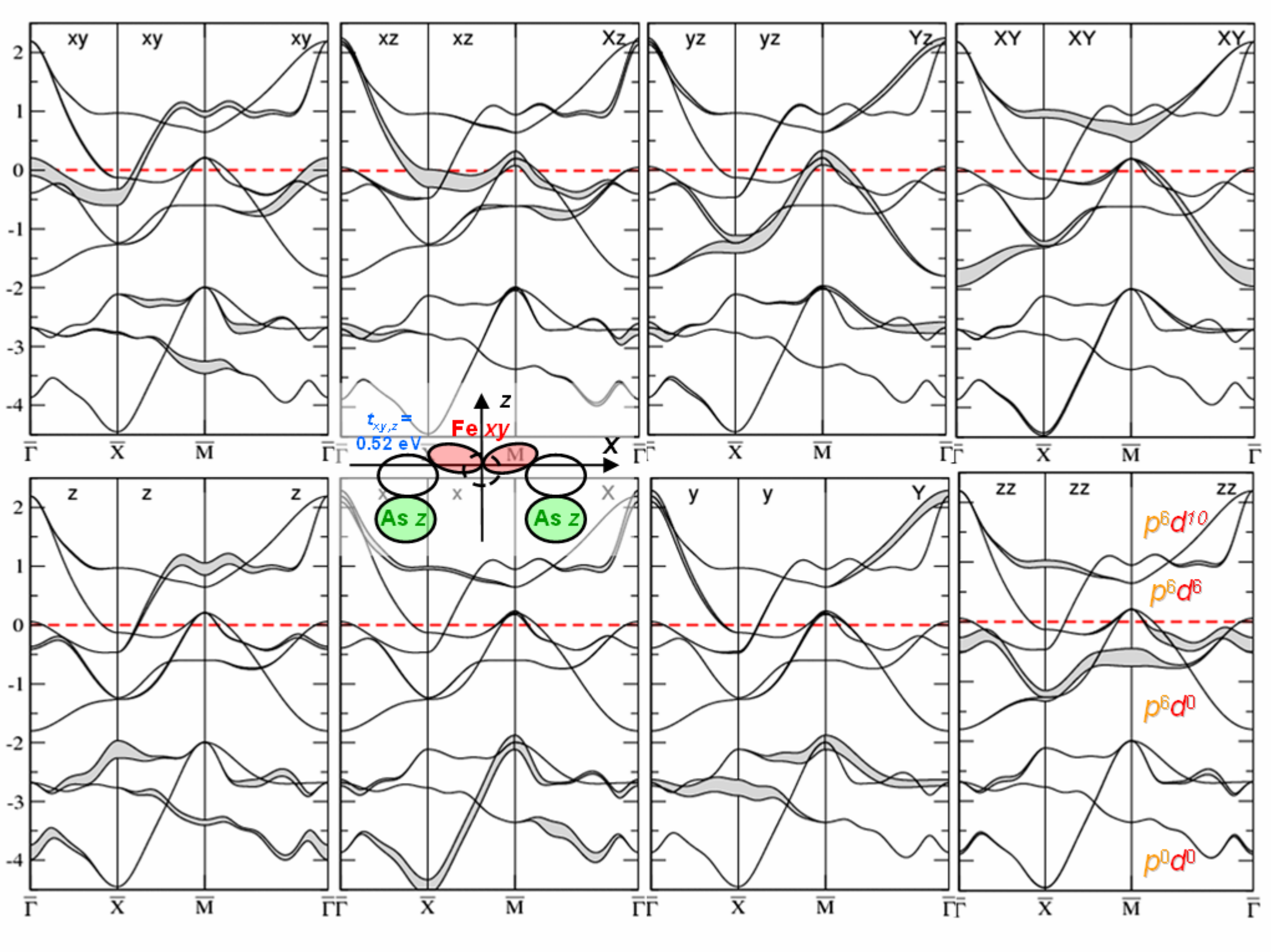
xy
xy
xy
xz
xz
Xz
yz
yz
Yz
XY
XY
XY
z
z
z
y
y
Y
zz
zz
zz
2
1
0
-1
-2
-3
-4
Γ̄
X̄
M̄
Γ̄Γ̄
$t_{xy,z}$ =
0.52 eV
Fe xy
z
X
M
As z
As z
p^6d^{10}
p^6d^6
p^6d^0
p^0d^0

Hybridized *xz/yz*-like hole bands near M

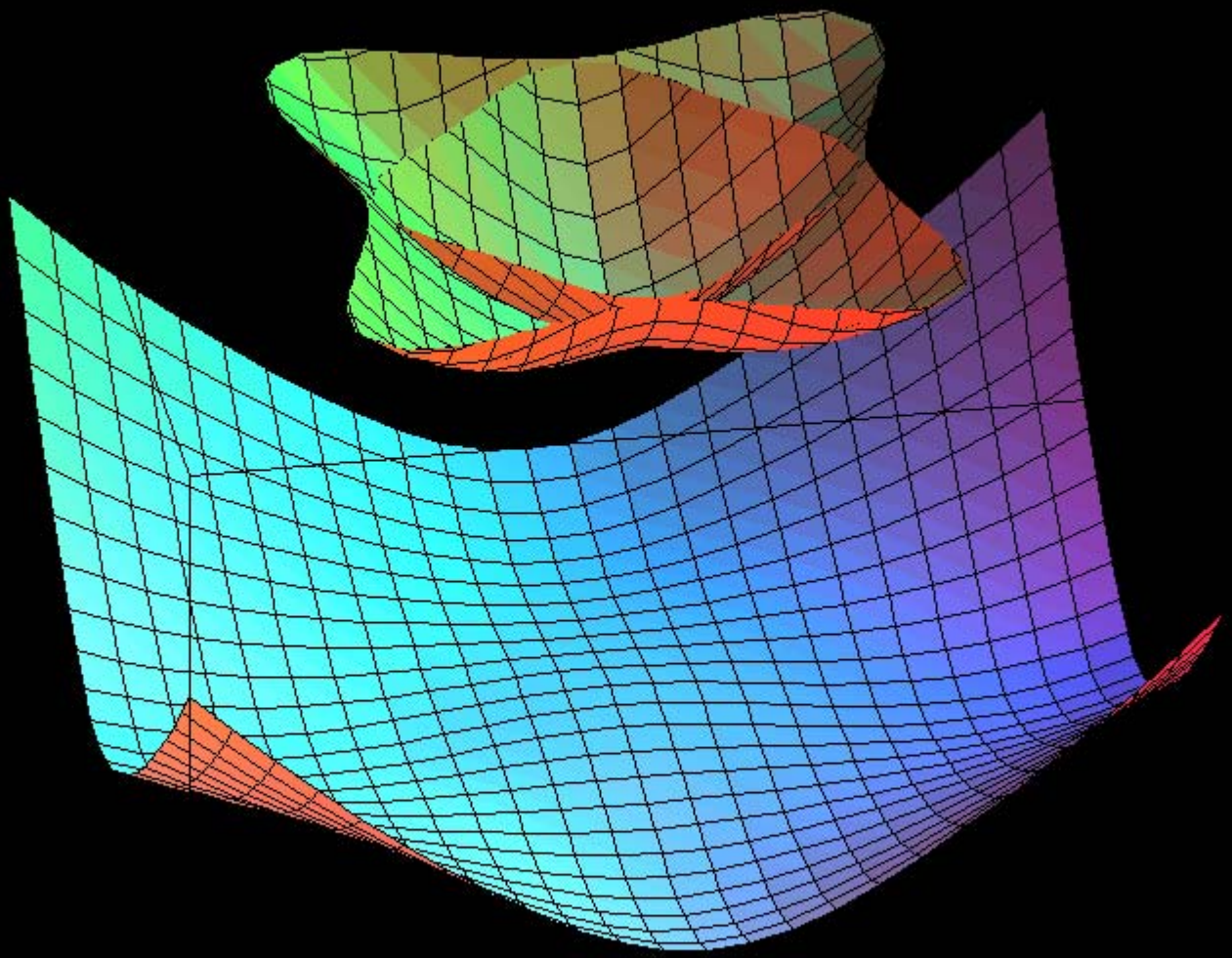

Antibonding *z/xy* band

Hybridized *xz*/*yz*-like
hole bands near M

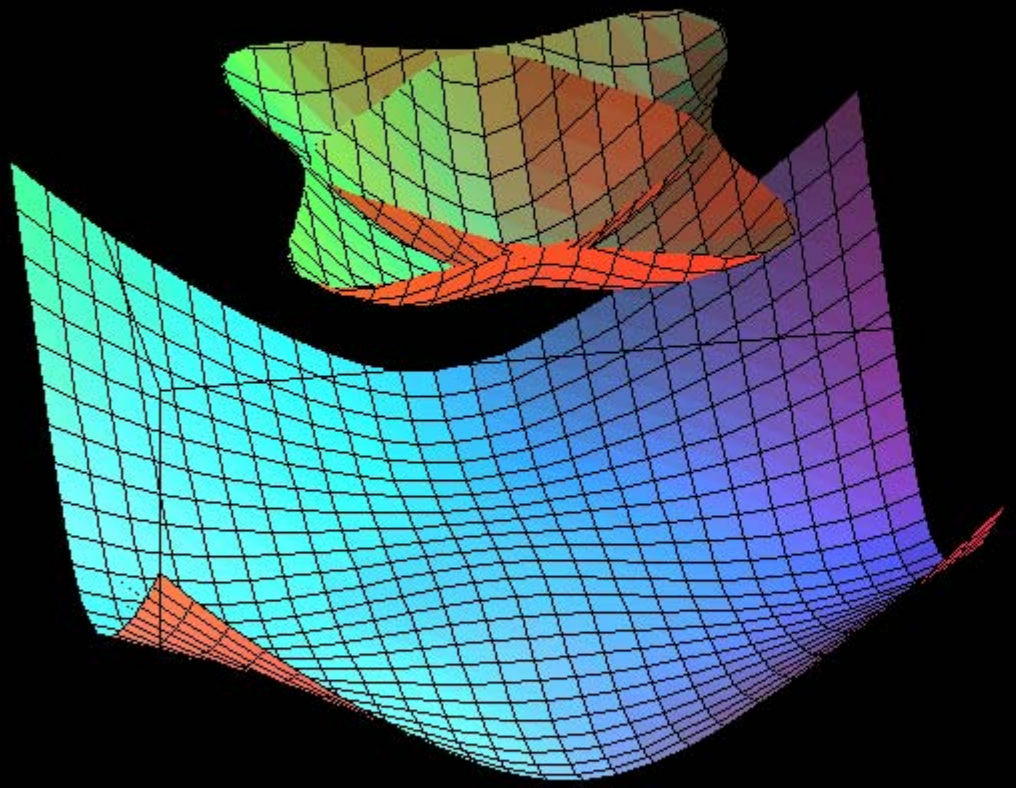

Hybridized *xz/yz*-like hole bands near M

The *z/xy* band cannot hybridize with *xz/yz* at M. But it can away from M, where the hybridization increases linearly with $k_{=}$.

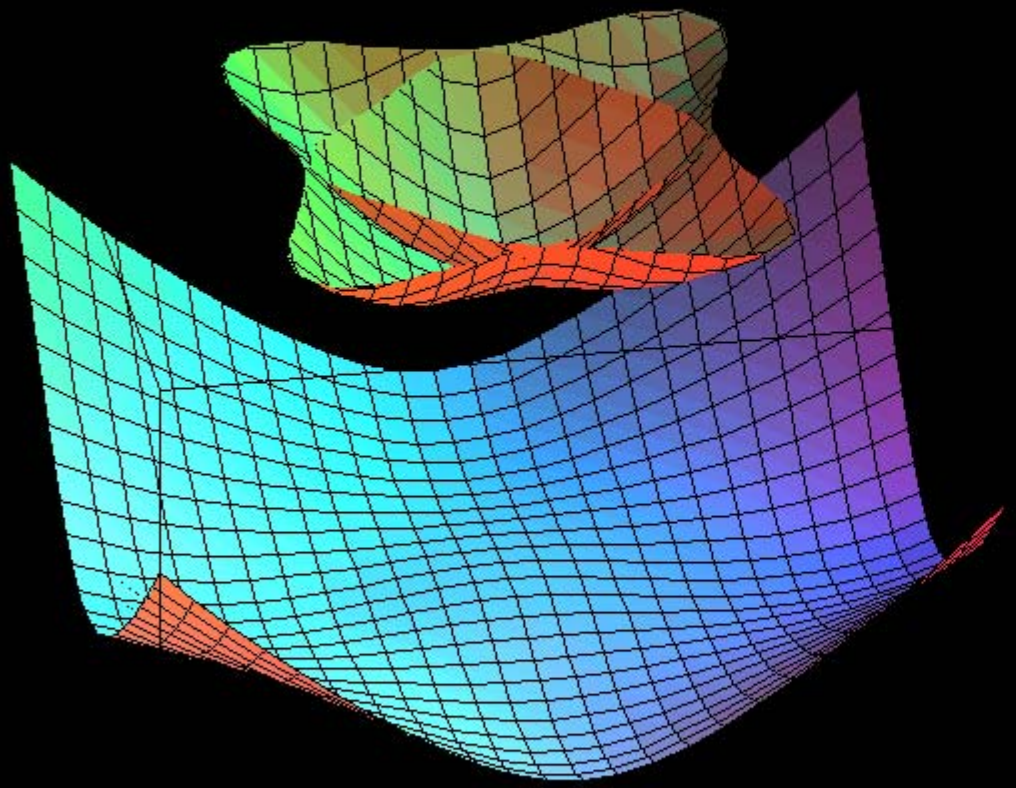

Hybridized *xz/yz*-like hole bands near M

The *z/xy* band cannot hybridize with *xz/yz* at M. But it can away from M, where the hybridization increases linearly with $k_{=}$.

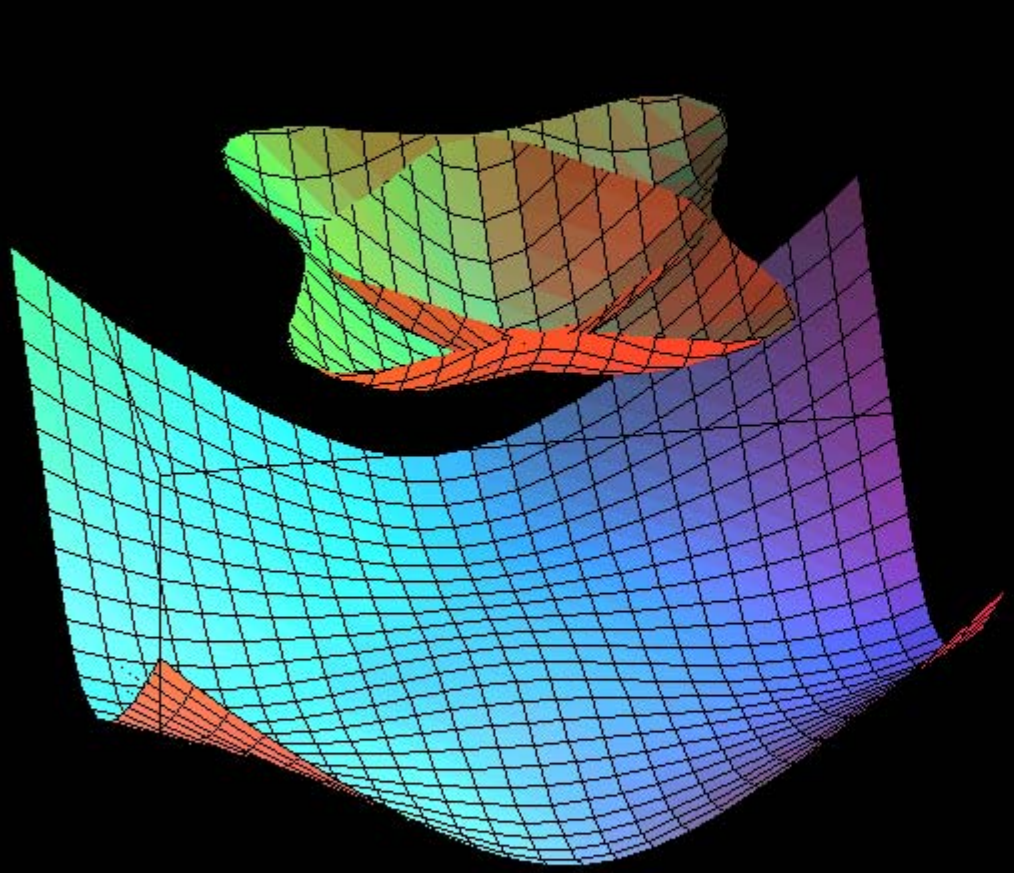

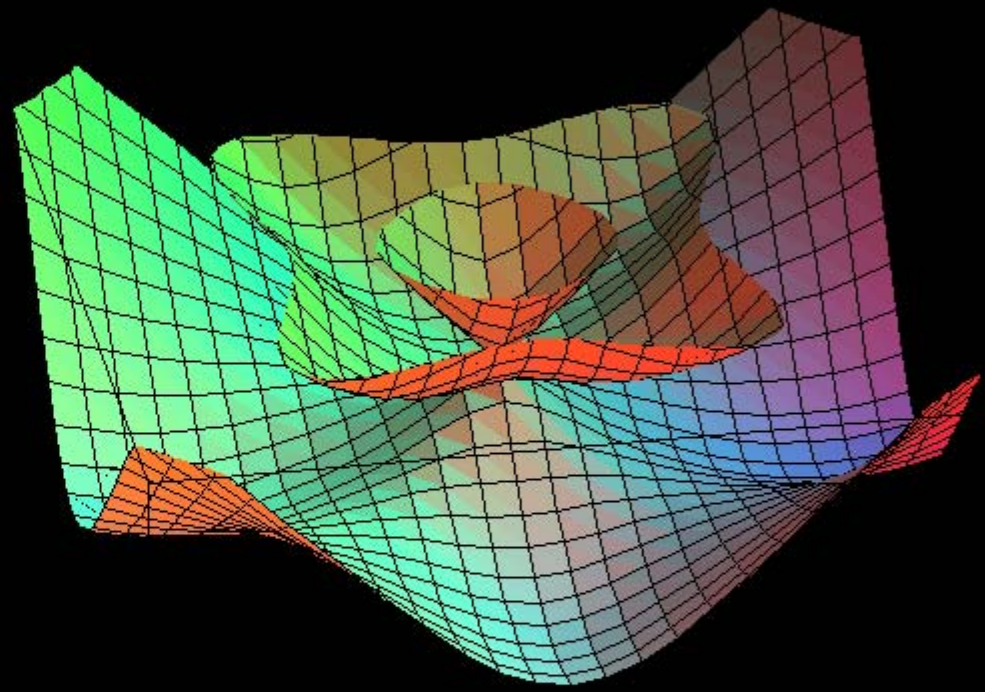

Hybridized *xz/yz*-like hole bands near M

The *z/xy* band cannot hybridize with *xz/yz* at M. But it can away from M, where the hybridization increases linearly with $k_=$.

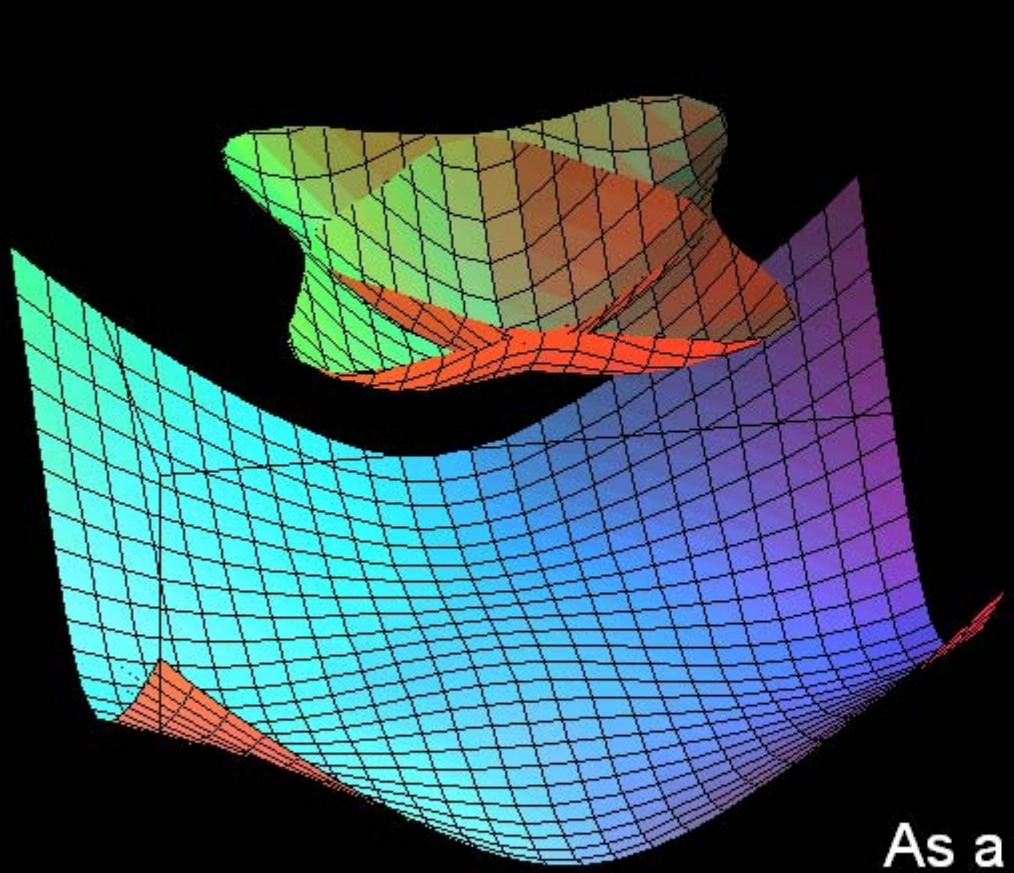

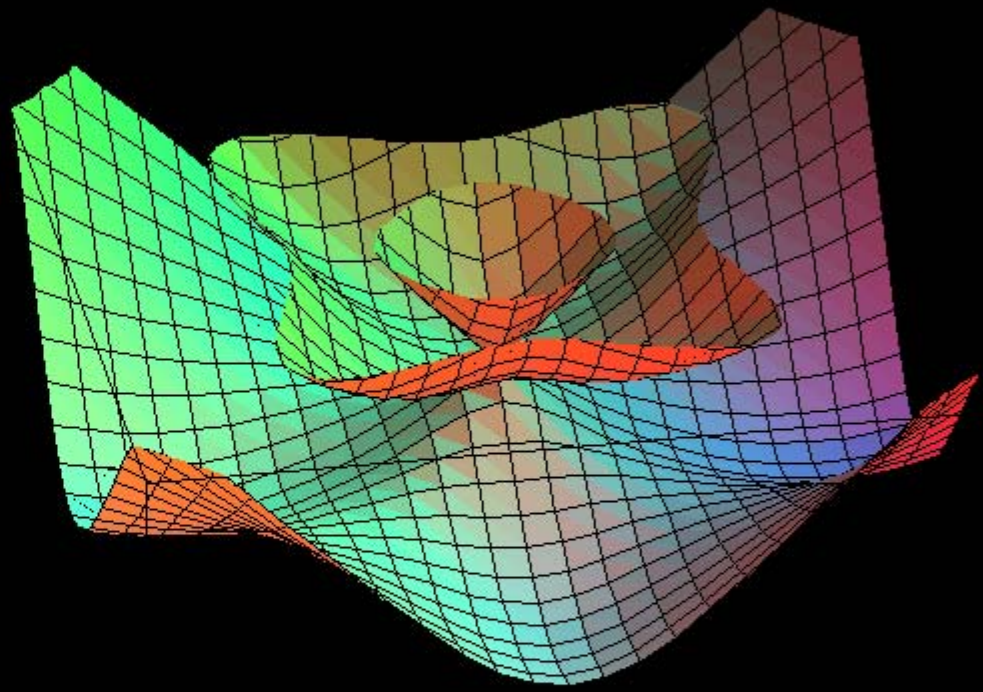

As a result, for the value of k_z where at M the *z/xy* and *xz/yz* bands become degenerate, the *z/xy* band and the inner *xz/yz* band form a *Dirac cone* with linear dispersion in $k_=$.

Main effect of tetraheder elongation

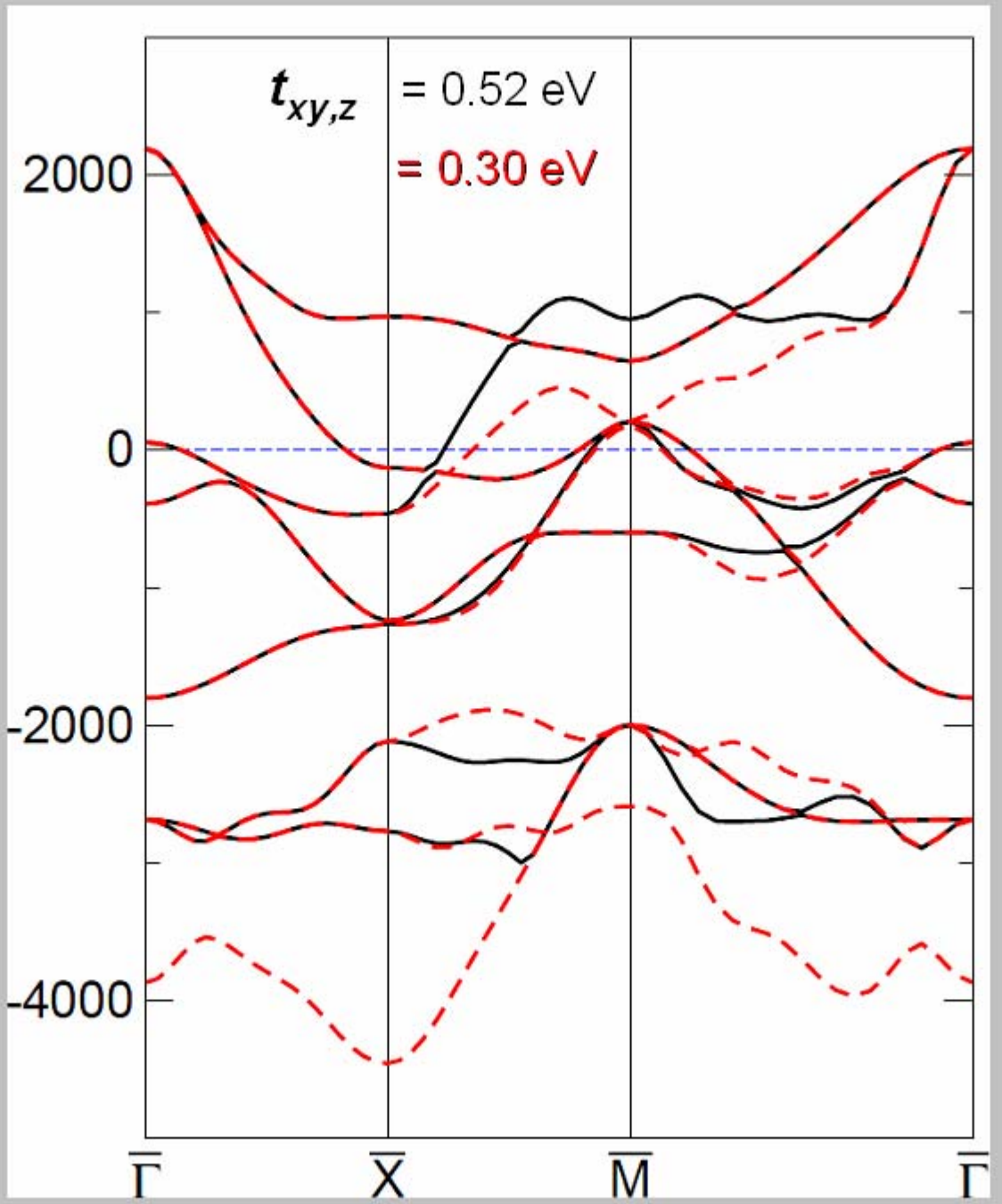

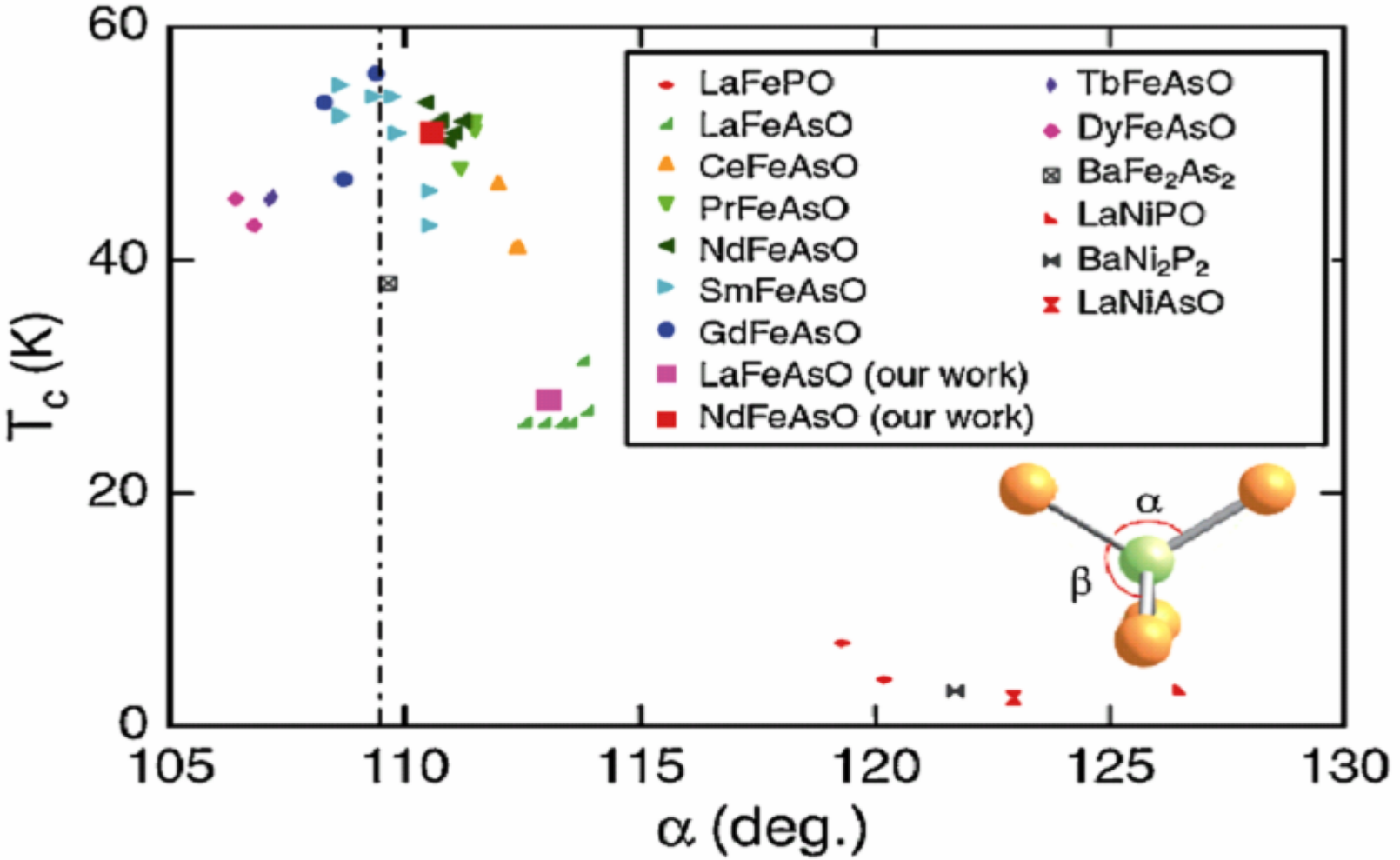

g. 31. (Color online) T_c vs As–Fe–As bond angle α for various pnictide superconductors. The formulas of parent compositions of superconductors are depicted in the inset. The crystal structure parameters of samples showing almost maximum T_c in each system are selected. The vertical dashed line indicates the bond angle of a regular tetrahedron ($\alpha = 109.4°$).[121] Figure reprinted from C.-H. Lee *et al.*: J. Phys. Soc. Jpn. 77 (2008) 083704. Copyright 2009 by the Physical Society of Japan.

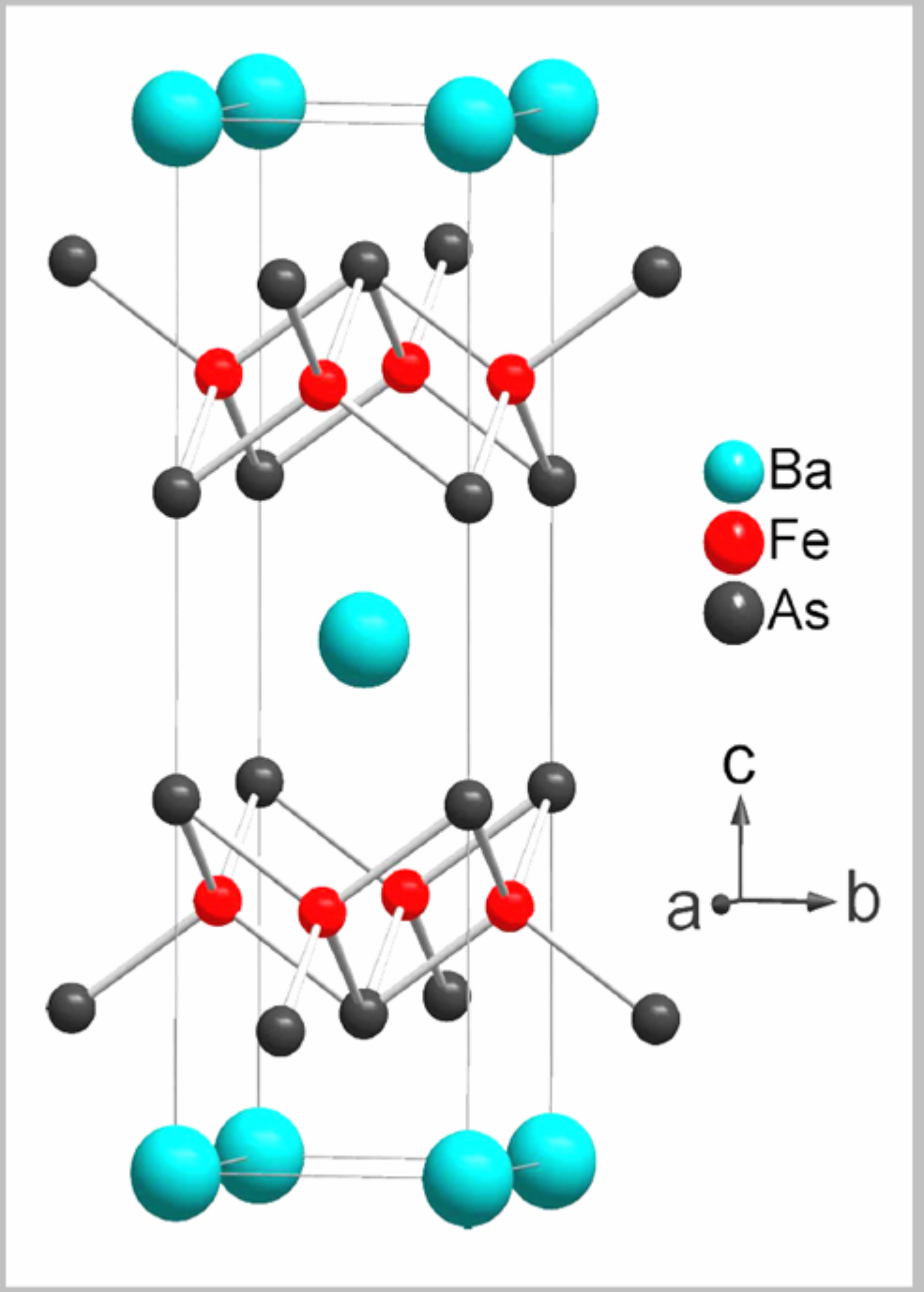

Fe chalcogenides have the same structure, but without Ba.

In all compounds, the Fe layeres are stacked on top.

A primitive translation along c should be associated with mirroring in the Ba and chacogenides compounds but not in the LnO.

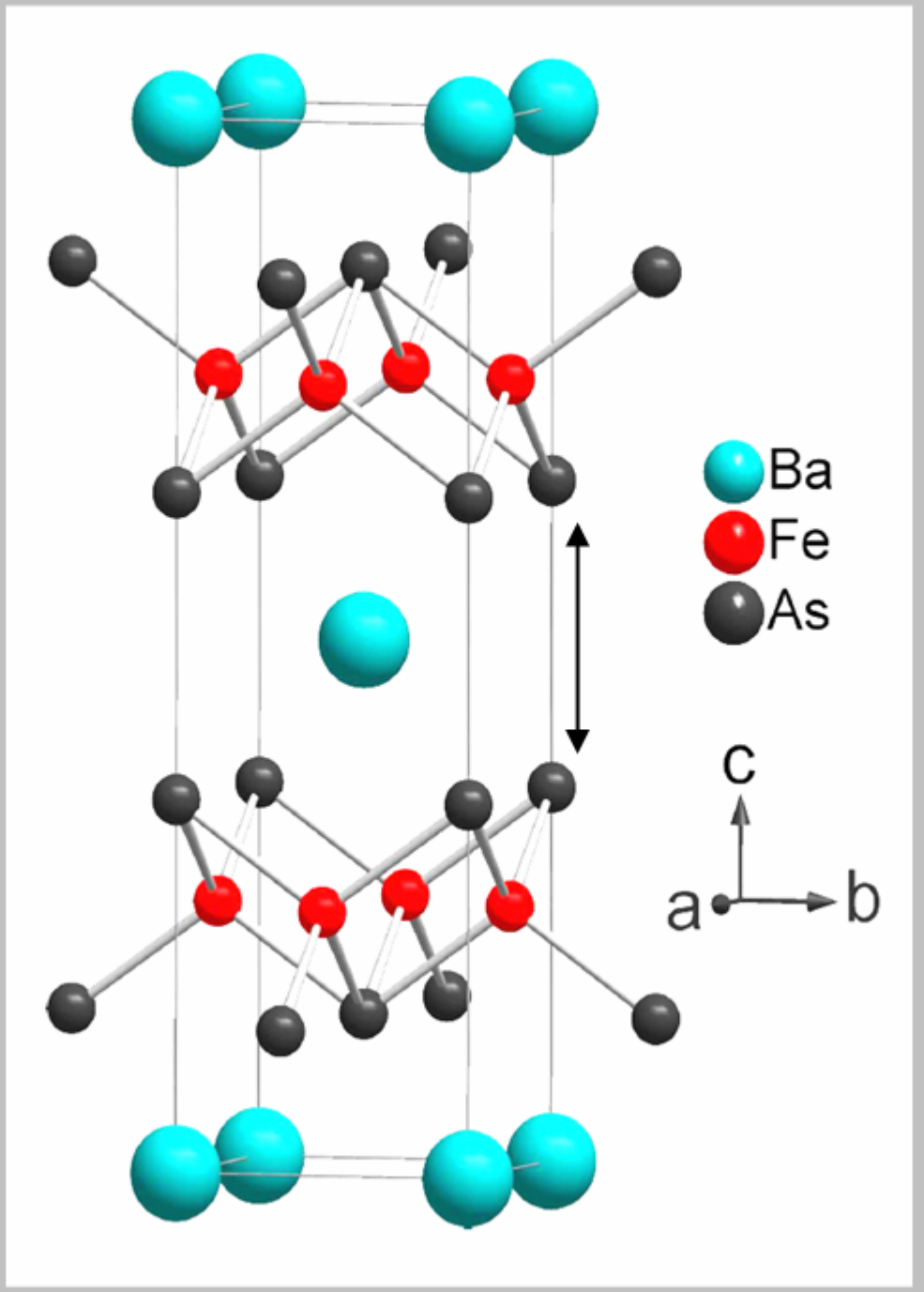

Fe chalcogenides have the same structure, but without Ba.

In all compounds, the Fe layeres are stacked on top.

A primitive translation along c should be associated with mirroring in the Ba and chacogenides compounds but not in the LnO.

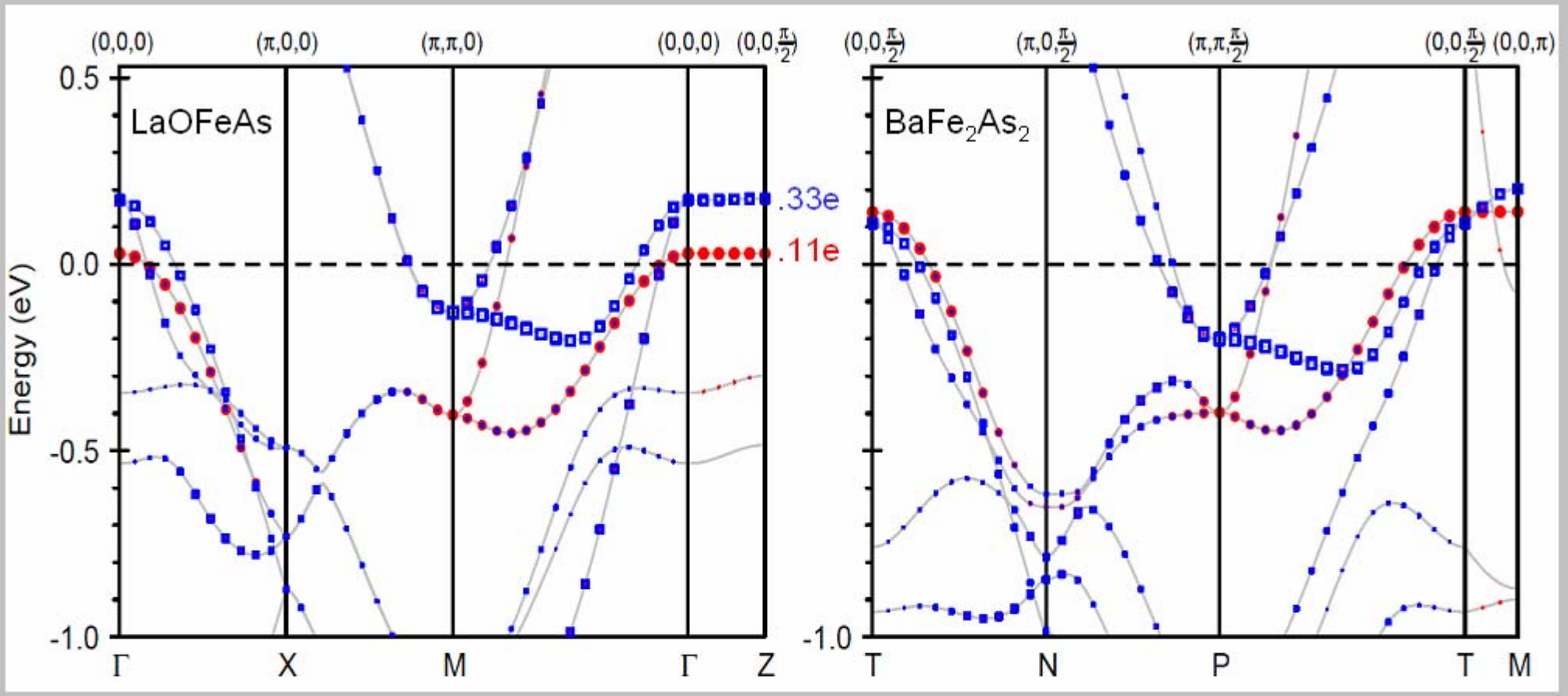
LaOFeAs
BaFe2As2
Energy (eV)
0.5
0.0
-0.5
-1.0
(0,0,0)
(π,0,0)
(π,π,0)
(0,0,0)
(0,0,π/2)
Γ
X
M
Γ
Z
(0,0,π/2)
(π,0,π/2)
(π,π,π/2)
(0,0,π/2)
(0,0,π)
T
N
P
T
M
.33e
.11e

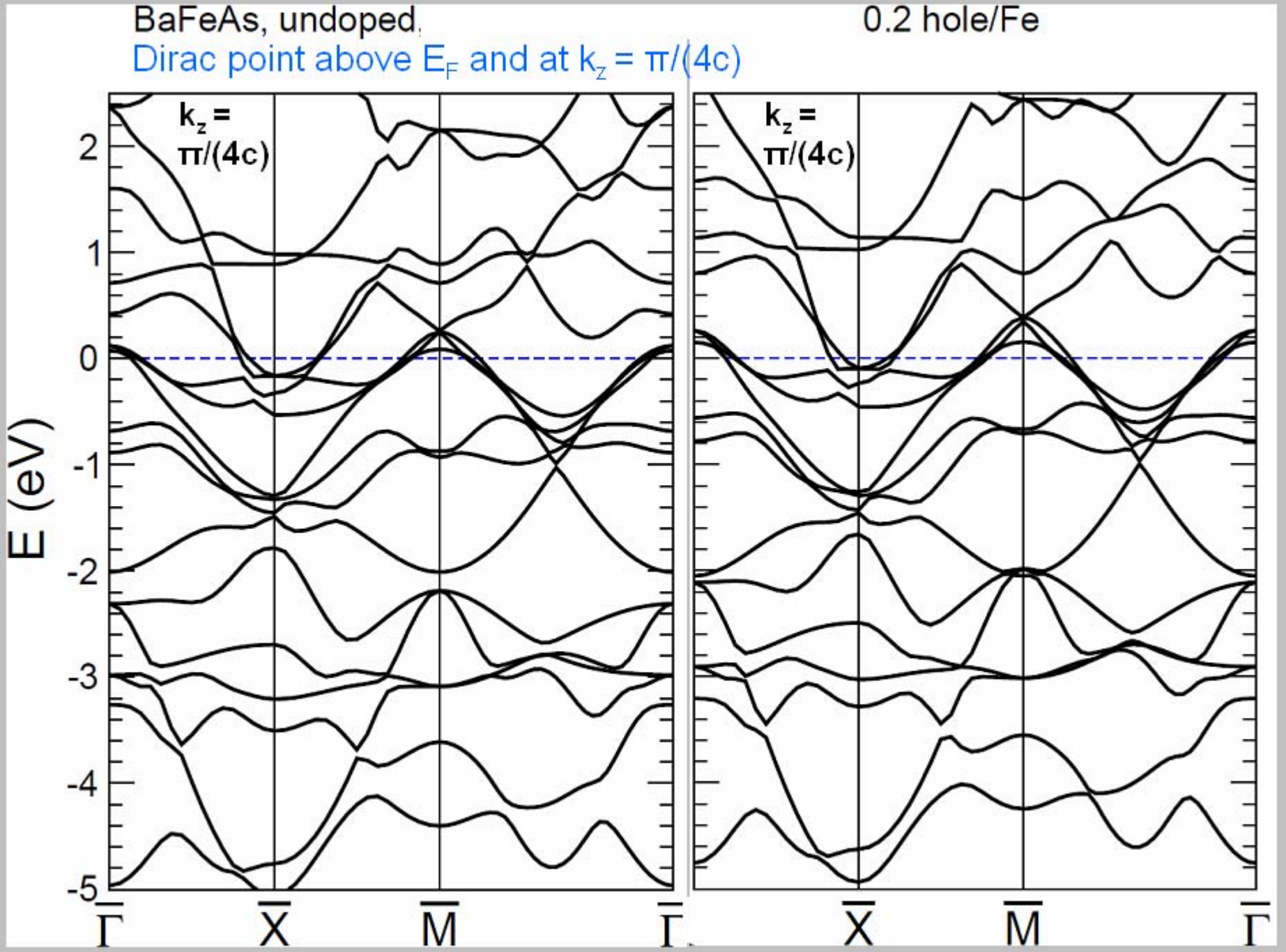
BaFeAs, undoped
Dirac point above E_F and at $k_z = \pi/(4c)$
0.2 hole/Fe
$k_z = \pi/(4c)$
$k_z = \pi/(4c)$
E (eV)
2
1
0
-1
-2
-3
-4
-5
Γ̄
X̄
M̄
Γ̄
X̄
M̄
Γ̄

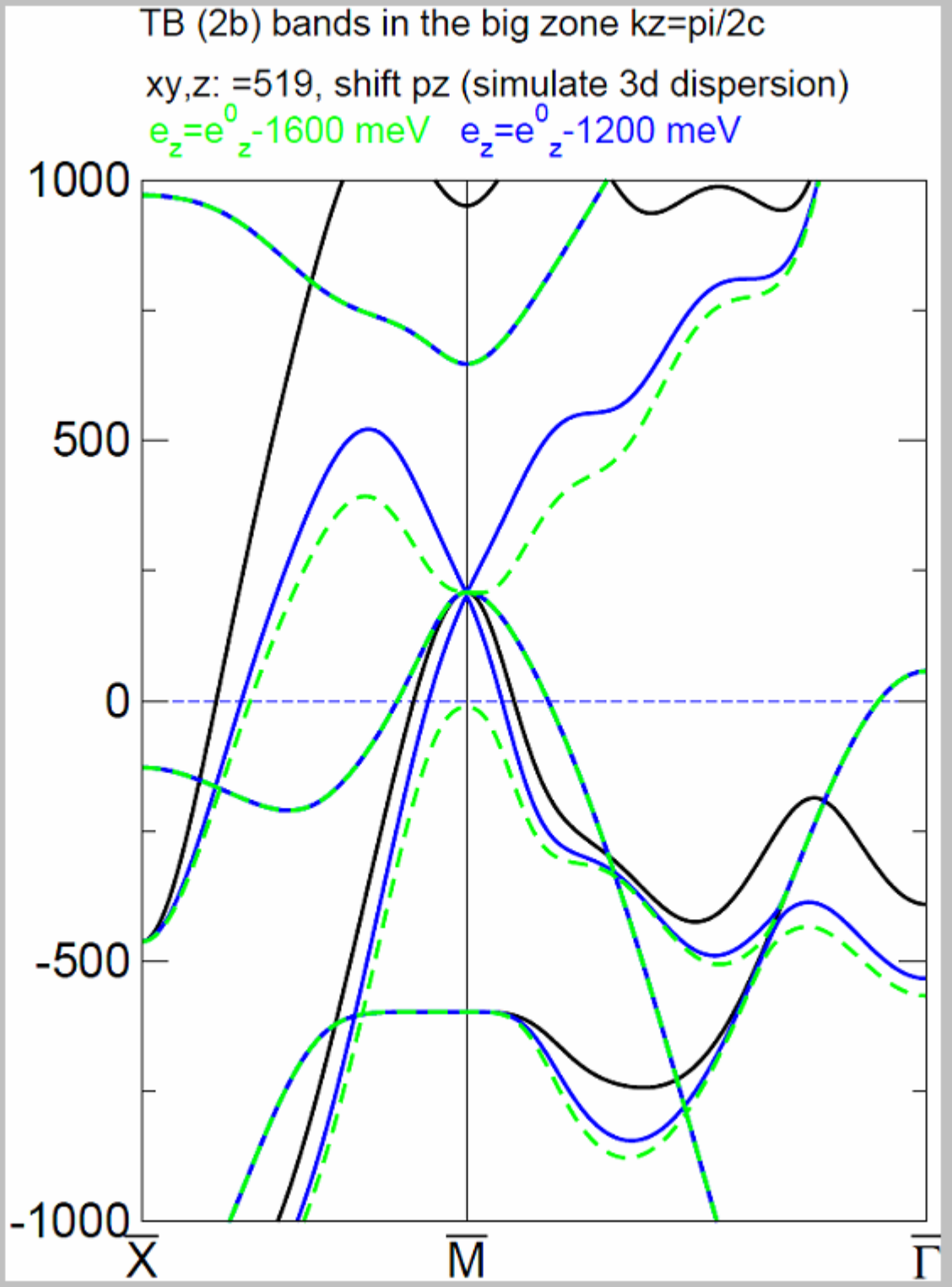
TB (2b) bands in the big zone kz=pi/2c
xy,z: =519, shift pz (simulate 3d dispersion)
e_z=e^0_z-1600 meV
e_z=e^0_z-1200 meV
1000
500
0
-500
-1000
X
M
Γ

Results of LAPW LDA and LSDA total energy

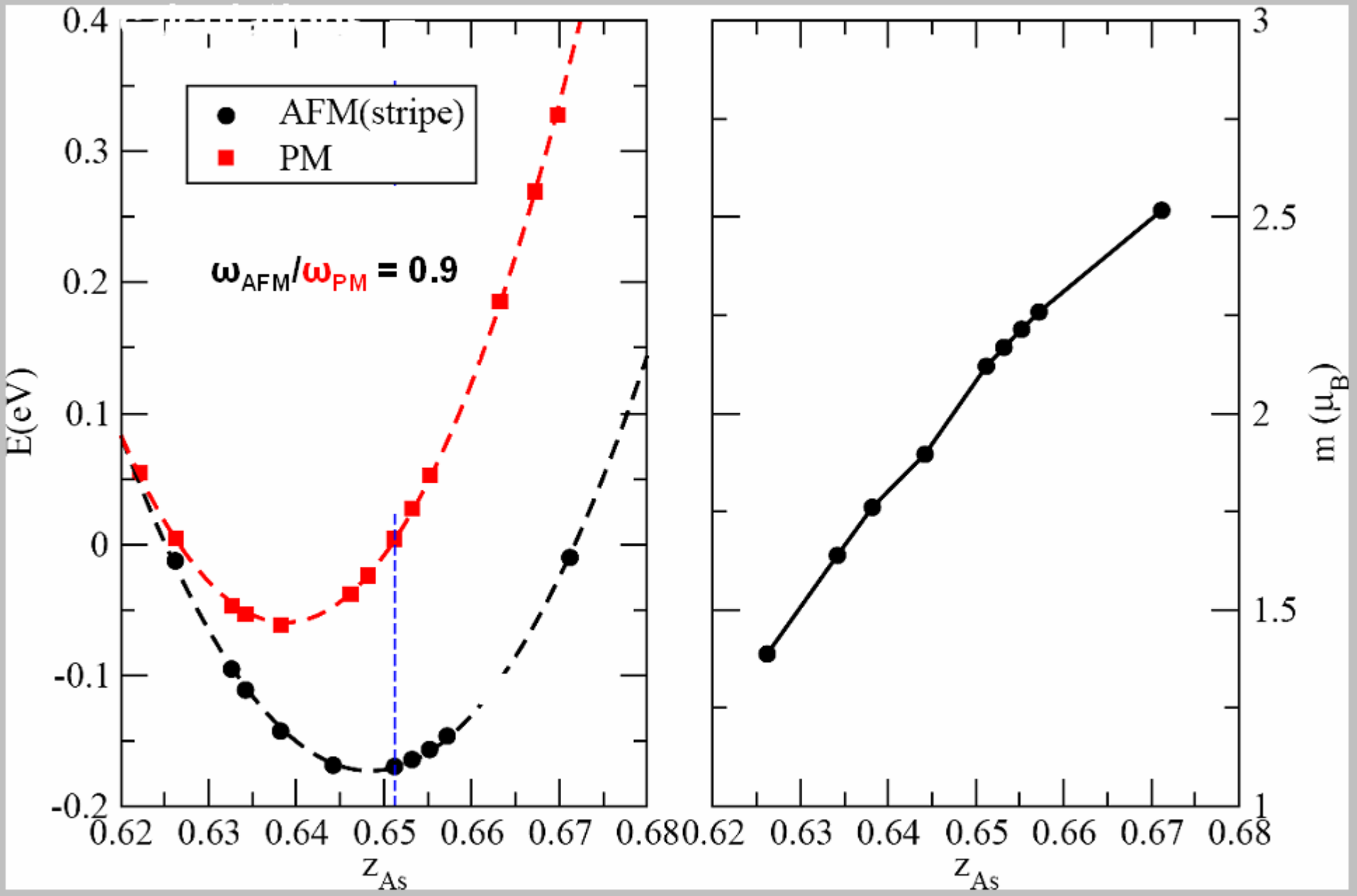

Exp value of the elongation of the $FeAs_4$ tetrahedron

As a first application of our *pd* model we have studied magnetism.

Striped AFM order corresponds to a SDW with q = (0,π) = Y.

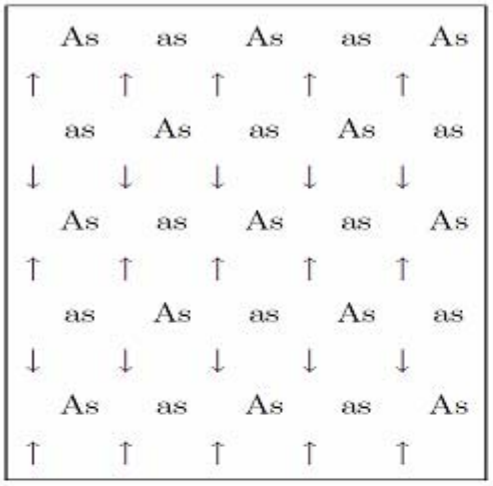

$$\mathbf{H}_{stripe} = \begin{bmatrix} \mathbf{H}(k_x, k_y) & \frac{1}{2}\mathbf{\Delta} \\ \frac{1}{2}\mathbf{\Delta} & \mathbf{H}(k_x, k_y + \pi) \end{bmatrix}$$

SDW Hamiltonian

$$\text{with } \mathbf{\Delta} = \Delta \times$$

Exchange splitting

$$\begin{bmatrix} 1 & 0 & 0 & 0 & 0 & 0 & 0 & 0 \\ 0 & 1 & 0 & 0 & 0 & 0 & 0 & 0 \\ 0 & 0 & 1 & 0 & 0 & 0 & 0 & 0 \\ 0 & 0 & 0 & 1 & 0 & 0 & 0 & 0 \\ 0 & 0 & 0 & 0 & 1 & 0 & 0 & 0 \\ 0 & 0 & 0 & 0 & 0 & 0 & 0 & 0 \\ 0 & 0 & 0 & 0 & 0 & 0 & 0 & 0 \\ 0 & 0 & 0 & 0 & 0 & 0 & 0 & 0 \end{bmatrix}$$

$$m(\Delta) = \sum_{\alpha=1}^{5} m_\alpha(\Delta) = \sum_{\alpha=1}^{5} \sum_{i\mathbf{k}} c_{\alpha,i\mathbf{k}} c^*_{\alpha,i\mathbf{k}+\mathbf{Q}}$$

Magnetic moment

$$\Delta = m(\Delta)\, I$$

Self-consistency condition

I is the Stoner- or Hund's-rule exchange coupling constant for Fe

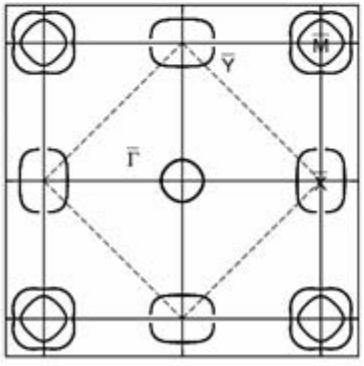

1) Start from PM bands

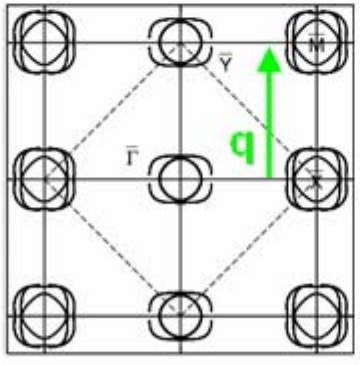

2) Fold in …

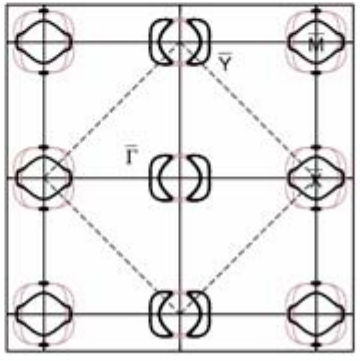

3) Couple with Δ…

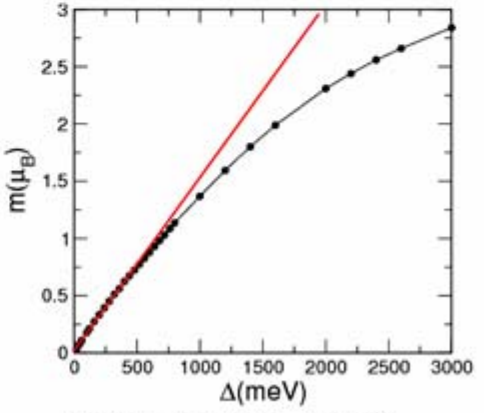

4) Compute *m*(Δ)

5) Solve *m*(Δ) = Δ/*I*

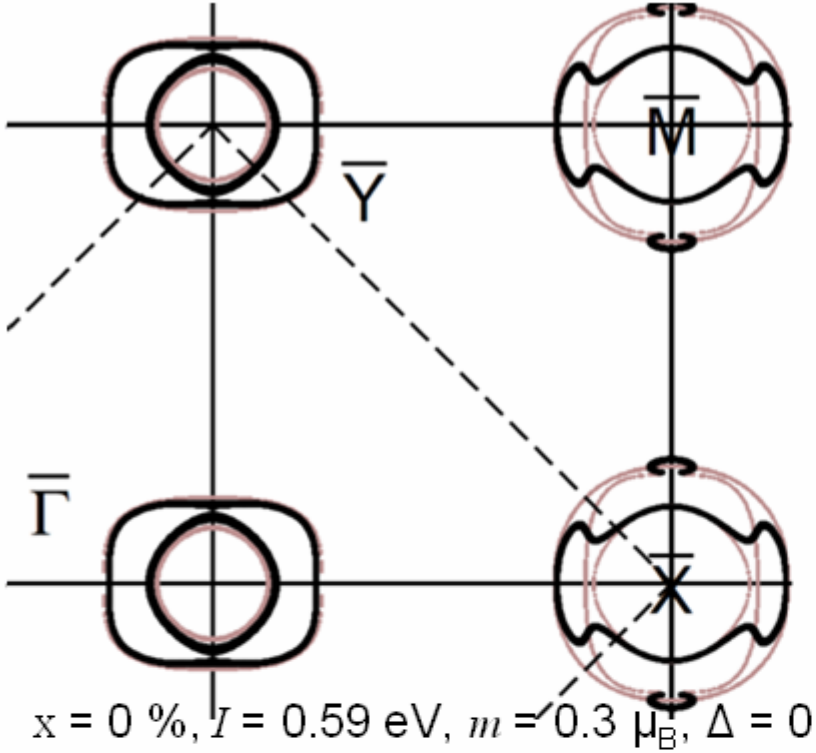

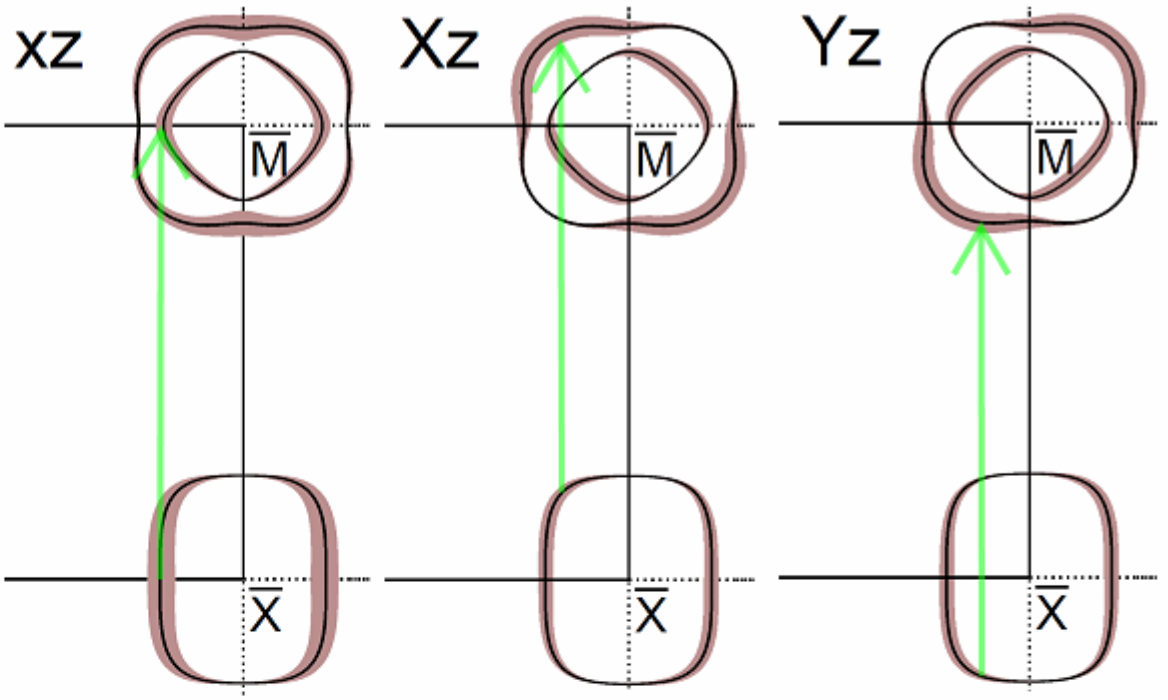

x = 0 %, I = 0.59 eV, m = 0.3 μ_B, Δ = 0.18 eV

The exchange-coupling matrix, **Δ**, is diagonal (to a good approximation) so that only Fermi-surface sheets with similar Fe characters couple. Below, to the right, we show the paramagnetic M-centered hole pockets and the X-centered electron pocket, decorated with the common Wannier-function characters, which are *xz*, *Xz,* and *Yz*. The stripe translation **Y**, brings those sheets on top of each other and, as seen on step to the left, those parts with good nesting and a common character do gap. The gapped Fermi surface has "propeller" shape, as was recently observed with ARPES by Borisenko et al.. The gapping of the *xz*, *Xz,* and *Yz* characters leads to "bonds" with those characters and hence, to a SDW-induced contraction along *x*, i.e. in the F-ordered direction. We believe that this is the observed orthorhombic distortion.

How does Doug's pairing compare with this (Maier et al 09)?

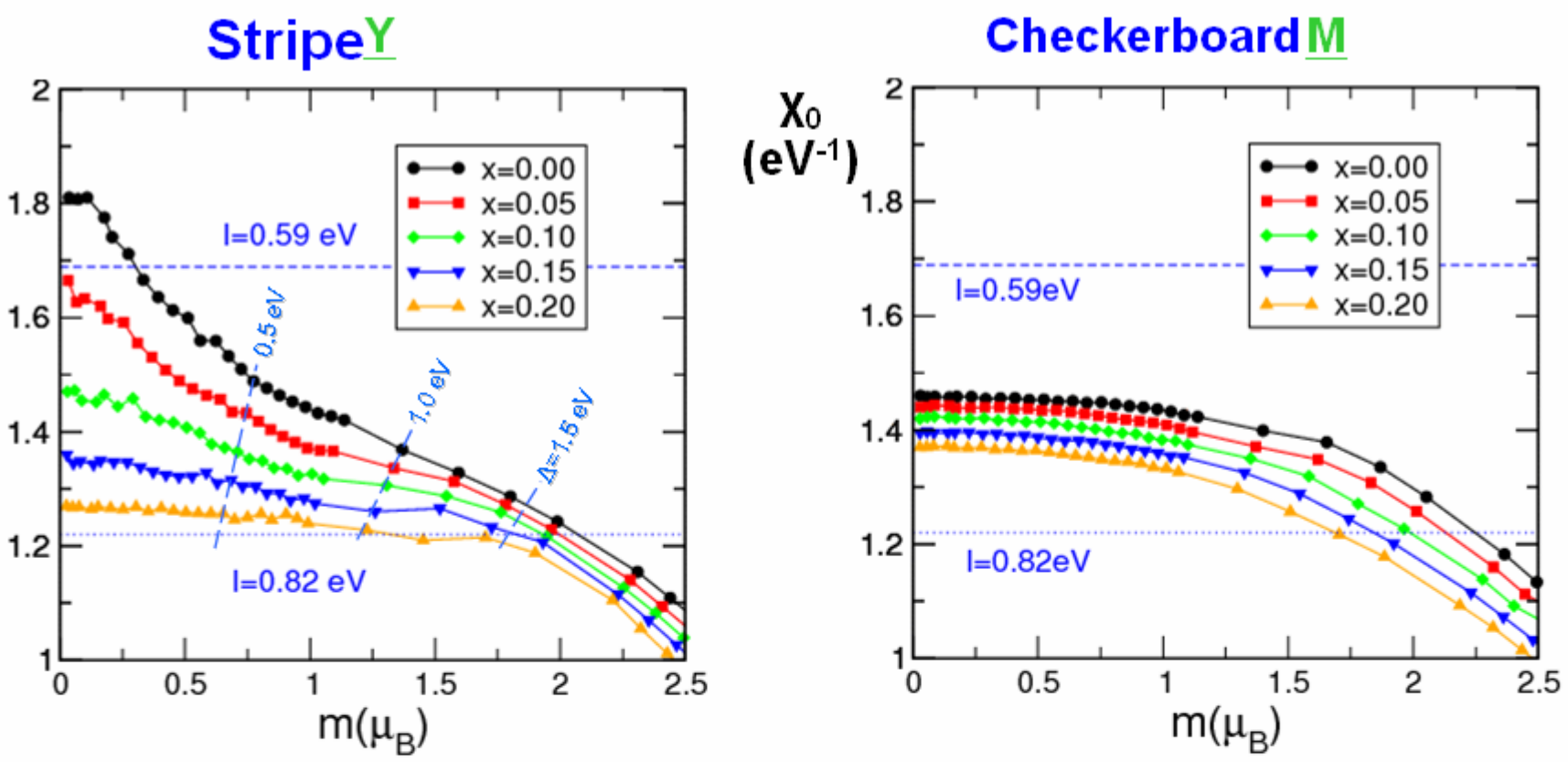

The curves below show for $LaO_{1-x}F_xFeAs$ the bare susceptibility, $\chi_0(m) = m(\Delta)/\Delta$, as a function of the induced moment, $m(\Delta)$, for striped (Y) and checkerboard (M) AFM order and various values of the electron doping x. For a given value of I, the stable moment is the solution of: $\chi_0(m) = 1/I$. The LSDA value I = 0.82 eV, predicts that both Y and M orders are stable and with moments $m \sim 2\ \mu_B$. Experimentally, only Y order is stable and $m \sim 0.3\ \mu_B$. This is consistent with the LDA bands and I = 0.59 eV; a reduction presumbly due to the strong As p character. With this value of I, our bands also reproduce the disappearance of the moment for x > 5% in accord with experiments.

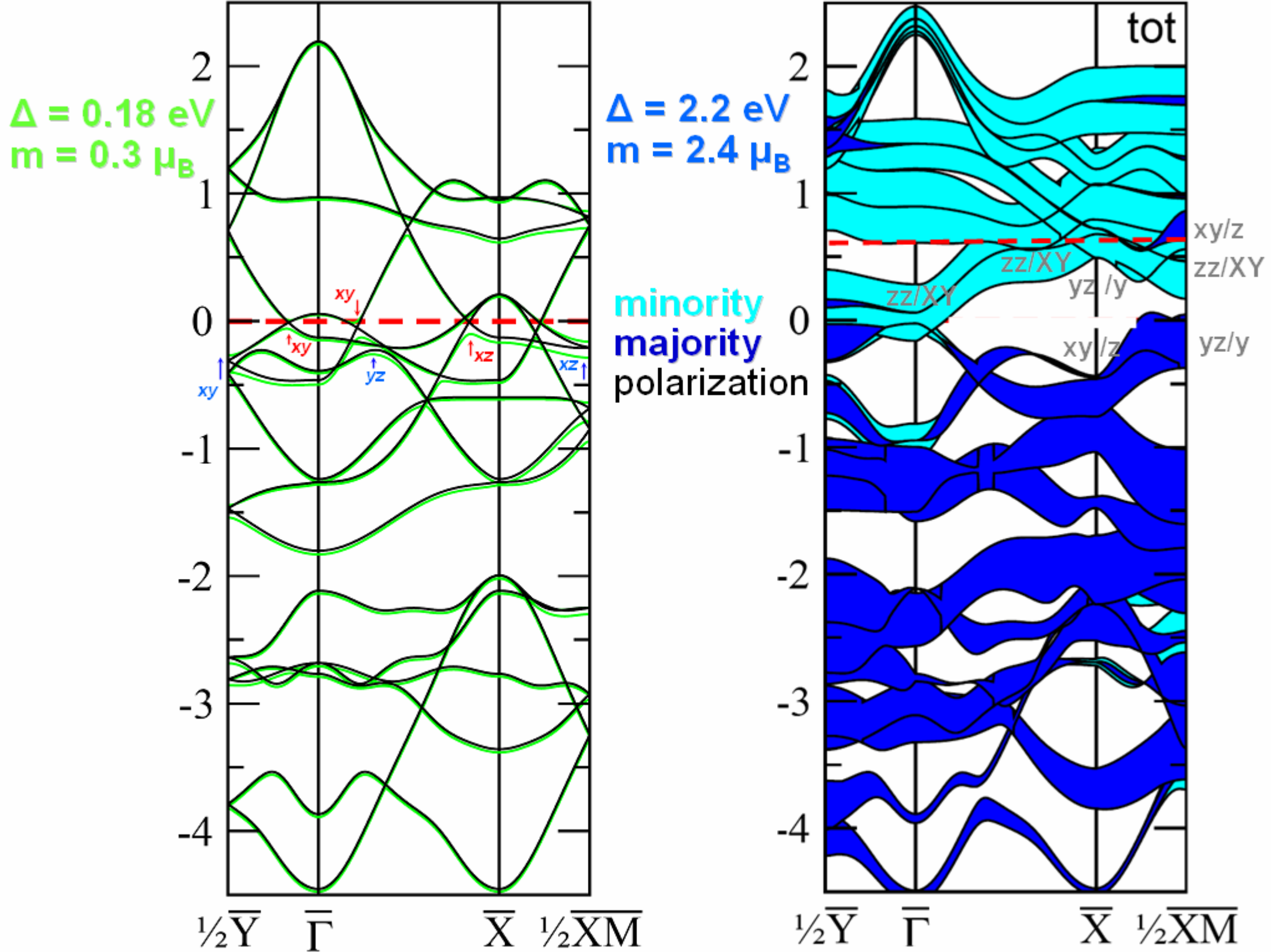
Δ = 0.18 eV
m = 0.3 μB
Δ = 2.2 eV
m = 2.4 μB
minority
majority
polarization
tot
xy/z
zz/XY
zz/XY
zz/XY
yz /y
xy /z
yz/y
xy
xy
yz
xz
xz
2
1
0
-1
-2
-3
-4
½Y
Γ
X
½XM

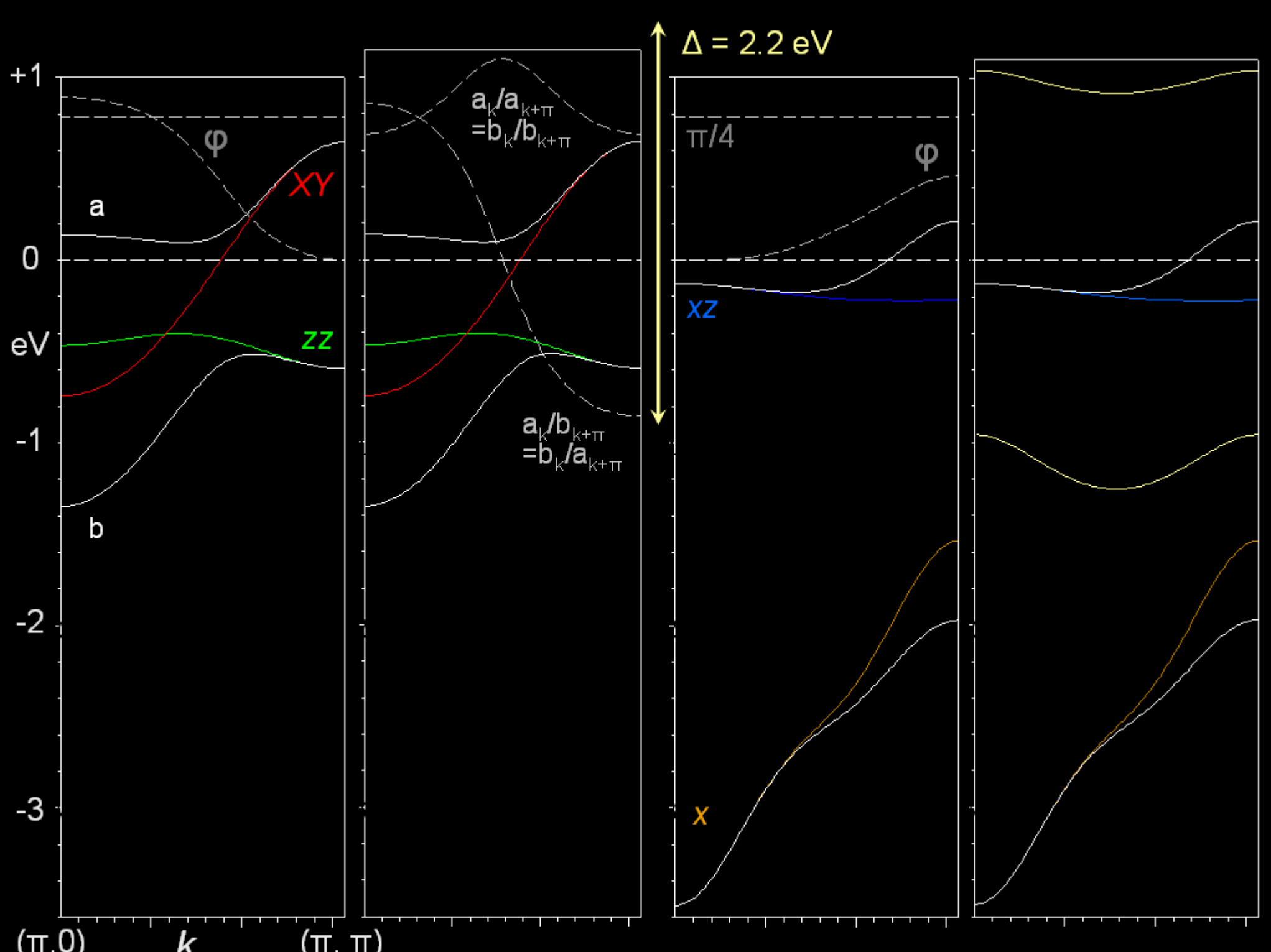
Δ = 2.2 eV
+1
0
-1
-2
-3
eV
φ
a
b
XY
ZZ
$a_k/a_{k+\pi}$
$=b_k/b_{k+\pi}$
$a_k/b_{k+\pi}$
$=b_k/a_{k+\pi}$
π/4
φ
XZ
X
(π,0)
k
(π, π)

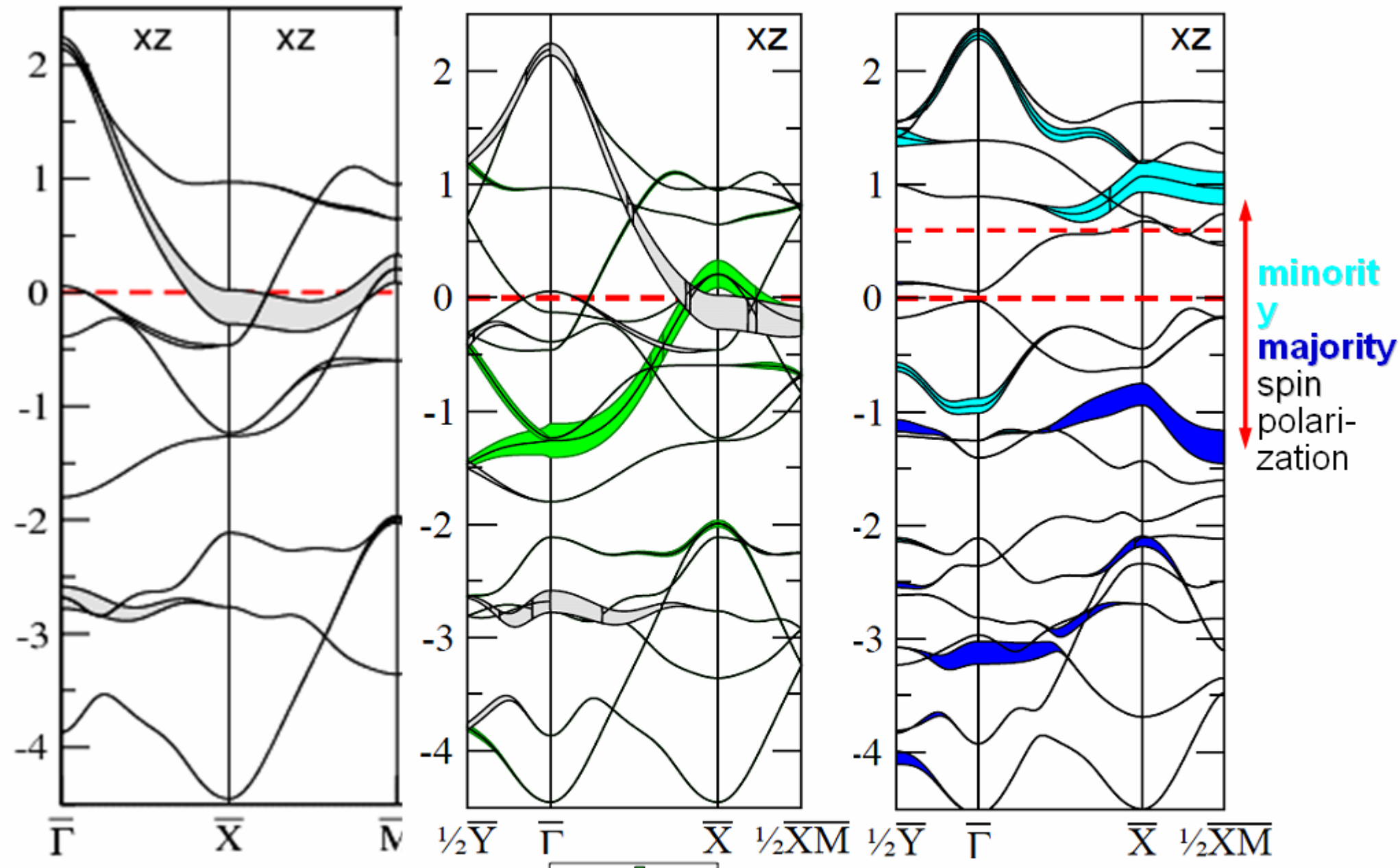

Preparing for the q=(0,π) stripes (folding into the small zone):

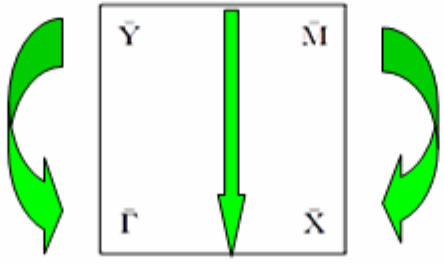

Coupling with $\Delta = mI = 2.2$ eV

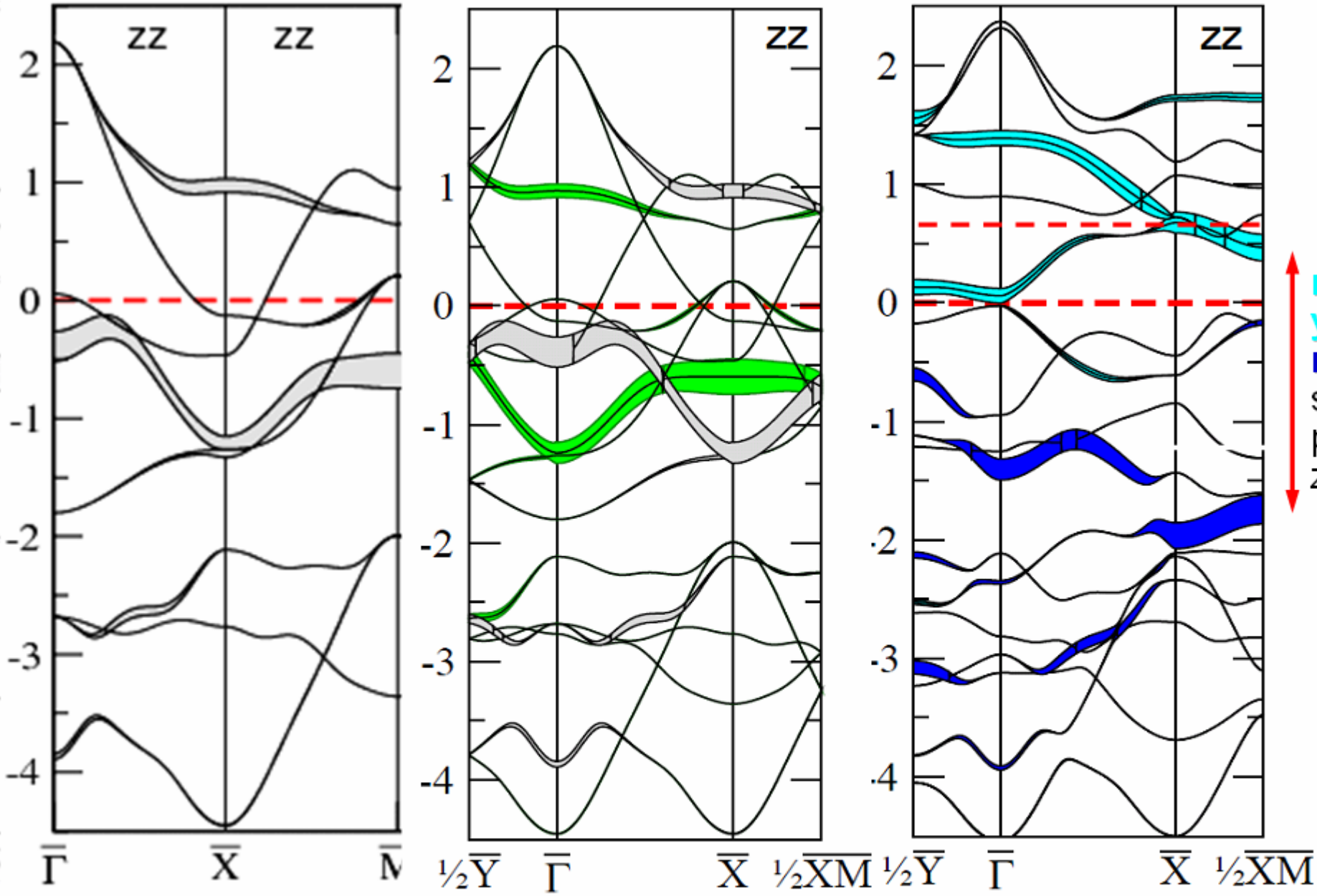

Preparing for the q=(0,π) stripes (folding into the small zone):

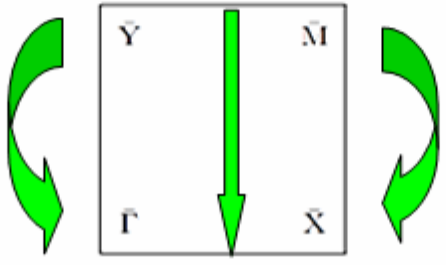

Coupling with $\Delta = mI = 2.2$ eV

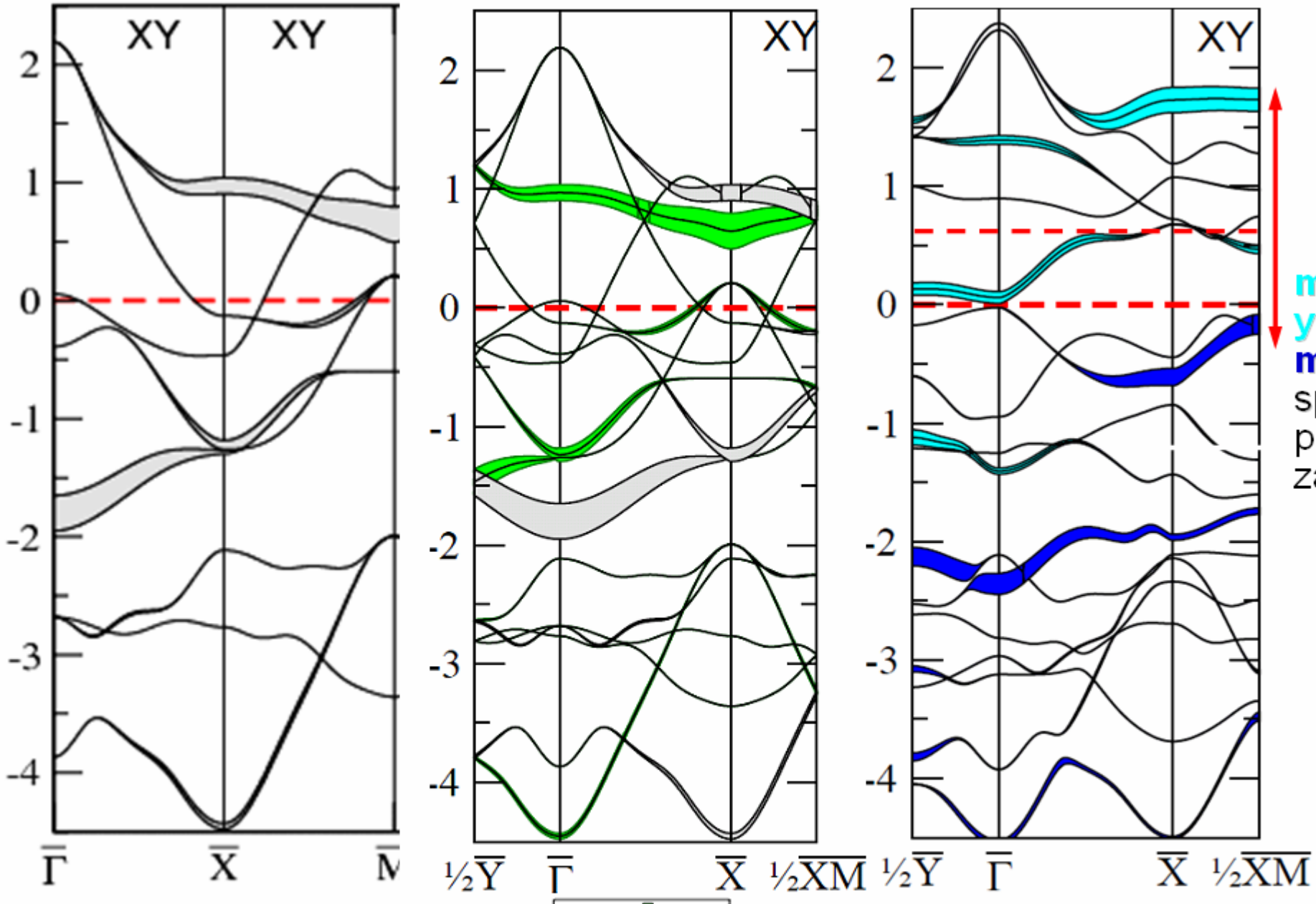

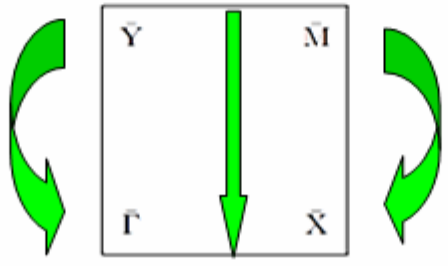

Preparing for the q=(0,π) stripes (folding into the small zone):

Coupling with $\Delta = mI = 2.2$ eV

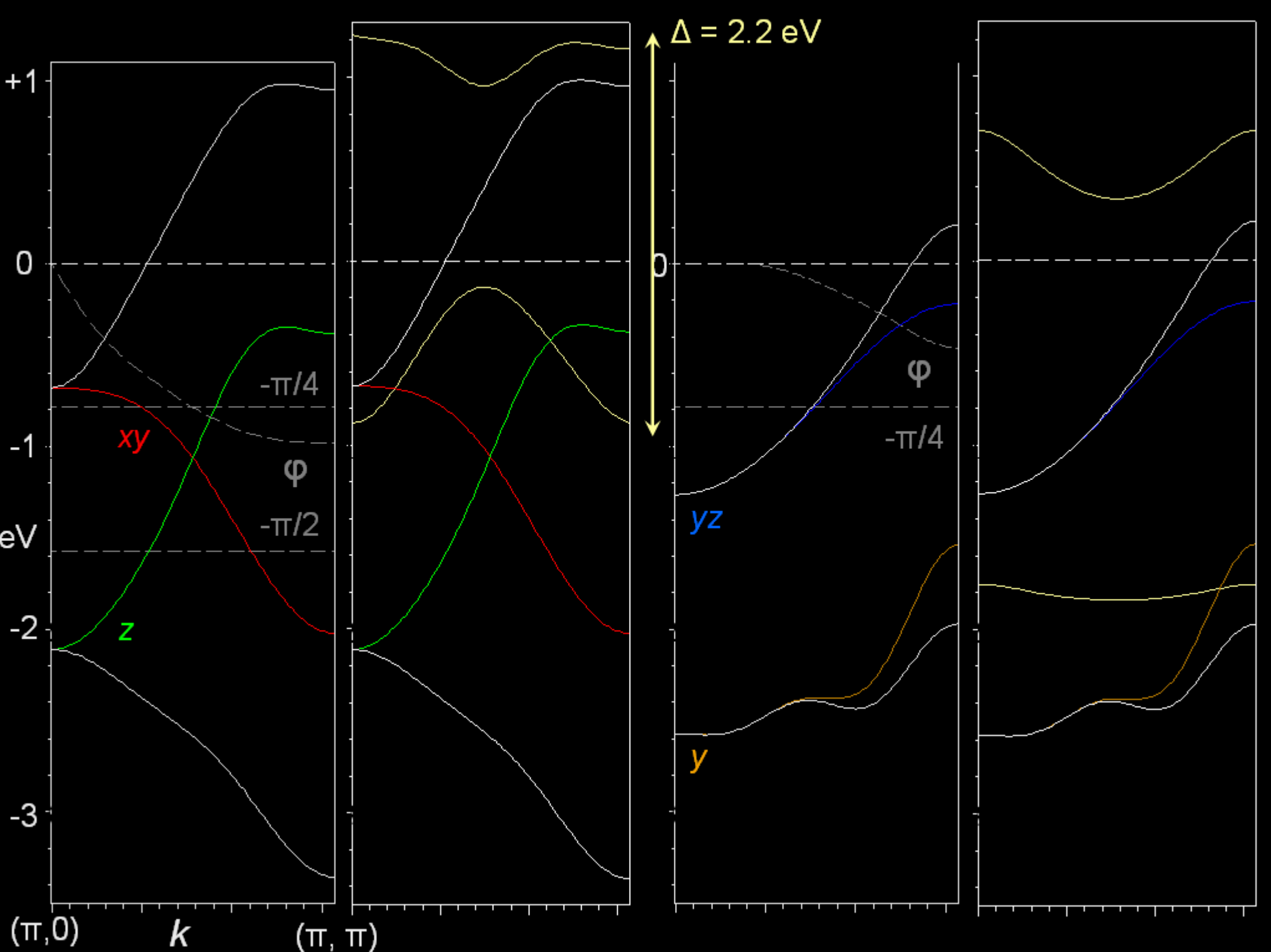
Δ = 2.2 eV
+1
0
-1
-2
-3
eV
-π/4
-π/2
φ
xy
z
yz
y
(π,0)
k
(π, π)

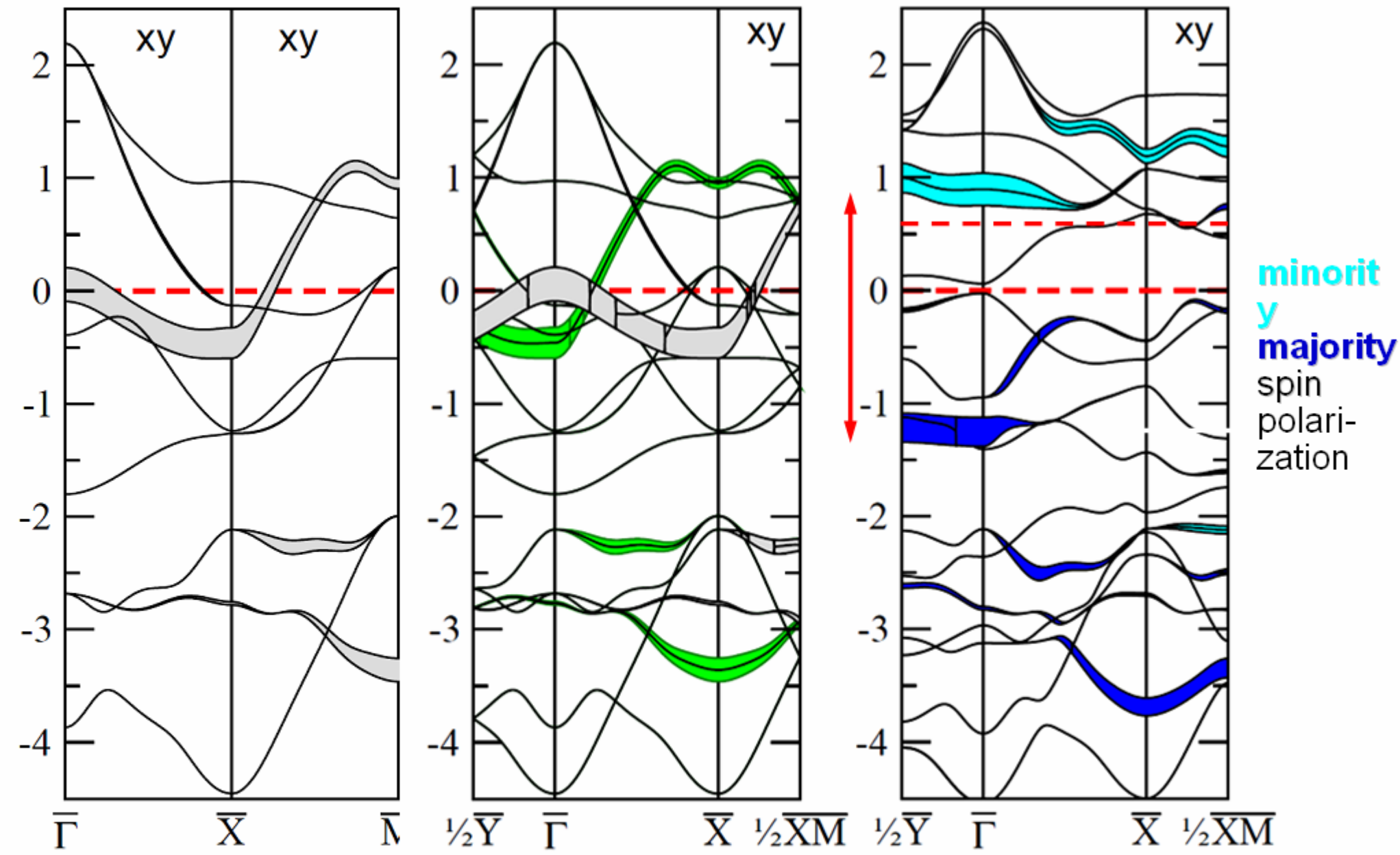

Preparing for the q=(0,π) stripes (folding into the small zone):

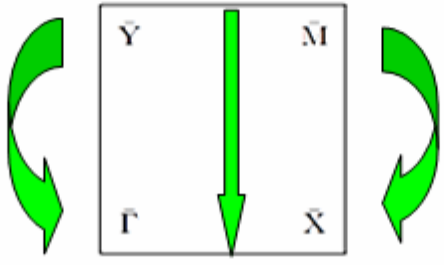

Coupling with $\Delta = mI = 2.2$ eV

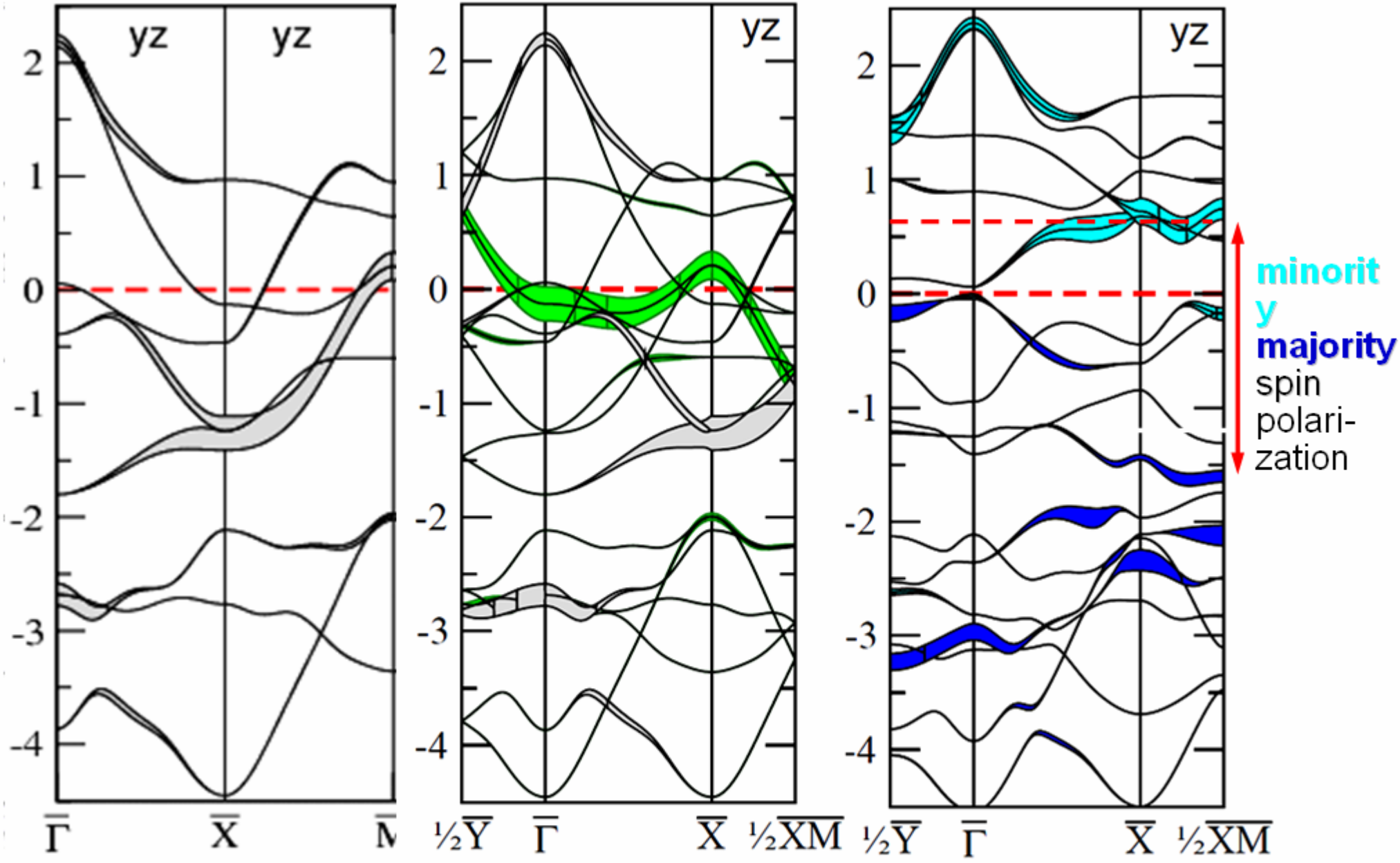

Preparing for the q=(0,π) stripes (folding into the small zone):

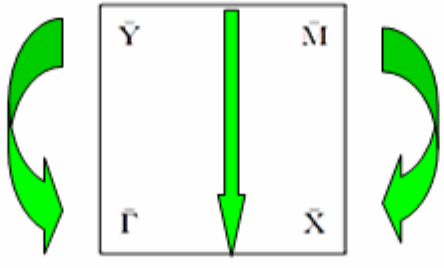

Coupling with $\Delta = mI = 2.2$ eV

1/5 ×

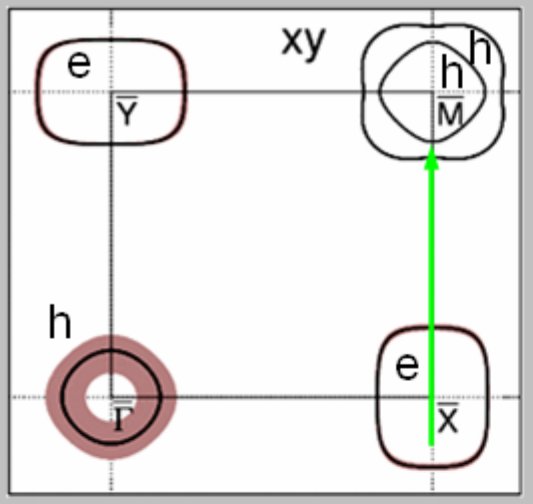

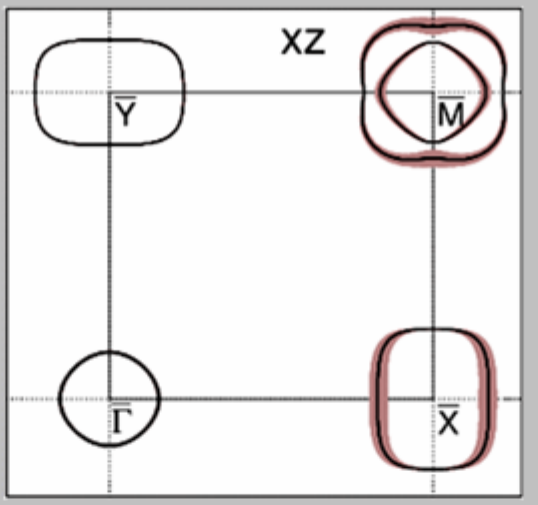

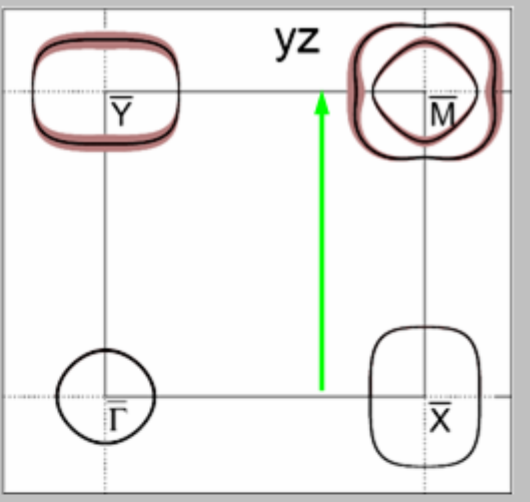

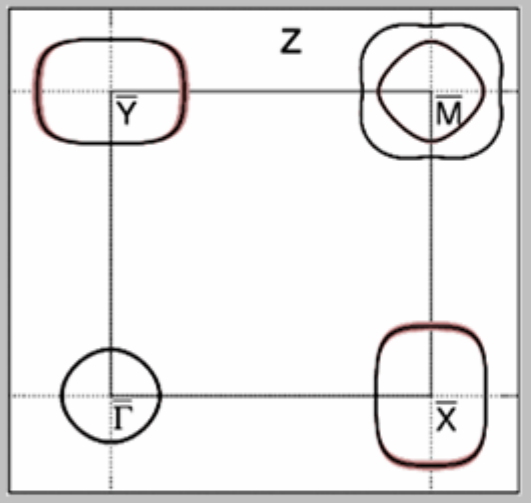

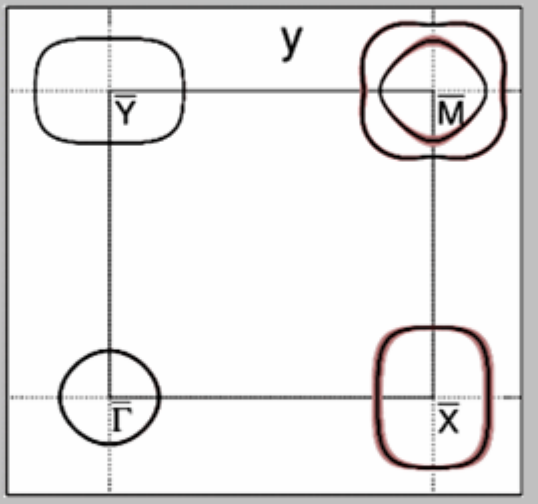

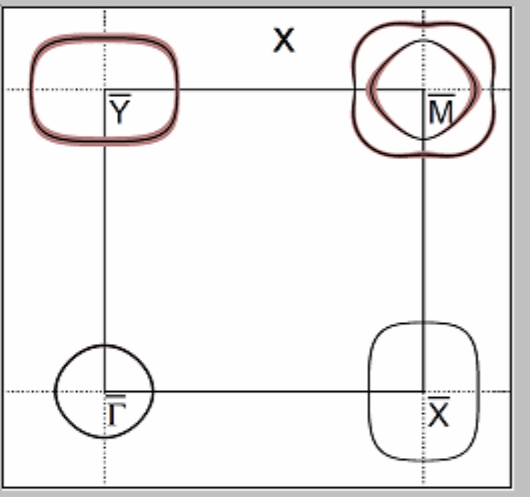

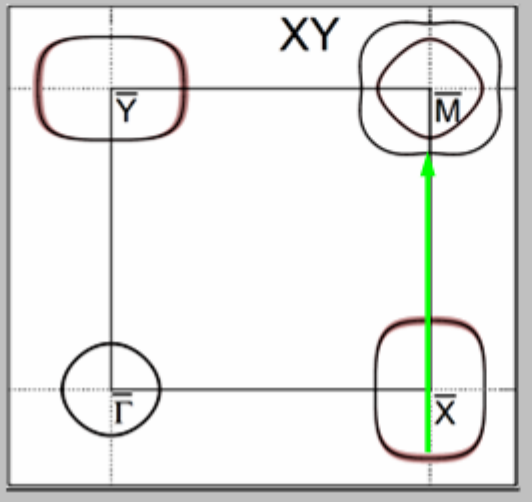

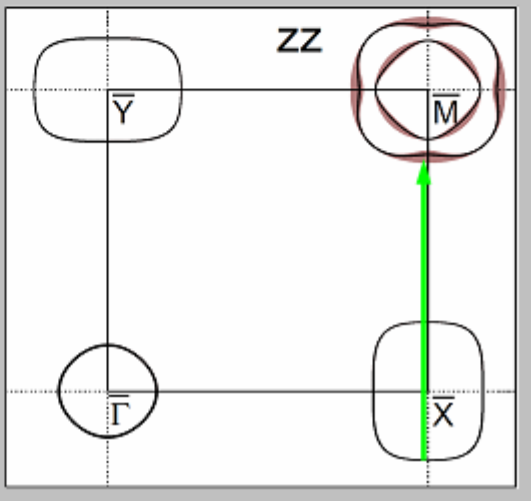

These ones do NOT get gapped around ε_F, and form the small FS on which SC might exist.

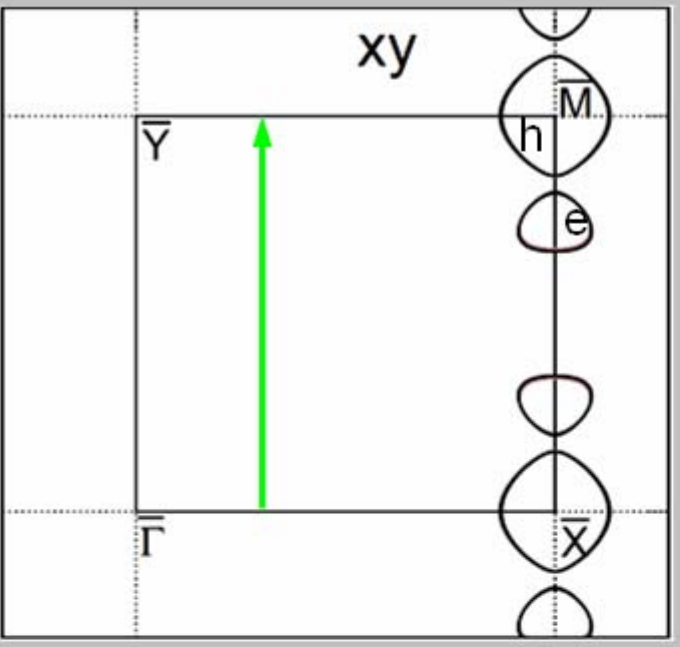

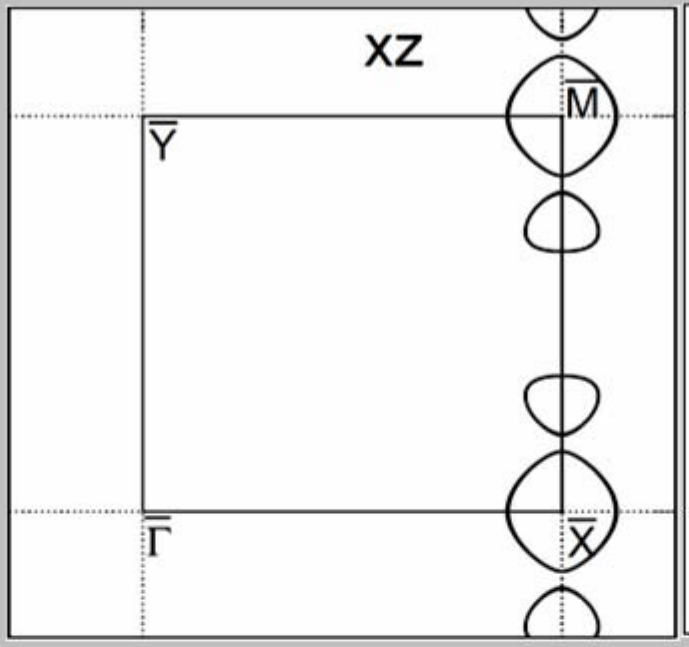

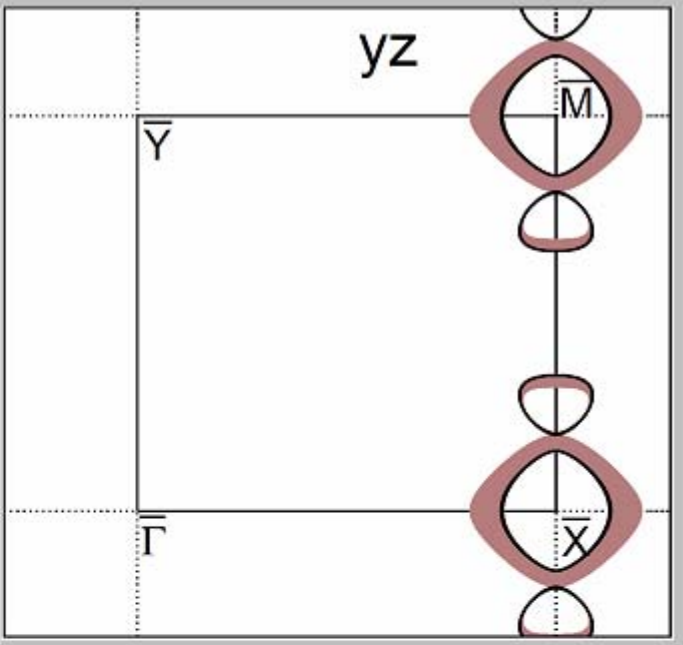

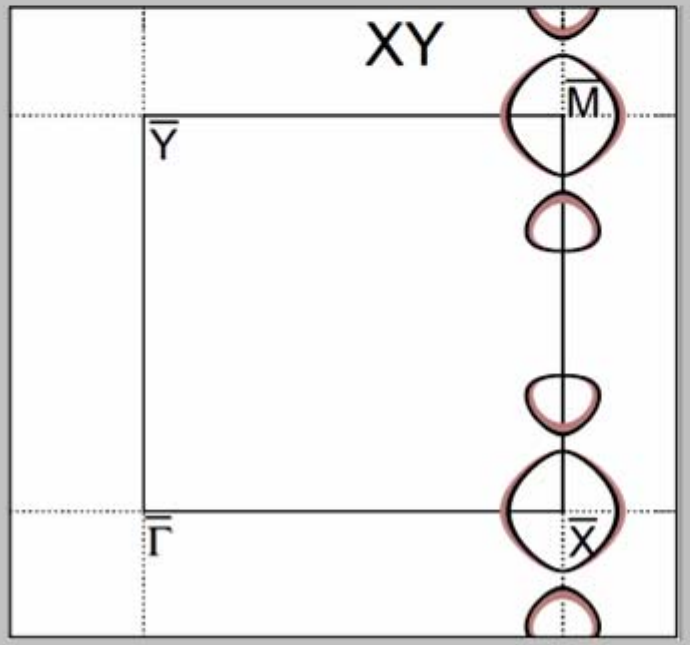

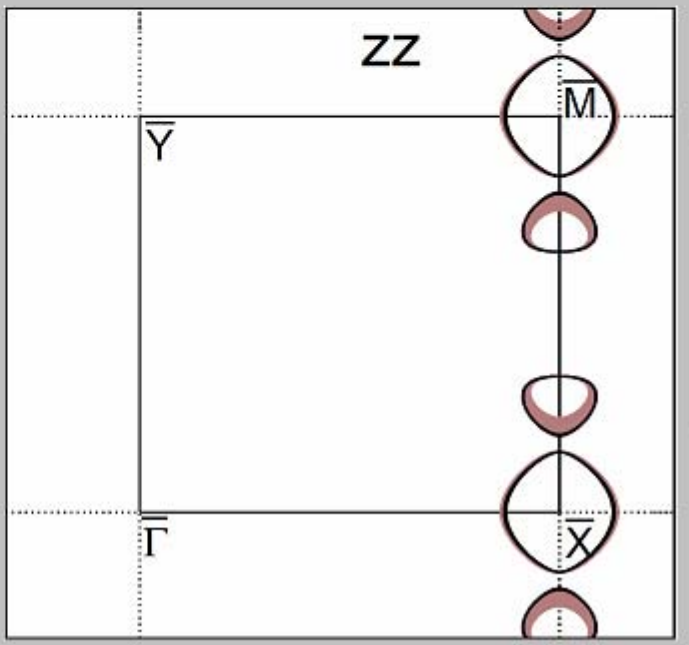

2 μ_B propeller. Mostly minority spins

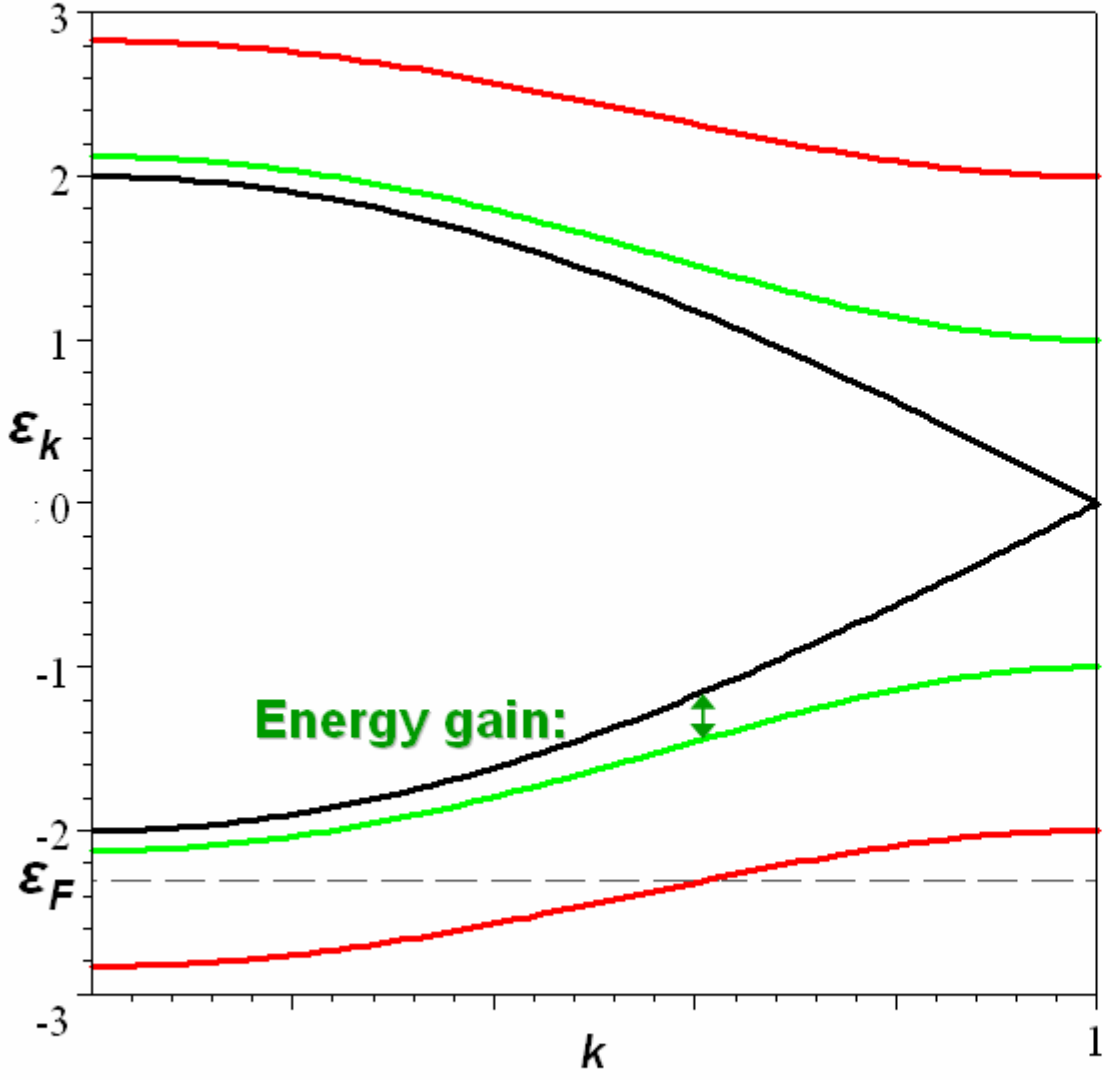

AFM band

AFM double-counting-corrected band

PM band folded into AF BZ

AFM double-counting-corrected band

AFM band

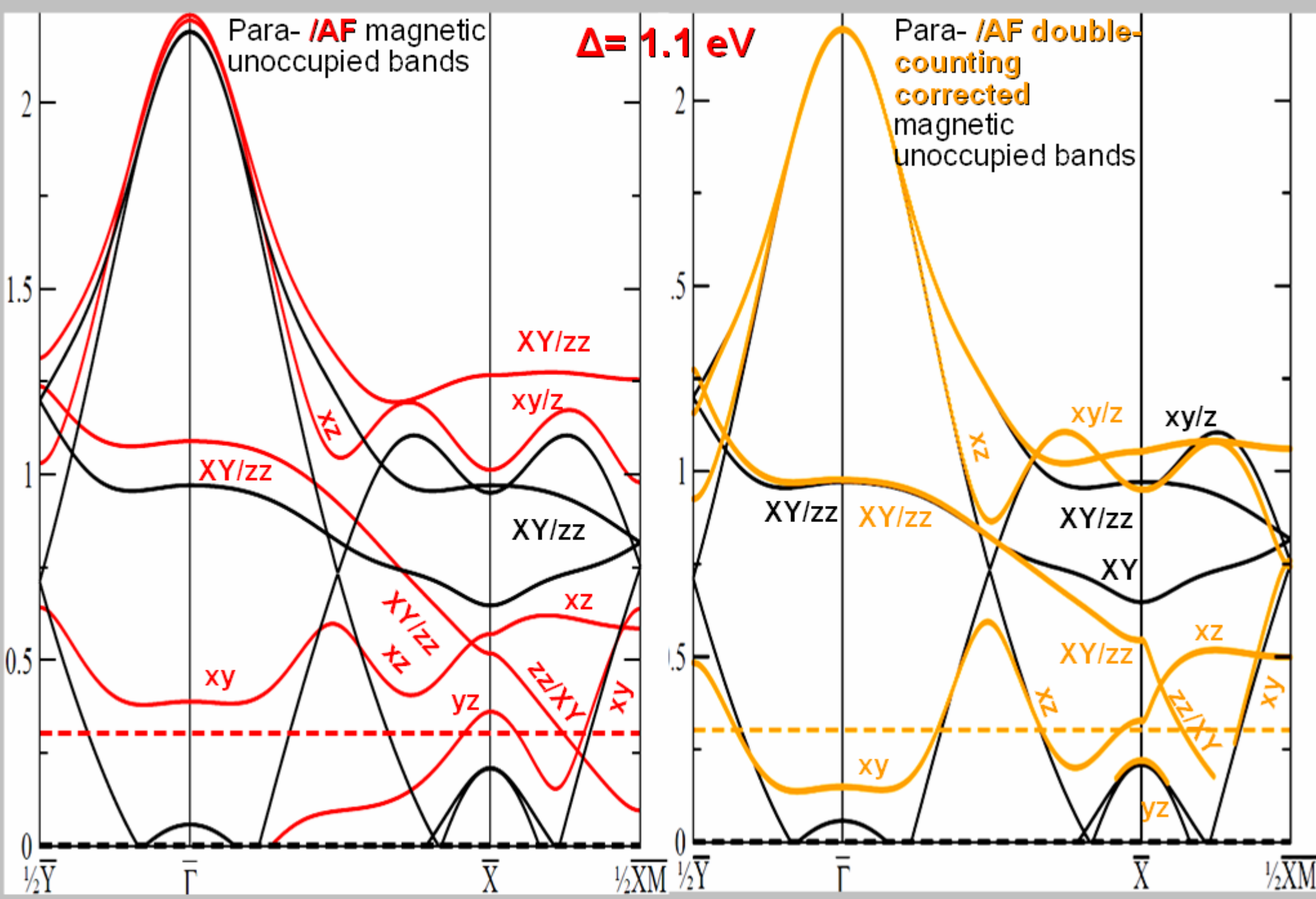
Para- /AF magnetic
unoccupied bands
Δ= 1.1 eV
Para- /AF double-
counting
corrected
magnetic
unoccupied bands
XY/zz
xy/z
xz
XY/zz
XY/zz
xz
xy
yz
zz/XY
xy
XY/zz
xz
xy/z
xy/z
XY/zz
XY/zz
XY/zz
XY
xz
XY/zz
xz
zz/XY
xy
xy
yz
2
1.5
1
0.5
0
½Y
Γ
X
½XM

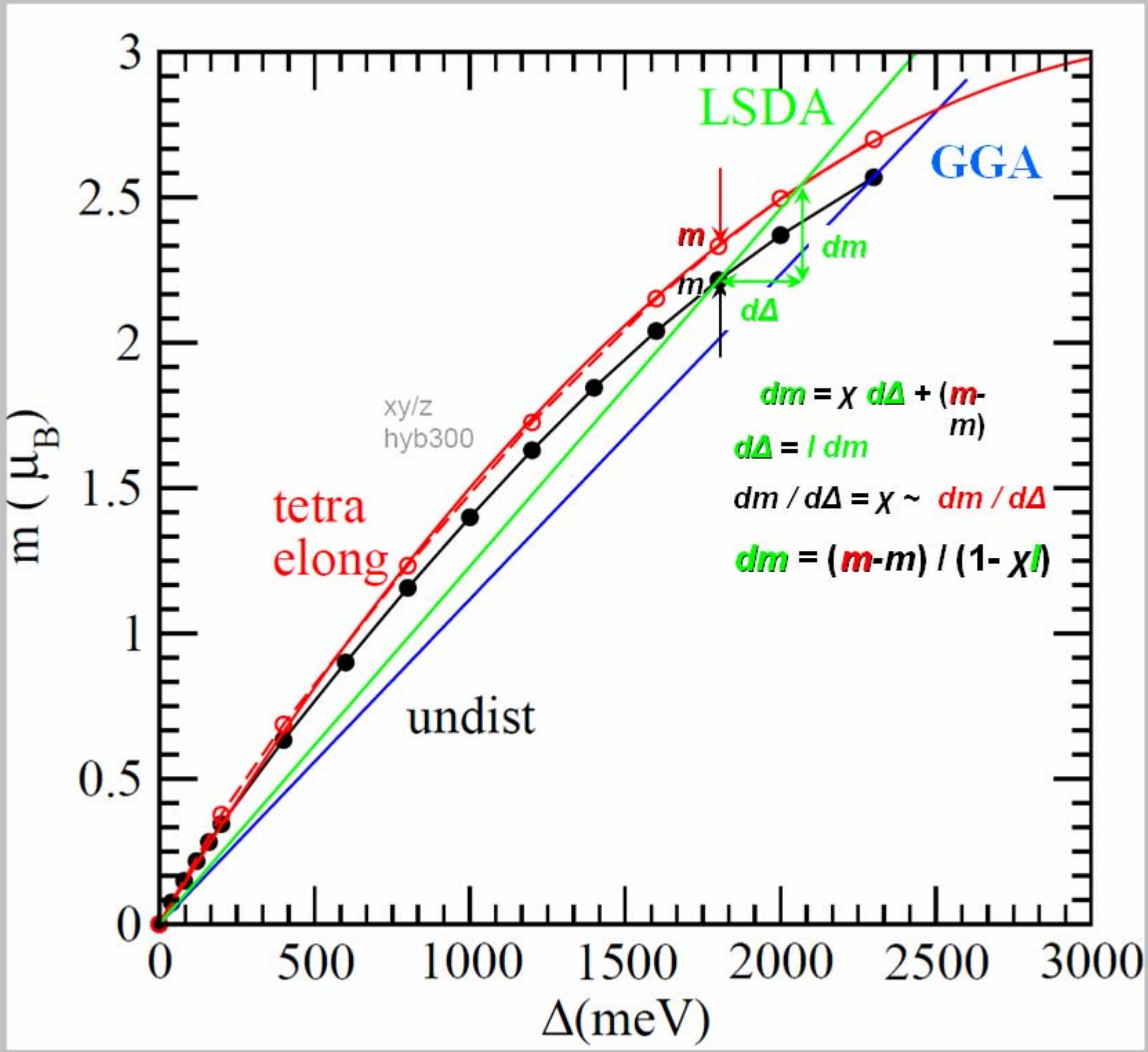
LSDA
GGA
m
m
dm
dΔ
dm = χ dΔ + (m-m)
dΔ = I dm
dm / dΔ = χ ~ dm / dΔ
dm = (m-m) / (1- χI)
xy/z
hyb300
tetra
elong
undist
m (μB)
Δ(meV)
0
0.5
1
1.5
2
2.5
3
0
500
1000
1500
2000
2500
3000

Fe sublattice magnetizations and magnetic energies of spin spirals calculated by LMTO-LSDA for the experimental structure.

A. Yaresko et al. PR B 79, 114503 (2009)

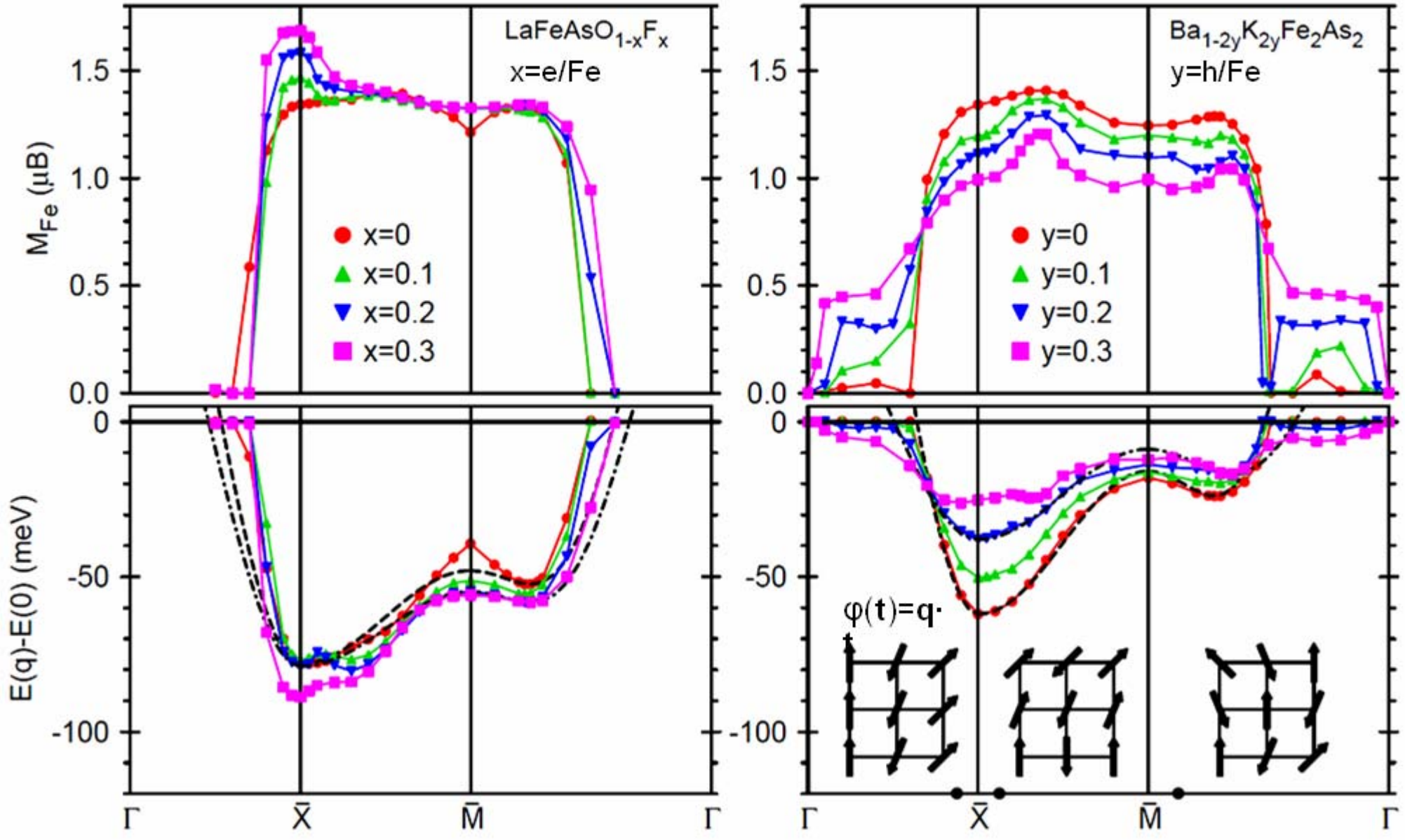

1/5 ×

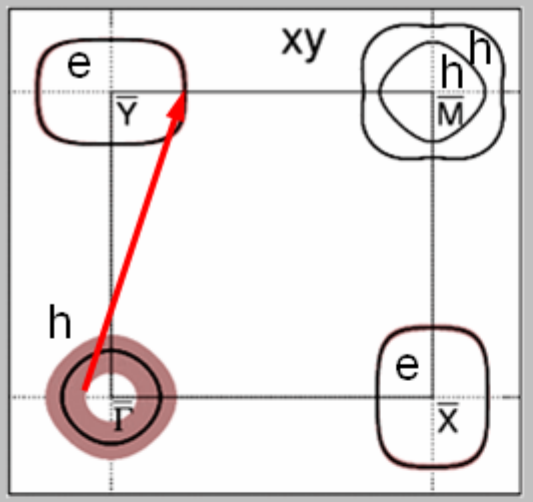

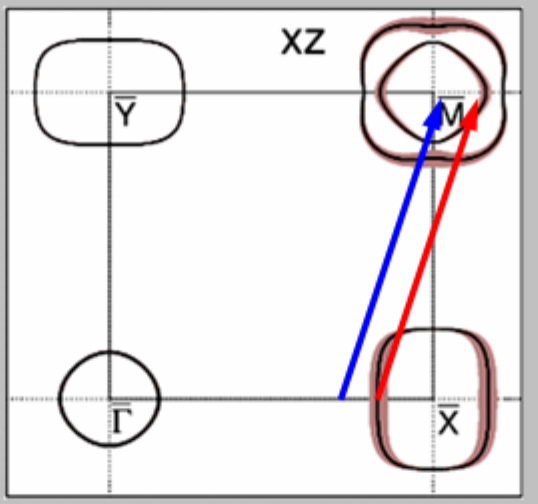

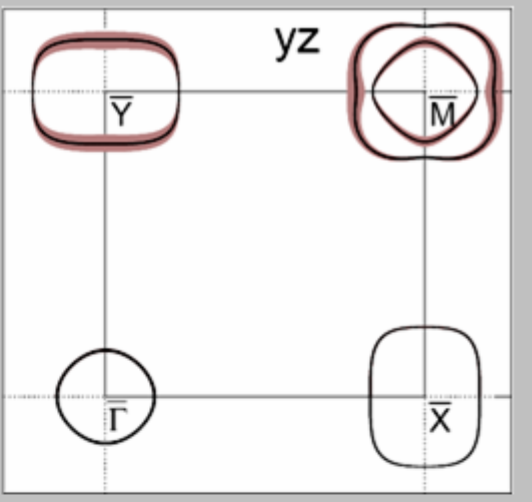

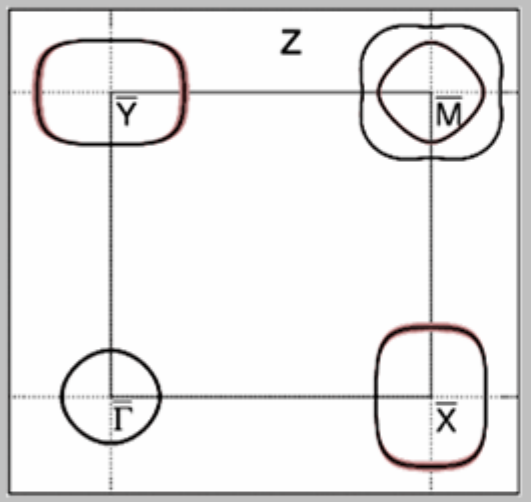

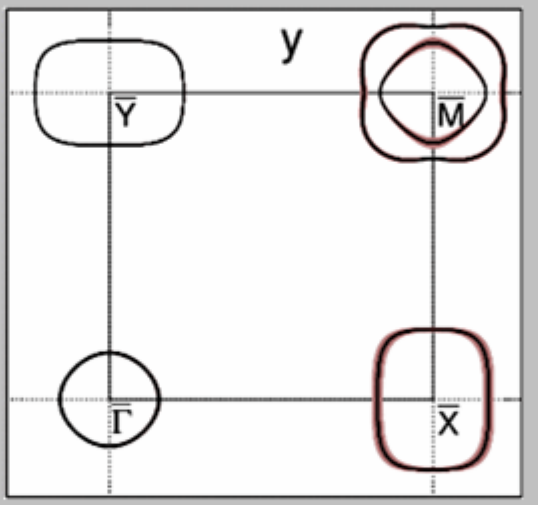

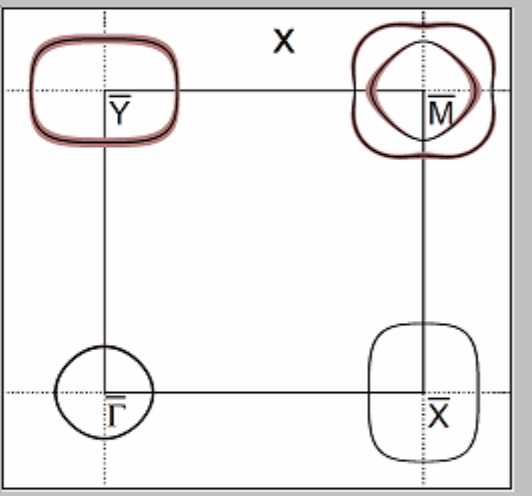

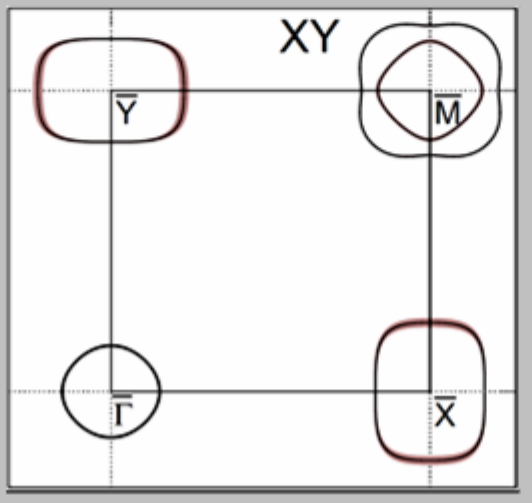

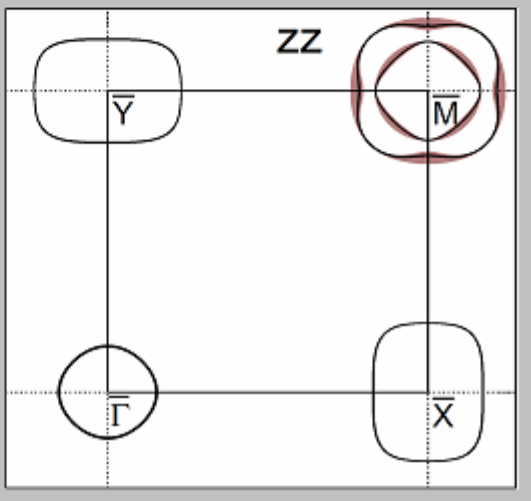

End of region of flat SDW energy for undoped LaOFeAs.

Second minimum for electron doping

does the Heisenberg model work for undoped compounds?

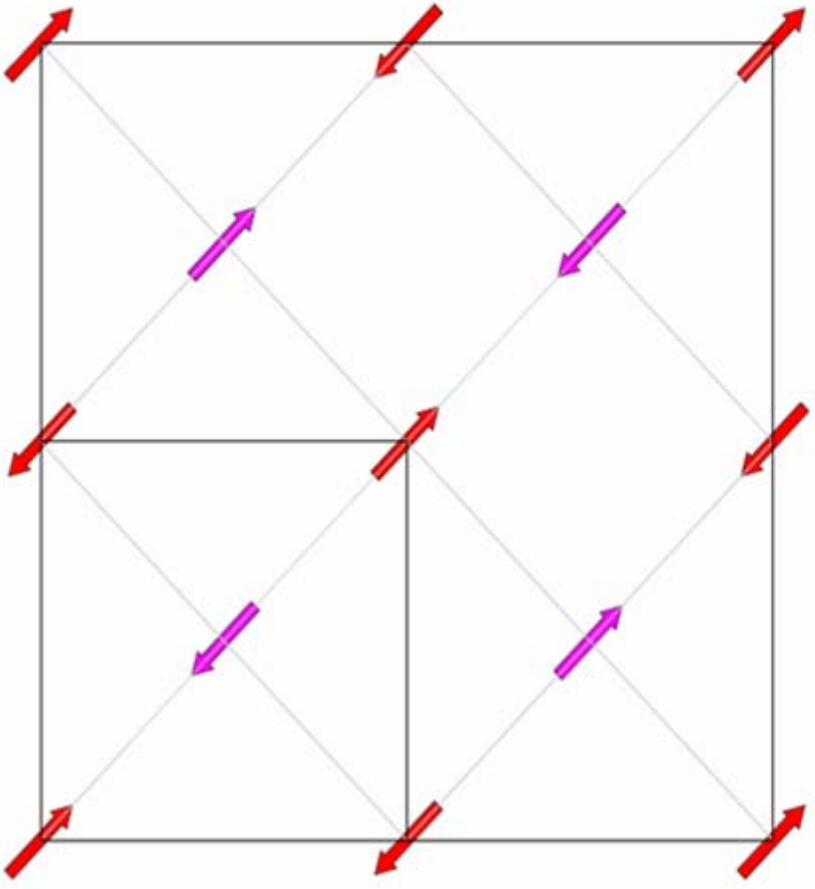

two AFM sublattices at $\mathbf{q}=(\pi,0)$
each Fe has two FM and two AFM n.n.:

$$\begin{aligned} E_H &= j_1[\cos\alpha + \cos(\pi-\alpha)] - 2j_2 \\ &= -2j_2 \end{aligned}$$

does the Heisenberg model work for undoped compounds?

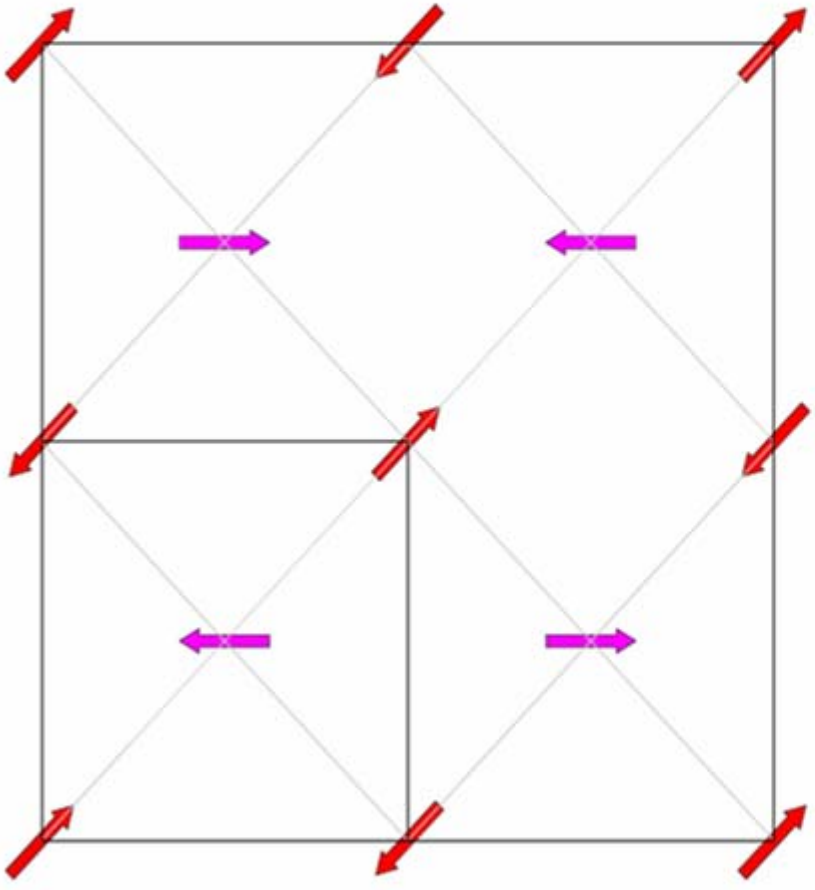

two AFM sublattices at $\mathbf{q}=(\pi,0)$
each Fe has two FM and two AFM n.n.:

$$\begin{aligned} E_H &= j_1[\cos\alpha + \cos(\pi-\alpha)] - 2j_2 \\ &= -2j_2 \end{aligned}$$

does the Heisenberg model work for undoped compounds?

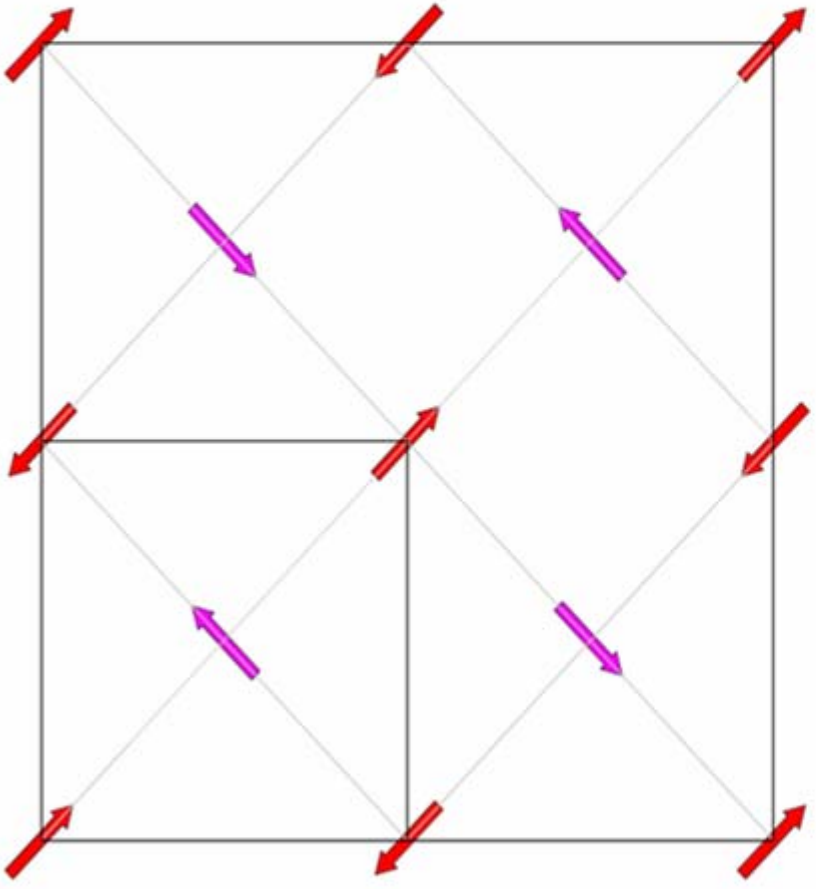

two AFM sublattices at $\mathbf{q}=(\pi,0)$
each Fe has two FM and two AFM n.n.:

$$\begin{aligned} E_H &= j_1[\cos\alpha + \cos(\pi-\alpha)] - 2j_2 \\ &= -2j_2 \end{aligned}$$

does the Heisenberg model work for undoped compounds?

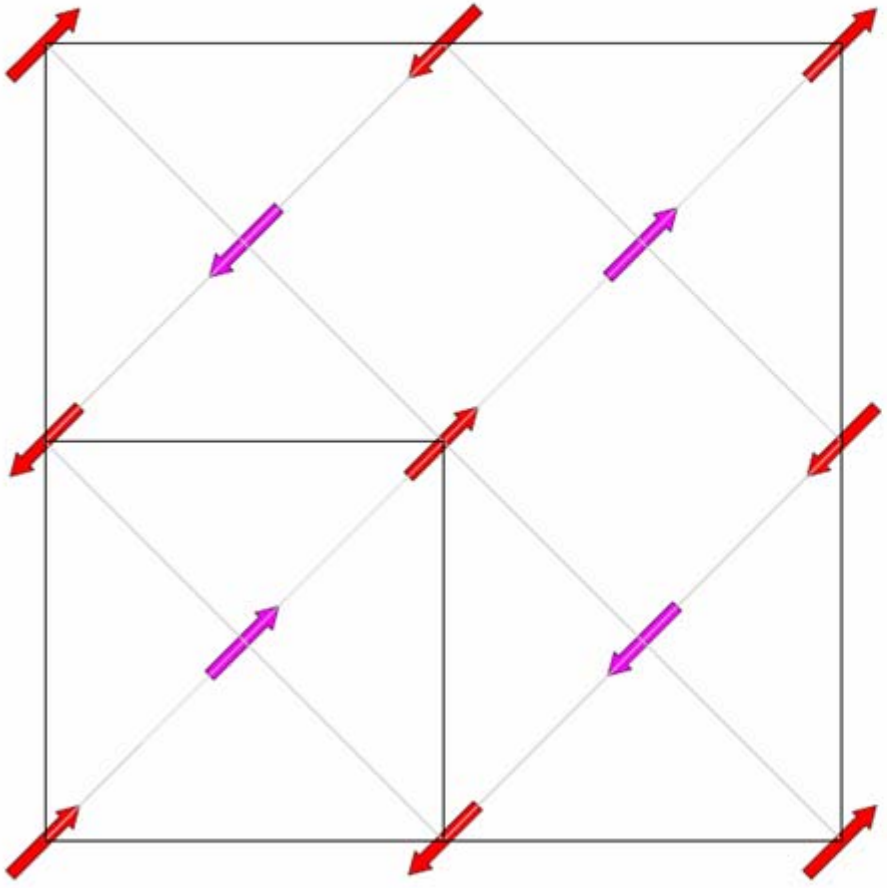

two AFM sublattices at $\mathbf{q}=(\pi,0)$
each Fe has two FM and two AFM n.n.:

$$\begin{aligned} E_H &= j_1[\cos\alpha + \cos(\pi-\alpha)] - 2 \\ &= -2j_2 \end{aligned}$$

NO!

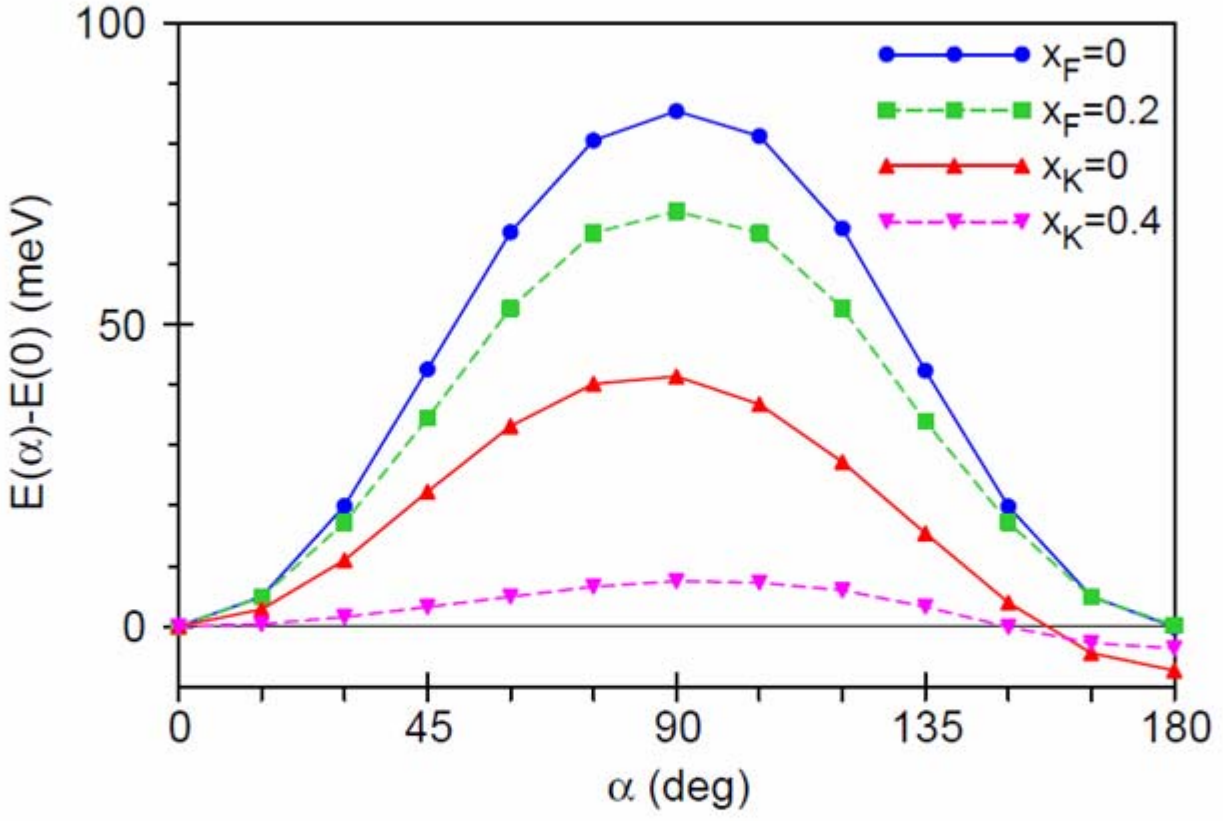

- collinear stripe AFM order is preferable
- $E(\alpha) \sim \sin^2 \alpha \sim -(\mathbf{S}_i \cdot \mathbf{S}_j)^2$
- the energy variation is suppressed by doping, especially in $BaFe_2As_2$.

The End